7. SITE 558[1]

Shipboard Scientific Party[2]

HOLE 558

Date occupied: 3 October 1981

Date departed: 11 October 1981

Time on hole: 196 hr.

Position (latitude; longitude): 37°46.2′N; 37°20.61′W

Water depth (sea level; corrected m, echo-sounding): 3754

Water depth (rig floor; corrected m, echo-sounding): 3764

Bottom felt (m, drill pipe): 3766

Penetration (m): 561

Number of cores: 44

Total length of cored section (m): 403.5

Total core recovered (m): 239.16

Core recovery (%): 59

Oldest sediment cored:
Depth sub-bottom (m): 408
Nature: Nannofossil chalk
Age: lower Oligocene

Basement:
Depth sub-bottom (m); 408
Nature: Basalt and serpentinized gabbro

HOLE 558A

Date occupied: 11 October 1981

Date departed: 12 October 1981

Time on hole: 28 hr.

Position (latitude; longitude): 37°46.2′N; 37°20.61′W

Water depth (sea level; corrected m, echo-sounding): 3754

Water depth (rig floor; corrected m, echo-sounding): 3764

Bottom felt (m, drill pipe): 3777

Penetration (m): 131.5

Number of cores: 16

Total length of cored section (m): 131.5

Total core recovered (m): 123.69

Core recovery (%): 94

Oldest sediment cored:
Depth sub-bottom (m): 131.5
Nature: Nannofossil ooze
Age: late Miocene

Principal results: Hole 558 (Site MAR-4) was drilled between Anomalies 13 and 15 on the west flank of the Mid-Atlantic Ridge about 30 miles south of the Pico Fracture Zone on a flow line passing through the FAMOUS area and the Leg 37 drilled sites (Fig. 1). The total penetration depth is 561 m, comprising 408 m of sediments and 153 m of basement.

In order to optimize the limited sediment program on this ocean crust leg, the shipboard scientists agreed that Site 558 would be suitable for continuous coring through the entire Neogene section and most of the Oligocene. The sediments recovered from the two holes cored at this site (558 and 558A) provide the first section of lower Oligocene through Pleistocene calcareous pelagic sediments from the North Atlantic.

The entire sediment layer (408 m) has been cored through a combination of piston coring and rotary coring; except for a 26-m gap where Holes 558 and 558A do not overlap. The recovered section provides an almost complete stratigraphic sequence from the Oligocene through the Pleistocene, with a minor hiatus in the lower Pliocene. There is a major change in the sediment lithology in the lower middle Miocene. The lower part of the section is characterized by a lower accumulation rate and a lower carbonate content. Nannofossils found within basalt breccias at the top of the basement are dated between 34 and 37 Ma, which is in agreement with the magnetic anomaly age. The magnetic reversal stratigraphy obtained from the lower part of the sedimentary section is very distinct and will provide strict limits for dating.

The upper 110 m of basement consisted almost entirely of aphyric pillow basalts and pillow breccias. Below this level, 43 m of serpentinized gabbros, serpentinite, and serpentinite mylonite were cored down to the bottom of the hole (561 m sub-bottom).

Six chemical units are distinguished within the pile of aphyric pillow basalts. Depleted (Nb = 3 ppm, Zr = 65 ppm), flat (Nb = 8.5 ppm, Zr = 83 ppm), and enriched (Nb = 15 ppm, Zr = 90 ppm) basalts are all represented. Interpretation of these results in terms of mantle plume and geodynamics will be very complex and will necessarily require isotopic and Ta/La data. These samples will be very valuable on the basis of fundamental and comparative geochemistry.

A complete set of logs was attempted. Because of poor hole conditions the logging runs were only partially successful.

OPERATIONS

Approach to Site 558

The criteria for Site 558 (MAR-4) were that it be on or near Anomaly 13 and on a flow line passing through the FAMOUS area and Site 335 of Leg 37 (Aumento, Melson, et al, 1977). The optimum sediment thickness was about 400 or 500 m, which we planned to continu-

[1] Bougault, H., Cande, S. C., et al., *Init. Repts. DSDP*, 82: Washington (U.S. Govt. Printing Office).

[2] Henri Bougault (Co-Chief Scientist), IFREMER (formerly CNEXO), Centre de Brest, 29273 Brest Cedex, France; Steven C. Cande (Co-Chief Scientist), Lamont-Doherty Geological Observatory, Columbia University, Palisades, New York; Joyce Brannon, Department of Earth and Planetary Sciences, Washington University, St. Louis, Missouri; David M. Christie, Hawaii Institute of Geophysics, University of Hawaii at Manoa, Honolulu, Hawaii; Murlene Clark, Department of Geology, Florida State University, Tallahassee, Florida; Doris M. Curtis, Curtis and Echols, Geological Consultants, Houston, Texas; Natalie Drake, Department of Geology, University of Massachusetts, Amherst, Massachusetts; Dorothy Echols, Department of Earth and Planetary Sciences, Washington University, St. Louis, Missouri (present address: Curtis and Echols, Geological Consultants, 800 Anderson, Houston, Texas 77401); Ian Ashley Hill, Department of Geology, University of Leicester, Leicester LE1 7RH, United Kingdom; M. Javed Khan, Lamont-Doherty Geological Observatory, Columbia University, Palisades, New York (present address: Department of Geology, Peshawar University, Peshawar, Pakistan); William Mills, Deep Sea Drilling Project, Scripps Institution of Oceanography, La Jolla, California (present address: Ocean Drilling Program, Texas A&M University, College Station, Texas 77843); Rolf Neuser, Institut für Geologie, Ruhr Universität Bochum, 4630 Bochum 1, Federal Republic of Germany; Marion Rideout, Graduate School of Oceanography, University of Rhode Island, Kingston, Rhode Island (present address: Department of Geology, Rice University, P.O. Box 1892, Houston, Texas 77251); and Barry L. Weaver, Department of Geology, University of Leicester, Leicester, LE1 7RH, United Kingdom (present address: School of Geology and Geophysics, University of Oklahoma, Norman, Oklahoma 73019).

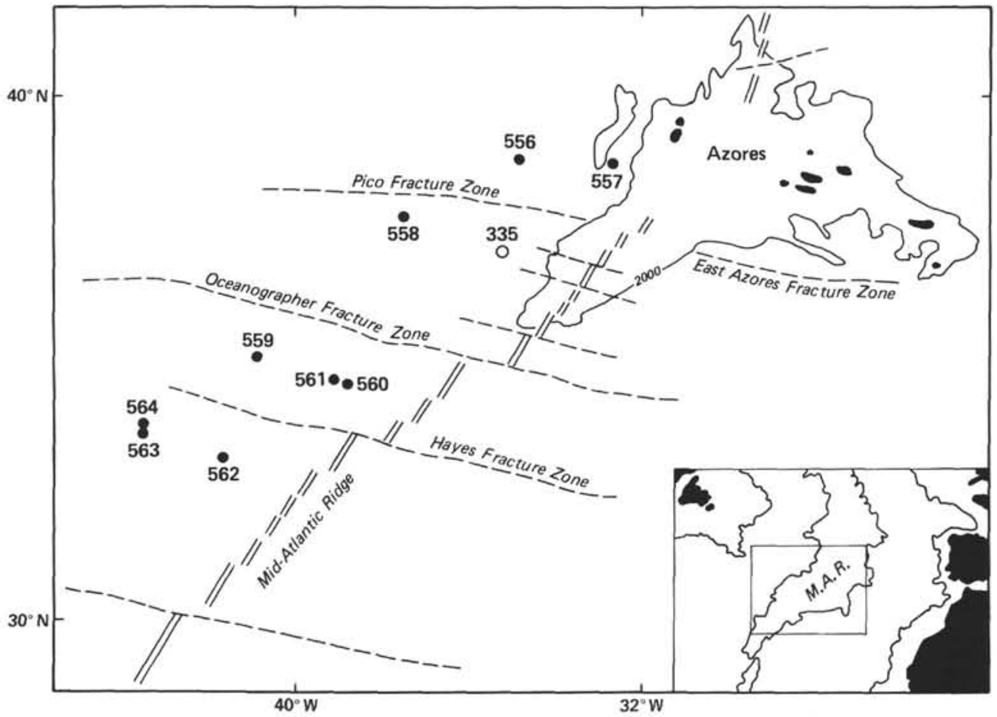

Figure 1. Site location map for Leg 82.

ously core. As at Sites 556 and 557, we wanted to avoid drilling on any irregular basement features that could not be considered typical oceanic crust.

The only existing geophysical data in the area were three magnetic lines (on which Anomalies 12 and 13 could be tentatively identified) and a poor quality seismic profiler record that showed an undulating basement with widely variable sediment thicknesses. Based on these data, we made a tentative site selection at 37°41′N, 37°19′W and laid out a track to survey it on the *Challenger* (Fig. 2). We were concerned that the site might be on one of the many fracture zones that offset the Mid-Atlantic Ridge near the FAMOUS area.

The survey on the approach to the site demonstrated that Anomaly 13 trended 12° *west* of north, which was unexpected because the trend of Magnetic Anomalies 12 and 13 further south near the Kane Fracture Zone is about 15° *east* of north. Basement relief is very irregular, and it is not clear whether the basement relief follows the same trend as the magnetic lineations. The reason for the anomalous trend of the magnetic lineations and the irregular basement relief is not known and requires more detailed surveying. It might reflect either oblique spreading at the ridge crest or possibly a series of small left lateral fracture zones that cannot be resolved at the spacing of our survey. We prefer the former interpretation of oblique spreading, because the peaks of Magnetic Anomaly 13 line up perfectly on all of the tracks with no hint of small, discrete offsets.

It was difficult to find a site within the survey area that met the requirements of a nominal 500 m of sediments underlain by a typical piece of oceanic basement. In general, the basement relief was quite irregular and the sediment cover was too thick to be continuously cored in a reasonable length of time. After completing the original planned survey of three east-west tracks parallel to the flow line, we found ourselves leaving the survey area without a prime site selected. At 1045Z, 3 October, we doubled back and headed for a site crossed at 0430Z on the north-south leg of the survey. However, we could not relocate this exact site and instead found a promising site about 5 miles north of our original tentative site selection (made before the survey was run). The beacon was dropped at 1146Z, 3 October, on a rolling basement hill covered with about 0.5 s of sediment (Fig. 3). Profiling was continued for a mile beyond the site and showed that the beacon had been dropped on a moderately steep slope. The actual site was offset 2500 ft. east of the beacon to a more level location in 3741 m of water.

The site is located on the negative anomaly between Anomalies 13 and 15 and has a theoretical age of 37 Ma based on the Lowrie and Alvarez (1981) time scale.

On-Site Operations

Hole 558 was spudded at 2122 hr. 3 October. No mudline core was taken and, in anticipation of hydraulic piston coring at the end of drilling operations, sediments were washed down to a depth of 158 m sub-bottom. Continuous coring was then started; the first core was on deck at 0220 hr. 4 October. Basement was reached around 1600 hr. 5 October at a depth of 406 m sub-bottom during cutting of Core 558-27. Coring within basement continued until 0754 hr. 9 October when, at a depth of 561 m sub-bottom, coring was halted because of a slow drilling rate and low recovery within thick serpentinite (Table 1). Total basement penetration was 155.5 m. After two attempts, the drill bit was dropped.

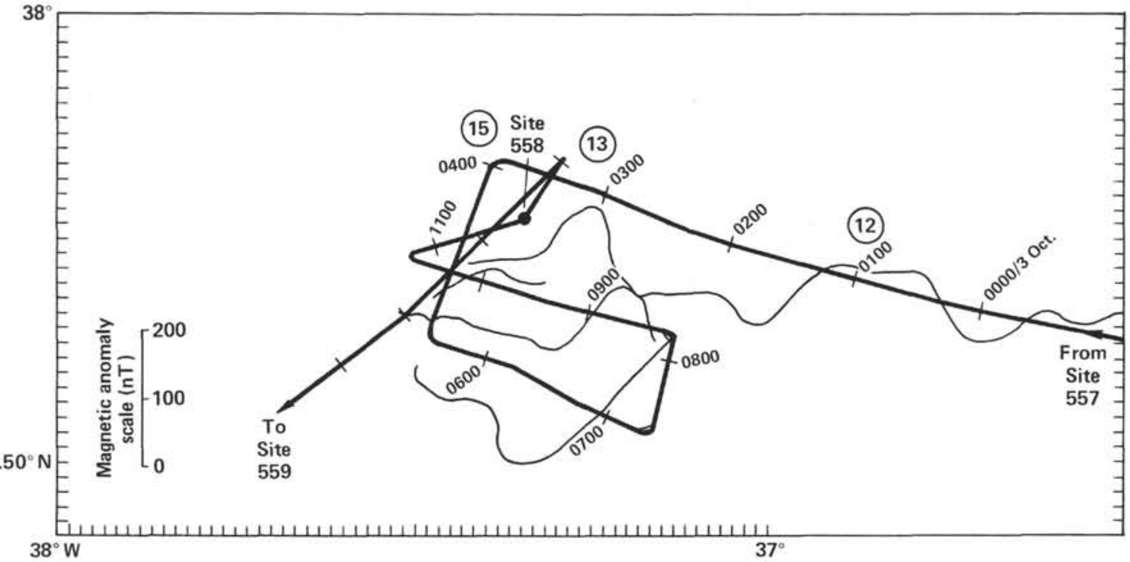

Figure 2. Approach and site survey tracks for Site 558. Heavy line is ship track with hour marks in GMT. Faint line is magnetic anomaly projected perpendicularly from the ship's track. Circled numbers are magnetic anomalies based on work at Lamont-Doherty Geological Observatory.

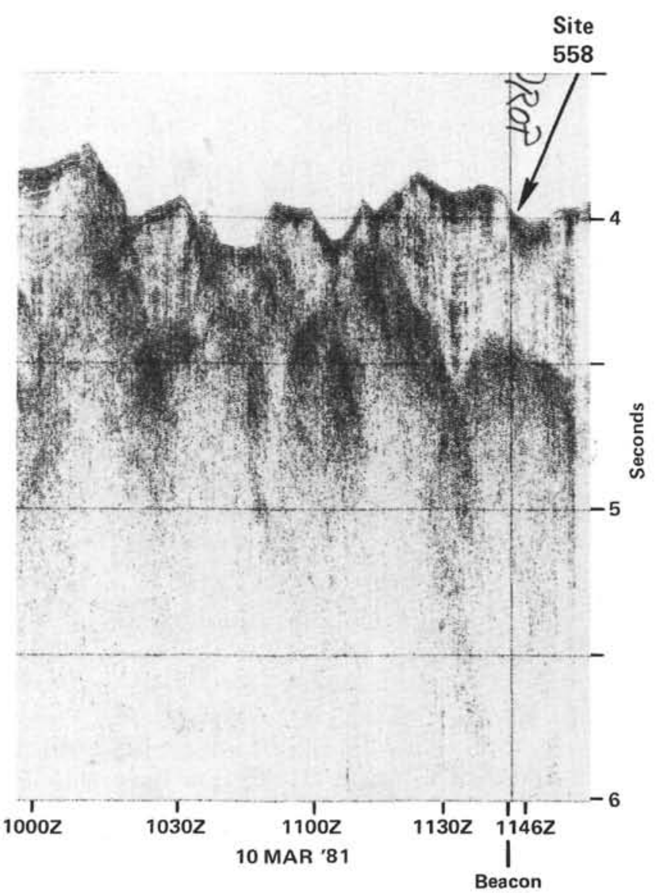

Figure 3. *Glomar Challenger* seismic profile approaching Site 558. For location of profile, see Figure 2.

Circulation was stopped at 1430 hr. 9 October and the end of the drill string pulled up to a depth of about 110 m sub-bottom. Logging operations were carried out between 1600 hr. 9 October and 0330 hr. 11 October. These operations are described in detail in the Downhole Measurements section. After logging was completed, preparations were made for hydraulic piston coring, which commenced at 1350 hr. 11 October and continued until 0930 hr. 12 October. A total of 132 m was piston cored (Table 1). Piston coring was halted before complete overlap of the sedimentary section when the pins holding the inner core barrel sheared and the core barrel became lodged in the hole, which forced us to abandon the hole. Piston coring operations were plagued repeatedly with the premature firing of the core barrel. However, this did not appear to affect the recovery of sediments, which was generally 100%. The *Challenger* was under way to Site 559 (MAR-8) by 1700 hr. 12 October. During the drilling of Holes 558 and 558A, operations were repeatedly hampered by a bad combination of current and swell that occasionally required a halt in operations for periods as long as 5 hr.

SEDIMENT LITHOLOGY

Two holes were cored at Site 558 in order to recover the upper portion of the sediment by hydraulic piston coring.

The first hole (558) was washed to 158 m before continuous rotary coring was begun. In this first hole a total of 561 m (measured from mudline) were penetrated, of which 408 m consisted of calcareous pelagic sediments.

After the first hole was successfully logged, Hole 558A was piston-cored to a depth of 131 m. Unfortunately, we were forced to stop operation at this depth before overlapping with the top of the cored interval from Hole 558. This left a gap of 26.5 m, which represents approxi-

Table 1. Coring summary, Site 558.

Core	Date (Oct. 1981)	Time (Z)	Depth from drill floor (m)	Depth below seafloor (m)	Length cored (m)	Length recovered (m)	Percent recovered
Hole 558							
H1	4	0039	3766.0–3924.0	0.0–158.0	0.0	0.00	0
1	4	0220	3924.0–3933.5	158.0–167.5	9.5	9.15	96
2	4	0353	3933.5–3943.0	167.5–177.0	9.5	8.78	92
3	4	0515	3943.0–3952.5	177.0–186.5	9.5	9.48	99
4	4	0652	3952.5–3962.0	186.5–196.0	9.5	9.65	100+
5	4	0800	3962.5–3971.5	196.0–205.5	9.5	9.40	99
6	4	0954	3971.5–3981.0	205.5–215.0	9.5	9.05	95
7	4	1120	3981.0–3990.5	215.0–224.5	9.5	0.89	9
8	4	1300	3990.5–4000.0	224.5–234.0	9.5	5.65	59
9	4	1450	4000.0–4009.5	234.0–243.5	9.5	3.28	35
10	4	1610	4009.5–4019.0	243.5–253.0	9.5	1.54	16
11	4	1740	4019.0–4028.5	253.0–262.5	9.5	2.74	29
12	4	1910	4028.5–4038.0	262.5–272.0	9.5	7.05	74
13	4	2055	4038.0–4047.5	272.0–281.5	9.5	9.00	96
14	4	2159	4047.5–4057.0	281.5–291.0	9.5	9.59	100+
15	4	2325	4057.0–4066.5	291.0–300.5	9.5	9.09	96
16	5	0057	4066.5–4076.0	300.5–310.0	9.5	9.70	100+
17	5	0236	4076.0–4085.5	310.0–319.5	9.5	7.43	78
18	5	0354	4085.5–4095.0	319.5–329.0	9.5	6.86	72
19	5	0525	4095.0–4104.5	329.0–338.5	9.5	7.60	80
20	5	0651	4104.5–4114.0	338.5–348.0	9.5	6.47	68
21	5	0805	4114.0–4123.5	348.0–357.5	9.5	3.64	38
22	5	0925	4123.5–4133.0	357.5–367.0	9.5	5.42	57
23	5	1045	4133.0–4142.5	367.0–376.5	9.5	9.36	99
24	5	1210	4142.5–4152.0	376.5–386.0	9.5	5.98	63
25	5	1340	4152.0–4161.5	386.0–395.5	9.5	8.97	94
26	5	1500	4161.5–4171.0	395.5–405.0	9.5	6.94	73
27	5	1801	4171.0–4180.5	405.0–414.5	9.5	3.78	40
28	5	2354	4180.5–4189.5	414.5–423.5	9.0	3.09	34
29	6	0553	4189.5–4198.5	423.5–432.5	9.0	3.29	37
30	6	1038	4198.5–4207.5	432.5–441.5	9.0	4.08	45
31	6	1538	4207.5–4216.5	441.5–450.5	9.0	2.20	24
32	6	2050	4216.5–4225.5	450.5–459.5	9.0	5.00	56
33	7	0435	4225.5–4234.5	459.5–468.5	9.0	3.79	42
34	7	0801	4234.5–4243.5	468.5–477.5	9.0	1.50	17
35	7	1110	4243.5–4252.5	477.5–486.5	9.0	4.12	46
36	7	1445	4252.5–4261.5	486.5–495.5	9.0	3.09	34
37	7	1928	4261.5–4270.5	495.5–504.5	9.0	1.29	14
38	8	0110	4270.5–4275.0	504.5–509.0	4.5	2.45	54
39	8	0605	4275.0–4284.0	509.0–518.0	9.0	4.83	54
40	8	0858	4284.0–4293.0	518.0–527.0	9.0	3.37	37
41	8	1350	4293.0–4302.0	527.0–536.0	9.0	4.10	46
42	8	1955	4302.0–4311.0	536.0–545.0	9.0	1.78	20
43	9	0224	4311.0–4320.0	545.0–554.0	9.0	1.30	14
44	9	0754	4320.0–4327.5	554.0–561.5	7.5	3.39	45
					403.5	239.16	59
Hole 558A							
1	11	1415	3777.0–3777.5	0.0–0.5	0.5	0.47	94
2	11	1523	3777.5–3787.0	0.5–10.0	9.5	9.36	99
3	11	1639	3787.0–3796.5	10.0–19.5	9.5	9.51	100+
4	11	1752	3796.5–3806.0	19.5–29.0	9.5	9.32	98
5	11	1920	3806.0–3815.5	29.0–38.5	9.5	9.71	100+
6	11	2040	3815.5–3825.0	38.5–48.0	9.5	9.70	100+
7	11	2145	3825.0–3834.5	48.0–57.5	9.5	8.22	87
8	11	2255	3834.5–3844.0	57.5–67.0	9.5	7.78	82
9	12	0025	3844.0–3851.0	67.0–74.0	7.0	4.76	68
10	12	0147	3851.0–3854.0	74.0–77.0	3.0	3.24	100+
11	12	0305	3854.0–3863.5	77.0–86.5	9.5	9.63	100+
12	12	0425	3863.5–3873.0	86.5–96.0	9.5	8.47	89
13	12	0546	3873.0–3880.0	96.0–103.0	7.0	6.98	100+
14	12	0652	3880.0–3889.5	103.0–112.5	9.5	9.65	100+
15	12	0810	3889.5–3899.0	112.5–122.0	9.5	8.11	85
16	12	0910	3899.0–3908.5	122.0–131.5	9.5	8.78	92
					131.5	123.69	94

mately 1–3 Ma of sedimentation. Because this gap represents such a short time span, and logging results through the same section in Hole 558 indicate that the lithology remains unchanged, we believe that we are justified in extrapolating sedimentation rates and lithology through this interval. Also for this discussion we have treated the cored sediment from both holes as one continuous section (see Fig. 4).

Based on carbonate and clay content (see Fig. 5) and the consequent color change, we have divided the sediment section into two major units. The lithologic unit descriptions are discussed in order of their deposition,

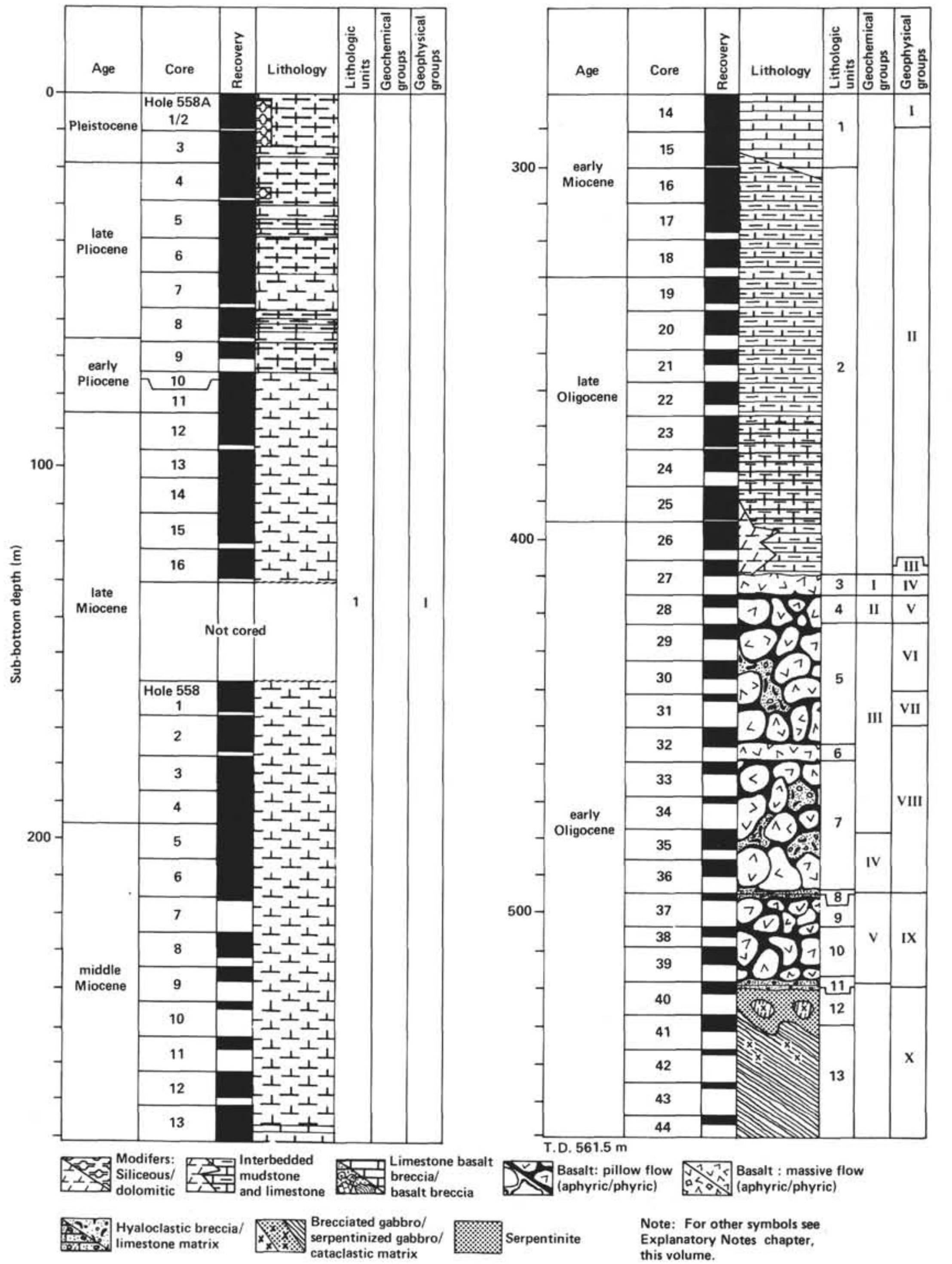

Figure 4. Lithologic column for Site 558. Water depth = 3766 m. T.D. = total depth. See Explanatory Notes chapter (this volume) for lithologic symbols.

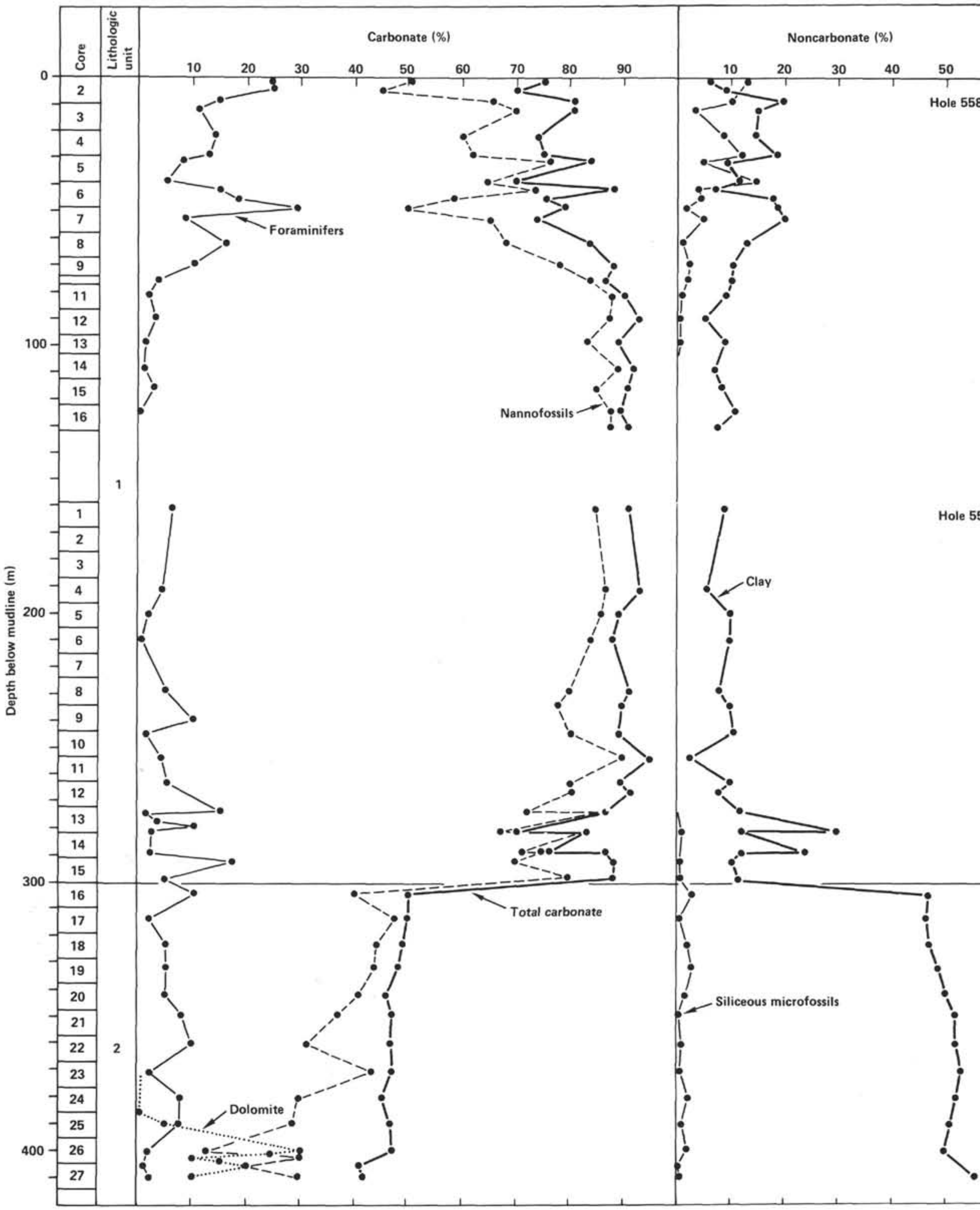

Figure 5. Percentage plot of major sediment components for Site 558.

beginning at the base of the sediment section with Unit 2 (summarized in Table 2).

Unit 2

This unit consists of 108 m (558-16-3, 40 cm through 558-27-2, 130 cm) of marly nannofossil chalk and limestone, marly foraminiferal nannofossil chalk, and dolomitic marly nannofossil chalk of the early Oligocene to early Miocene time (from 17–19 to 34–37 Ma). Colors of the chalks and limestones vary from brown (10YR 5/3) and yellowish brown (10YR 5/4) to pale brown (10YR 6/3). The color changes are usually gradational

Table 2. Sedimentary lithologic units at Site 558.

Interval	Lithologic unit	Sub-bottom depth (thickness) (m)	Main colors	Main lithology	Main components	Structure	Age
All of Hole 558A and 558-H1 to 558-16-3, 40 cm	1	0–300.0 (300)	Shades of white to pale brown	Nannofossil ooze; siliceous foraminiferal-nannofossil ooze; foraminiferal-nannofossil ooze	Nannofossils, foraminifers	Uniform with moderate mottling	late Pleistocene to early Miocene
558-16-3, 40 cm to 558-27-2, 130 cm	2	300.0–408.0 (108)	Yellowish brown to brown	Marly nannofossil chalk and limestone; marly foraminiferal-nannofossil chalk; dolomitic marly nannofossil chalk/ limestone	Nannofossils, foraminifers, clay, dolomite	Uniform with moderate to intense mottling	early Miocene to early Oligocene

with few sharp contacts. These color changes reflect the change in carbonate versus clay content, although in Cores 26 and 27 the presence of dolomite may be the cause of darker shades of brown.

We observed no sediment transport textures or structures. Bedding is massive. Bioturbation/mottling is moderate to intense. Burrows (2–3 cm in diameter) have white halos around darker cores and are somewhat ellipsoid. Open ocean pelagic sedimentation began at this site in the early Oligocene and has continued to the present. But the deposition of sediments characterized by low carbonate values (40–50%) and high clay content (45–55%) ended in the late early Miocene. The presence of clay minerals is confirmed by X-ray diffraction analysis. Clay percentages were calculated by subtracting the percentage of carbonate (determined by carbonate bomb analysis), siliceous microfossils, feldspar, and other components (estimated from smear-slide examination) from 100 (Fig. 5).

Throughout this unit, siliceous microfossils and volcanic-derived debris (i.e., volcanic glass, feldspar, palagonite, and heavy minerals) occur in only trace amounts to a few percent. Manganese micronodules are also present in trace quantities in all the cores, although in Cores 558-17 through 558-15, larger nodules (1–3 cm in diameter) do occur. The presence of these manganese nodules suggests a low sediment deposition rate. This observation is supported by an average sedimentation rate of about 8 m/Ma calculated from biostratigraphic data (Fig. 7).

Carbonate values change very little within Unit 2 with a slight increase from 41% at the bottom of the unit to 50% at the top (see Fig. 5). Discussion of the carbonate component in terms of foraminifer-nannofossil ratios is complicated by the presence of authigenic dolomite rhombs in Cores 27 through 23. In the chalks and limestones of Core 27, the dolomite content is between 15 and 20%, then increases rapidly to 30% in Core 26. From Cores 26 to 23, the dolomite decreases to trace amounts and is absent from the rest of the sediment section. The constant carbonate composition through this section and the decrease in foraminiferal and nannofossil components with increase in dolomite would suggest that the dolomite is forming at the expense of the original carbonate constituents. Dolomite was observed encrusting (and possibly replacing) tests of washed foraminifers. In smear-slide examination, the majority of the dolomite rhombs are euhedral, although some show textures of previous resorption and recrystallization. Occurrence of the dolomite is discussed further in the Pore Water Chemistry section of this report.

The foraminiferal content changes from 5% or less in the zone of maximum dolomitization to an estimated 10% at the top of the dolomitized section in Core 25 and continues through Core 21 at 8–10%, with lower values in some samples (Fig. 5). Between Cores 21 and 16, the foraminiferal content is less than 5%, but increases erratically upward from the upper part of Unit 2 in Core 558-17 through the transition zone into Unit 1, reaching a maximum of 15% in Core 558-13.

The nannofossil abundance curve is essentially a mirror-image of the foraminifers, except in the dolomitized portion where both are in reduced abundance. Again beginning in the top of the dolomitized zone, nannofossils increase from an estimated 35% in Core 558-25 to 55% just below Core 558-16 and maintain values averaging 40–50% until the top of the unit in Core 558-16. Nannofossil percentages in the transition zone between Unit 1 and Unit 2 average between 60 and 70%.

Unit 1

This unit consists of 300 m (Hole 558A to 558-16-1, 0 cm) of nannofossil ooze and chalk, foraminiferal-nannofossil ooze and siliceous foraminiferal-nannofossil ooze. Unit 1 represents a period of deposition from the late early Miocene to the late Pleistocene (0 to 17–19 Ma) and is a continuation of the open ocean pelagic sedimentation from Unit 2, but with less clay deposition and higher sedimentation rates averaging 16 m/Ma.

We observed no sediment transport textures or structures. Bedding is massive. Bioturbation/mottling is moderate, when observed, although the lack of color contrast may have resulted in underestimating the degree of intensity or in overlooking these structures.

The lower portion of Unit 1 is transitional from Unit 2. In fact the first signs of the transition begin within Unit 2 at 558-18-4, 90 cm with the first minor occurrences of white (10YR 8/1) to light brownish gray (10YR 6/2) nannofossil chalk. These interbeds of nannofossil chalk (10–20 cm thick) continue irregularly uphole until

558-15-5, 40 cm, where they become the dominant lithology. The pale brown (10YR 6/3) to very pale brown (10YR 8/3) clayey interbeds persist uphole to 558-13-4, 60 cm, becoming less frequent, thinner, and less clayey (less than 10%). The change in lithification from chalk to ooze also takes place here.

Within the transition zone the nannofossil content (60–70%) varies inversely with the clay content (see Fig. 5). The foraminifers vary erratically from 1 to 15%. Because the total carbonate values are calculated from carbonate bomb data, a more reliable method than smear slide estimates, the variation shown by its curve (range 70 to 90%) demonstrates best the transitional nature of the lower portion of Unit 1.

Most of Unit 1 above the transition zone, through Core 558A-8 is very uniform in composition and this is reflected in coloration that varies only in shades of white (2.5YN 8 to 10YR 8/1). The total carbonate curve (Fig. 5) maintains a rather uniform average value of 90% with a range of 83 to 97%. Through this interval, nannofossil abundances range between 70 and 90% and foraminiferal abundances range from trace amounts to less than 10%. Clay, like the total carbonate curve, remains rather consistent at 10% with a range of 2 to 17%. Siliceous microfossils along with volcanic-derived material are absent or occur in trace amounts only. Micronodules of either pyrite or manganese minerals are present in trace or small amounts and may produce black streaks on the cut surface of the cores as a result of the core-splitting process.

Above Core 558A-8, the sediment color is white (5YR 8/1) up to 558A-1, which is pale brown (10YR 6/3), and sediment constituents depart from their uniform nature as previously described. Although overall clay content departs very little from its previous average value of 10%, except for a tendency to decrease near the top of the sediment section, a noticeable difference in the clay abundance curve is the increased variation in the range of values (2–20%).

This increase in range and variation is common to all the sediment constituents, although noticeable trends are observed with sedimentation (uphole). The total carbonate range is from 70 to 88%, with a decreasing trend with younger sedimentation. Nannofossils, while still the dominant sediment component, have a range of 80 to 45% with a decreasing trend with younger sedimentation. Foraminifers have a range of 2 to 29% with an increasing trend with younger sedimentation. Siliceous microfossils like the foraminifers also increase with younger sedimentation and have a range of trace amounts to 20%.

The relative increase of ratio of foraminifers and siliceous microfossils to nannofossil abundances may reflect an increase of productivity of the surface water. The higher variability may be due to cyclic environmental changes that cannot be resolved by our sampling density.

Miscellaneous Sediments

Intrapillow-basalt (volcaniclastic) limestone is common throughout the basalt units. It occurs either between pillow margins or as fillings in basalt cracks. Colors vary from light brownish yellow (10YR 6/4) to white (10YR 8/2). The volcaniclasts are mostly derived from the adjacent vitric rims of basalt pillows. Along with these volcaniclasts, foraminifers and micronodules are roughly stratified (geopetal texture?).

The degree of recrystallization of the former pelagic ooze is variable. The present limestone is mostly composed of micritic calcite, along with some rare unrecrystallized nannofossils, although irregular patches of sparite are common. These limestones have been heavily mineralized by dendritic manganese oxides.

BIOSTRATIGRAPHY

At Site 558, located near Anomaly 13, two holes were drilled; Hole 558 and Hole 558A. Hole 558 was washed down to a depth of 158 m and then sediments were continuously cored to a total penetration above basement of 408 m. The sediments recovered range from late Miocene to early Oligocene. The age of the oldest sediment, based on the microfossils, is in agreement with the estimated age of basement at the site.

Hole 558A had been piston-cored to a total depth of 132 m when mechanical problems in the inner core barrel forced termination before biostratigraphic overlap was accomplished. Sediments recovered from Hole 558A are Pleistocene to upper Miocene.

The combined section recovered from Holes 558 and 558A as dated by calcareous nannofossils ranges from Pleistocene to lower Oligocene. All major zones of Okada and Bukry (1980) are represented except CN11a and b, CN10b and c, and CN8. Nannofossil preservation is generally good in Hole 558A and remains so down to Core 558-5, which is middle Miocene. Preservation is only moderate from Core 558-5 down to the base of the sediment column.

Figure 6 shows the cored intervals, approximate ages based on foraminifers and position of the biostratigraphic gap. Foraminiferal ages are in general agreement with the nannofossil dates. Planktonic foraminifers are common to abundant and preservation moderate to good throughout most of the section (except for the middle and upper Miocene sections where there is evidence of dissolution and in the Oligocene section above the basalt where there is evidence of destruction of foraminifers by the growth of dolomite crystals in and on the tests).

Benthic foraminifers are fairly common and diversified and are indicative of deep water.

Other elements of the fauna such as well-preserved diverse ostracodes, radiolarians, sponge spicules, fish teeth, echinoid spines and *Bolboforma* (calcareous algae?) are significant (see Echols, this volume, for discussion of *Bolboforma*).

Calcareous Nannofossils

Hole 558

Hole 558 was washed down to a depth of 158 m where Core 558-1 was taken. Core 558-H1,CC contains an upper Miocene assemblage that includes *Discoaster neoha-*

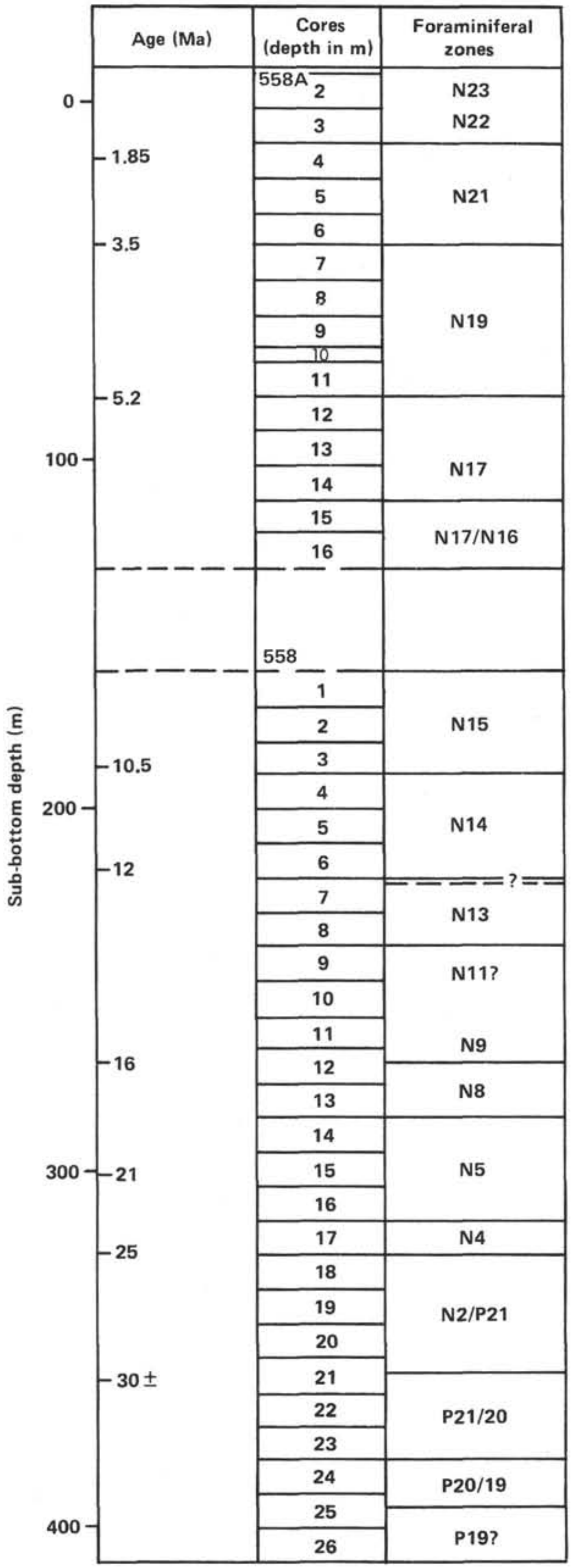

Figure 6. Preliminary zonation of Holes 558 and 558A.

matus, Calcidiscus macintyrei, D. bellus, and *Triquetrorhabdulus rugosus* and is characteristic of the *D. neohamatus* Zone CN8 of Okada and Bukry (1980) NN10. Because of the common occurrence of *D. bellus*, it is possible that Core 558-H1 corresponds to the lower part of the *D. neohamatus* Zone.

Cores 1 to 3 were recovered by rotary methods and are assigned to the upper middle Miocene to lower upper Miocene based on the occurrence of *D. hamatus* and *Catinaster calyculus*. *D. hamatus* is the index species for CN7 (NN9) and according to Okada and Bukry (1980), the base of *C. calyculus* is the marker for Subzone CN7b.

The core catcher of Core 558-4 contains *C. coalitus* without *D. hamatus* and is placed within the *C. coalitus* Zone CN6 (NN8), which is middle Miocene.

Cores 5 to 11 occur between the first appearance of *C. coalitus* and the last appearance of *Sphenolithus heteromorphus*. This interval is assigned to the *D. exilis* Zone CN5 (NN6–NN7) and indicates an accelerated accumulation rate for the middle Miocene. *D. exilis* is abundant and occurs with *D. variabilis, D. bollii, Calcidiscus macintyrei, Coccolithus pelagicus*, and *T. rugosus*.

Cores 12 to 14 are assigned to the middle Miocene because of the presence of *S. heteromorphus* with the common occurrence of long-armed discoasters. Core 15 contains *S. heteromorphus* but the long-armed discoasters are absent, creating an overall change in the appearance of the assemblage. This suggests that Core 15 probably should be attributed to the *Helicosphaera ampliaperta* Zone CN3 (NN4–NN3). *H. ampliaperta* is absent in Cores 12 to 15, so the first appearance of the long-armed discoasters is used to separate Zones CN3 and CN4.

The core catcher of Core 16 is lower Miocene, based on the presence of *S. belemnos* CN2 (NN3-2).

The Oligocene/Miocene boundary occurs within Cores 17 and 18, which are placed into the *T. carinatus* Zone CN1 (NN1–NP25). The assemblage is characterized by *T. carinatus, D. deflandrei*, and *Cyclicargolithus floridanus*.

The interval 558-19,CC through 558-22,CC contains *S. ciperoensis and is assigned to the upper Oligocene S. ciperoensis* Zone CP19 (NP24–NP25). *S. distentus*, whose last appearance datum marks the boundary between Subzones 19b *Dictyococcites bisectus* and 19a *C. floridanus*, is not present until 558-21,CC. The interval 558-19,CC through 558-21,CC is assigned to Subzone 19b, and 558-22,CC is assigned to Subzone 19a.

The core catcher of Core 23 is assigned to the lower upper Oligocene *S. distentus* Zone CP18 (NP23) because of the occurrence of *S. distentus* without *S. ciperoensis*. A lower upper Oligocene CP17 (NP23) assignment is inferred for 558-24,CC because of the presence of *S. predistentus* in the absence of *S. distentus* or *Reticulofenestra umbilica*.

The presence of rare *R. umbilica* in 558-25,CC indicates that this sample occurs within CP16c (NP22) *H. reticulata* Zone, *R. hillae* Subzone. The core catcher of Core 26 and 558-27-2, 42 cm contain *R. umbilica* and *Coccolithus formosus*, which indicate that this interval belongs to the *H. reticulata* Zone, *C. formosus* Subzone CP16b (NP21). Cores 25 to 27 are lower Oligocene.

Hole 558A

Hole 558A was cored by the hydraulic piston corer (HPC), and 123.69 m of sediment were recovered. Core 1 contains abundant *Gephyrocapsa caribbeanica* and *G. oceanica*, indicating the upper Pleistocene. The presence of *Emiliania huxleyi* is indefinite because of the difficulty in recognizing this species with the light microscope. Core 1 contains common and well-preserved *Ceratolithus telesmus* and *C. cristatus*. Although 558A-2,CC is Pleistocene, assignment to a particular zone is questionable because of the small size of the nannofossils present: exceptions are *Cycloccolithus leptoporus* and *Helicopontosphaera sellii*. *Calcidiscus macintyrei* is encountered in Core 3 above the extinction of *Discoaster brouweri*. This sample corresponds to the lower Pleistocene *C. macintyrei* Zone of Gartner (1977) (NN19).

Cores 4 to 7 are upper Pliocene and are assigned to the *D. brouweri* Zone CN12 of Okada and Bukry (1980) (NN16, NN17, NN18) on the basis of the occurrence of *D. brouweri* above the last appearance of *Reticulofenestra pseudoumbilica*. The core catcher of Core 4 contains *C. macintyrei* and *D. brouweri* without *D. pentaradiatus*. This indicates the uppermost Subzone CN12d of the *D. brouweri* Zone of Okada and Bukry (1980). Cores 5 and 6 contain *D. pentaradiatus* and possibly *D. surculus* and are placed within the Subzones CN12b–c. *D. tamalis* is first encountered in 558A-7,CC, and the sample is therefore assigned to Subzone CN12a.

Very rare *R. pseudoumbilica* are found in 558A-8,CC, as well as *D. tamalis* and *Ceratolithus rugosus*. Because specimens of *R. pseudoumbilica* are so rare and *Sphenolithus abies* is absent, this sample is assigned to the *D. brouweri* Zone, *D. tamalis* Subzone CN12a (NN16).

The core catcher of Core 9 contains a color change that marks the position of a lower Pliocene hiatus. The top of the core catcher contains *R. pseudoumbilica, D. asymmetricus*, and *D. tamalis* and is assigned to the *D. asymmetricus* Subzone of the *R. pseudoumbilica* Zone CN11b (NN15). The lower part of the core catcher contains *Amaurolithus primus, A. delicatus*, and a possible *C. acutus*. Two specimens of *Triquetrorhabdulus rugosus* are also present but may be reworked. This places the lower part of 558A-9,CC in either the *C. acutus* or *T. rugosus* Subzone of the *A. tricorniculatus* Zone CN10a,b (NN12). Subzone CN11a and CN10c of the lower Pliocene are absent, signaling a hiatus during this interval.

The interval from 558A-10,CC to 558A-12,CC contains *T. rugosus* with *A. primus, A. delicatus*, and *A. tricorniculatus*. This indicates that this interval is uppermost Miocene. Because the presence of *D, quinqueramus* could not be clearly established, Cores 10 and 11 are thought to occur within the *A. tricorniculatus* Zone, *T. rugosus* Subzone CN10a (NN12).

The interval from 558A-13,CC to 558A-14,CC is attributed to the upper Miocene *D. quinqueramus* Zone, *A. primus* Subzone CN9b (NN11). *D. quinqueramus* is observed in these samples as well as *A. amplificus* and *A. primus*. The core catcher samples from Cores 15 and 16 also belong to the *D. quinqueramus* zone. The absence of *A. primus* and the presence of *D. berggrenii* place this interval within the *D. berggrenii* Subzone CN9a (NN11).

Foraminifers

Hole 558

Miocene (upper)

Hole 558 was washed down to a depth of 158 m. The first rotary core taken recovered a white nannofossil-foraminiferal ooze with an abundant and well-preserved middle-upper-Miocene fauna. Although placement is tentative, abundant specimens of the *Globorotalia menardii-(cultrata)* s.l. lineage and the presence of *Globigerina nepenthes, Globoquadrina altispira, G. dehiscens, Sphaeroidinellopsis subdehiscens* and *S. seminulina* seem to be indicative of foraminiferal Zone N15 (10–10.5 Ma). The core catchers of Cores 2 and 3 contain a similar fauna, but the planktonic foraminifers in 558-3,CC show signs of fragmentation. The core catcher of Core 4, which also shows fragmentation and/or dissolution, is assigned to lower Zone N15/upper N14 because of the presence of very abundant *Globigerina nepenthes*,which makes its first appearance at approximately 12 Ma.

Miocene (middle)

The core catcher of Core 5, Zone N14, is significant in the marked increase in numbers of *Globoquadrina dehiscens* and *G. advena* and for the interesting tiny spherical to flattened spherical calcareous forms found in the finest fractions. These forms probably belong to the *incertae sedis Bolboforma*, originally described from the Oligocene and Miocene of northwestern Germany by Daniels and Spiegler in 1974. Since then the forms have been recorded from Miocene sediments drilled during DSDP Legs 35, 48, and 80 (Rögl and Hochuli, 1976; Murray, 1979; and Graciansky, Poag, et al., in press, respectively). In these reports they have been referred to as cysts or reproductive bodies of an unknown algae, and it has been suggested, because the species described have distinct stratigraphic ranges, that they may be regional markers in deep-sea sediments (see Echols, this volume).

The core catcher of Core 6, which is older than 12 Ma, shows considerable fragmentation of the planktonic forms and, because of the selective dissolution, a high proportion of large, well-preserved diverse benthic foraminifers. The rare specimens of *Globigerina nepenthes* present are attributed to uphole contamination. In 558-7,CC, planktonic forms are common and moderately well preserved. *Sphaeroidinellopsis seminulina* and *S. subdehiscens* are the dominant forms in the assemblage. This sample is assigned to the middle Miocene Zone N13. The fauna in 558-8,CC shows some fragmentation and overgrowths on the globorotalid forms. The core catcher of Core 9 has a fairly abundant but fragmented fauna. *Globorotalia peripheroronda*, which becomes extinct around 14+ Ma, is first encountered in this sample. *Orbulina universa* and *O. suturalis* are also present in fair numbers, indicating an age older than 14 Ma and less than 16 Ma. This sample is assigned to Zone N11. The core catchers of Cores 10 and 11 are also middle Miocene but are heavily contaminated with Pleistocene and Pliocene material. In 558-12,CC, foraminifers are common but fractured. *G. peripheroronda, S. subdehiscens*, and *S. seminulina* are common, and *Globigerinoides sicanus* is rare.

Miocene (lower)

The core catcher of Core 13 is assigned to the foraminiferal Zone N8, upper part of the lower Miocene. In this sample *Globigerinoides sicanus, Globoquadrina dehiscens*, and *Globigerinoides trilobus* are common and *Orbulina* species are absent. In this sample the siliceous element is apparent; radiolarians, diatoms, and sponge spicules are very abundant and diverse. The core catcher of Core 14, lower Miocene, contains abundant and well-preserved *Globoquadrina dehiscens* and globorotalid forms, such as *Globorotalia praemenardii* and *G. praescitula*.

The core catcher of Cores 15 and 16 are also lower Miocene. In the larger fraction these samples contain very abundant *Globoquadrina dehiscens*, and in the finer fractions abundant *Catapsydrax* and *Globigerinoides*. The core catcher of Core 17 is assigned to Zone N4 based on the assemblage of *Catapsydrax dissimilis, Globorotalia kugleri, Globoquadrina dehiscens*, and *Globigerina tripartita*.

Oligocene (upper)

The core catchers of Cores 18 and 19 are considered uppermost Oligocene. The core catcher of Core 18, although contaminated with Pliocene-Pleistocene material, does contain abundant *Globigerina tripartita, G. venezuelana*, and *Catapsydrax dissimilis*. The core catcher of Core 19 also contains these forms in abundance along with *Globoquadrina baroemoenensis* (= *dehiscens* of some authors), *Globigerina gortanii* (*Catapsydrax* of some authors), and rare *Globorotalia opima*. Very large specimens of *C. dissimilis* have been used, where other markers are missing, for the Oligocene assignment (the *Globorotalia opima opima* Zone). The core catcher of Core 19 is assigned to N2/P21 *G. opima opima* Zone.

The core catchers of Cores 20 and 21 have essentially the same abundant well-preserved fauna, whereas 558-22,CC and 558-23,CC have in addition abundant well-developed *Chiloguembelina cubensis, Globorotaloides suteri, Globigerina praebulloides*, and *Globorotalia opima nana*. This assemblage is assigned to the lower part of P21, or upper part of P20.

Oligocene (lower)

The core catchers of Cores 24 and 25 have a similar fauna with abundant *Chiloguembelina cubensis* and in addition, abundant *Pseudohastigerina* sp. These samples are assigned to the zonal interval P20/P19.

The core catcher of Core 26 contains abundant *Pseudohastigerina* sp., planispirally coiled specimens common in the lower Oligocene, and a similar fauna to that found in the preceding cores. Although this sample is not particularly diagnostic, it is tentatively assigned to P19.

Of interest in this sample is the fact that the foraminifers show some destruction, and dolomite rhombs are growing in and on the foraminiferal tests. The pan fraction of this sample consists of dolomite crystals and tiny corroded foraminifers.

Basalt was reached in 558-27,CC at approximately 408 m. The washed residue of a sample 1 m above the basalt contains nothing but dolomite rhombs, rare fragments of foraminifer shells, and manganese(?) nodules.

Age of basement based on the foraminifers is estimated at 32–35 Ma.

Hole 558A

Pleistocene

Sixteen HPC cores, to a total depth of 131.5 m, were drilled into Hole 558A. Core 558A-1,CC, a white nannofossil-foraminiferal ooze at 5 m, recovered Pleistocene sediments. Dominant elements of the foraminiferal fauna that are characteristic of Zones N22/N23 are *Globorotalia truncatulinoides, G. inflata, G. scitula, Globigerina bulloides, Globigerinoides ruber, G. obliquus, Neogloboquadrina pachyderma*, and *Orbulina universa*. Benthic foraminifers, ostracodes, and abundant beautiful diverse radiolarians are well preserved.

Sample 558A-2,CC (which is also Pleistocene) contains essentially the same fauna with an increase in the abundance of *Globorotalia truncatulinoides* and the addition of abundant *G. tumida, G. flexuosa*, and *G. crassaformis*.

Pliocene-Pleistocene

Core 558A-3,CC at 19.5 m is lower Pleistocene–uppermost Pliocene. Besides the fauna found above it contains abundant *Pulleniatina obliquiloculata*. Core 558A-4,CC is considered uppermost Pliocene (N21) and is characterized by a reduction in numbers of Pleistocene species and by the appearance of the gradational forms in the *Globorotalia truncatulinoides* lineage (i.e., *G. ronda* and *G. tosaensis*). The core catchers of Cores 5 and 6 are also upper Pliocene (N21). *G. truncatulinoides* is very rare in 558A-5,CC and absent from 558A-6,CC.

Pliocene (lower)

The core catchers of Cores 7 and 8 contain foraminifers indicative of the lower Pliocene (N19). (Zone N20 of Blow, 1969, if it exists, was not recognized in this hole.) Both samples have very abundant, well-preserved foraminifers in a white nannofossil-foraminiferal ooze. The core catcher of Core 7 has very abundant and large *Orbulina* species, abundant *Globorotalia crassaformis* (*crassula*), *G. ronda, Globigerinoides conglobata, G. sacculifer*, and pink *G. ruber*. The core catcher of Core 8 contains essentially the same fauna in different proportions and in addition large well-preserved *Globorotalia pertenuis*. The fauna indicates a warm-temperate climate.

Samples from 558A-9,CC are also assigned to Zone N19; but the fauna indicates a slightly older age. As a matter of fact, reexamination of the core catcher seems to indicate that the Miocene/Pliocene boundary may have been penetrated in this section between 558A-9,CC and 558A-10-1.

Therefore, until detailed zonation is complete, 558A-10,CC and 558A-11,CC are tentatively assigned to the lowermost Pliocene–uppermost Miocene.

Miocene (upper)

The core catchers of Cores 12 through 15 are upper Miocene and are assigned to the N17 foraminiferal zone. Zone N18 is either missing from the section or just not apparent in the core catcher material. Further study of the sections may resolve this question. The planktonic fauna in the core catchers of Cores 12 through 14 show fracturing and/or dissolution in all size fractions, and the forms are considerably smaller in size than the preceding sample. This may be more apparent than real and due to the fact that the larger forms are fractured. The core catcher of Core 15 contains very abundant *Globigerina nepenthes* and may be representative of the lower part of N17.

The core catcher of Core 16 at 131.5 m, the last HPC core recovered from Hole 558A, contains a well-preserved, diverse, robust fauna of abundant *G. nepenthes, Sphaeroidinellopsis seminulina, S. subdehiscens*, large *G. bulloides* (*praebulloides*?), *G. atlantica*, and *Orbulina*. This sample is assigned to N16 and may be dated at approximately 8 Ma+.

Biostratigraphic overlap with Hole 558 was not accomplished (Fig. 6).

SEDIMENT ACCUMULATION RATES

Sediment accumulation rates are plotted from foraminiferal and nannofossil biostratigraphic zone determinations from core catcher samples. Because preliminary age designations show some differences between nannofossil and foraminiferal dates, we have plotted the age ranges at each core catcher depth (Fig. 7) and have calculated an average sediment accumulation rate for each stratigraphic interval, based on the boundaries determined from nannofossils and foraminifers respectively (Fig. 7; Table 3).

The changes in sediment accumulation rates correspond approximately with stratigraphic boundaries. The most obvious change in sediment accumulation rate (from 16.6–26.2 m/Ma to 4.7–5.8 m/Ma) near the top of the lower Miocene corresponds to the boundary of Lithologic Units 1 and 2. This boundary is defined by a downhole decrease in carbonate content and an increase in the clay content. In the transition zone between the two lithologic units (approximately 277 to 304 m), we calculated a sediment accumulation rate of 7 to 9 m/Ma.

The causes of the quite abrupt decrease in sediment accumulation rate and carbonate content (to less than 50%) were discussed extensively on board ship but no conclusions were reached. The following are possible factors that were considered. (1) Dissolution may account for only part of the reduction. Preservation of the nannofossils is only moderate throughout the interval from the top of the lower Miocene to the base of the sediment section, although the site has probably been above the calcite compensation depth (CCD) throughout its history. (Backtrack curves for this area in the vicinity of the Azores Triple Junction have greater uncertainty.) Dissolution resulting from characteristics of the Oligocene to early Miocene water mass is also a possibility. (2) Changes in carbonate productivity may have some affect. (3) Possibly, the carbonate underwent some dissolution and some proportion of the nannofossils may have been "winnowed" away by bottom water movement, reworking, and bioturbation, leaving reduced nannofossil percentages and increasing clay and foraminiferal percentages. The irregular basement topography and the fact that the site is situated on a basement high could well be the key cause. Similar problems have been discussed by Berger and von Rad (1972).

In the upper portion of the hole, above the lower Pliocene hiatus, the upper Pliocene has an extremely high sediment accumulation rate (40.8 m/Ma). This high rate may correspond to increased productivity of the surface waters. As shown in Figure 5, this same interval shows an increase in siliceous microfossils content. The presence of siliceous microfossils is used as an indicator of surface water productivity.

PORE WATER CHEMISTRY

The results of the interstitial water chemistry analysis for Hole 558 and Hole 558A are shown in Figure 8 and tabulated in Table 4.

The values of pH, alkalinity, and chlorinity remain fairly constant with depth. The salinity values, on the other hand, are very erratic, which may reflect contamination by surface seawater (seawater is used as a drilling fluid in rotary coring).

Except for the sample taken immediately above the basalt, the calcium and magnesium concentration gradients are typical for calcareous pelagic sediments overlying basalt; that is, the pore waters are enriched in calcium and depleted in magnesium. However, the pore waters sampled immediately above the basalts are just the opposite, being depleted in calcium and enriched in magnesium. The possible cause for these anomalous values could be the result of seawater contamination, but note that this pore water sample was taken from dolomitic (authigenic, 20%) nannofossil chalk.

IGNEOUS PETROLOGY AND GEOCHEMISTRY

Igneous rocks, consisting mainly of pillow basalts and varying amounts of interpillow breccia (hyaloclastite limestone breccia) occur below 408 m sub-bottom depth throughout the drilled basement section. Two thin, massive basalt flows were encountered within and above the pillow layers. Serpentinite rocks, initially moderately altered grading down through fresh serpentinite to highly sheared serpentinite mylonite, were drilled from 520 m

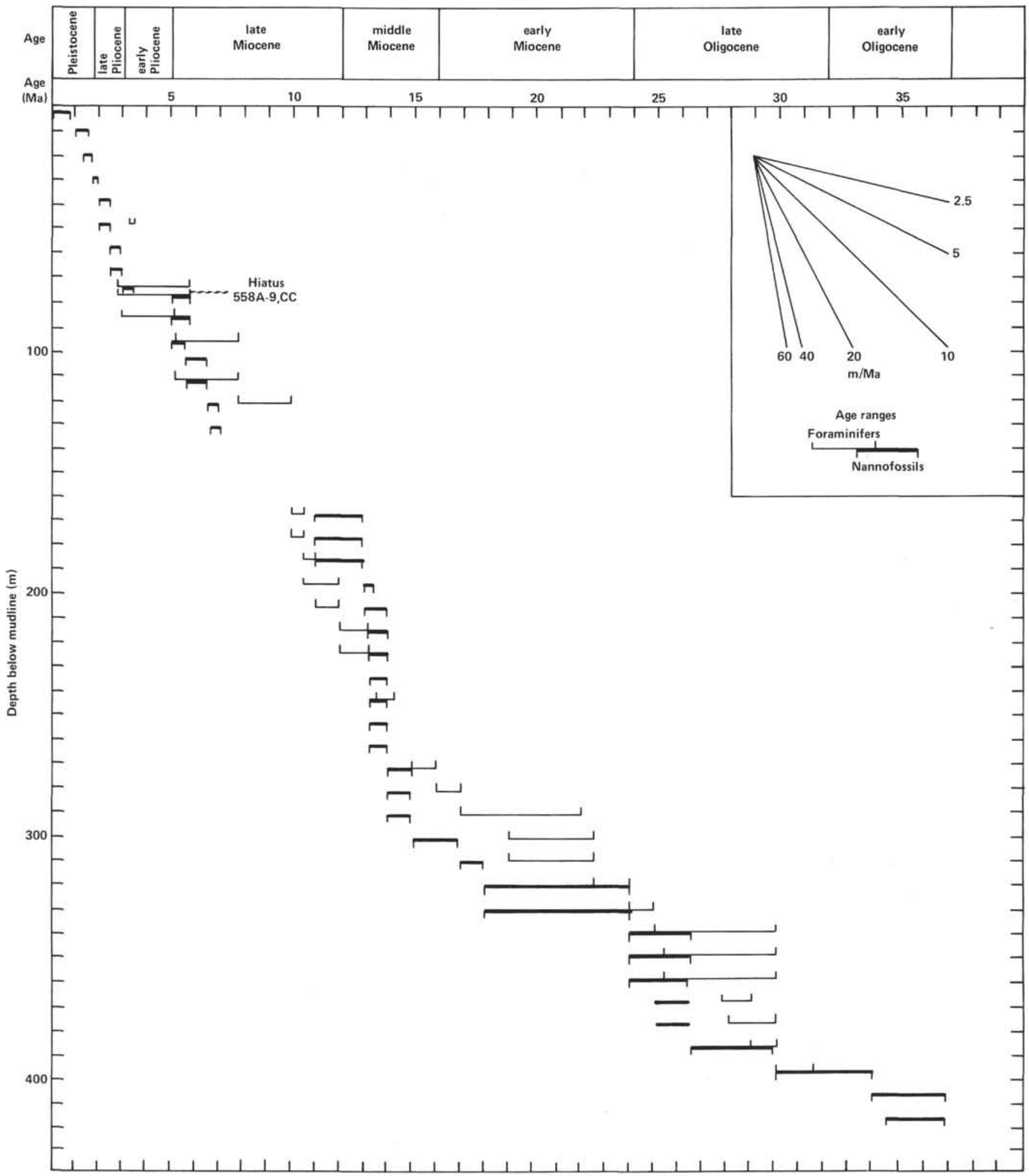

Figure 7. Sediment accumulation rates, Site 558.

Table 3. Sediment accumulation rates.

Stratigraphic unit	Age (Ma)	Nannofossils Depth (m)	Nannofossils Rate (m/Ma)	Foraminifers Depth (m)	Foraminifers Rate (m/Ma)
Pleistocene	1.8	0-18	10.0		
upper Pliocene	1.8-3	18-67	40.8		
lower Pliocene	3-5	67-74			
		Hiatus			
upper Miocene	5-12	74-186	16	86-205	17
middle Miocene	12-16	186-291	26.2	205-272	16.7
lower Miocene	16-24	291-329	4.7	272-319	5.8
upper Oligocene	24-32	329-386	7.1	319-395	9.5
lower Oligocene	32-37	386-414	5.6		

to the end of drilling at 561.5 m. Eleven lithologic units and six chemical groups have been identified in the basement at Site 558 (Units 3-13, Figs. 9 and 10).

Lithologic Units

Unit 3 (408-414.9 m)

The first igneous rock unit, occurring below sedimentary Units 1 and 2 is a moderately altered, weathered, fine-grained aphyric massive basalt flow. Unit 3 has been interpreted as a massive flow because it lacks glass or other evidence of internal cooling margins. Variolitic basalt is observed in the upper 40 cm of this unit. The size

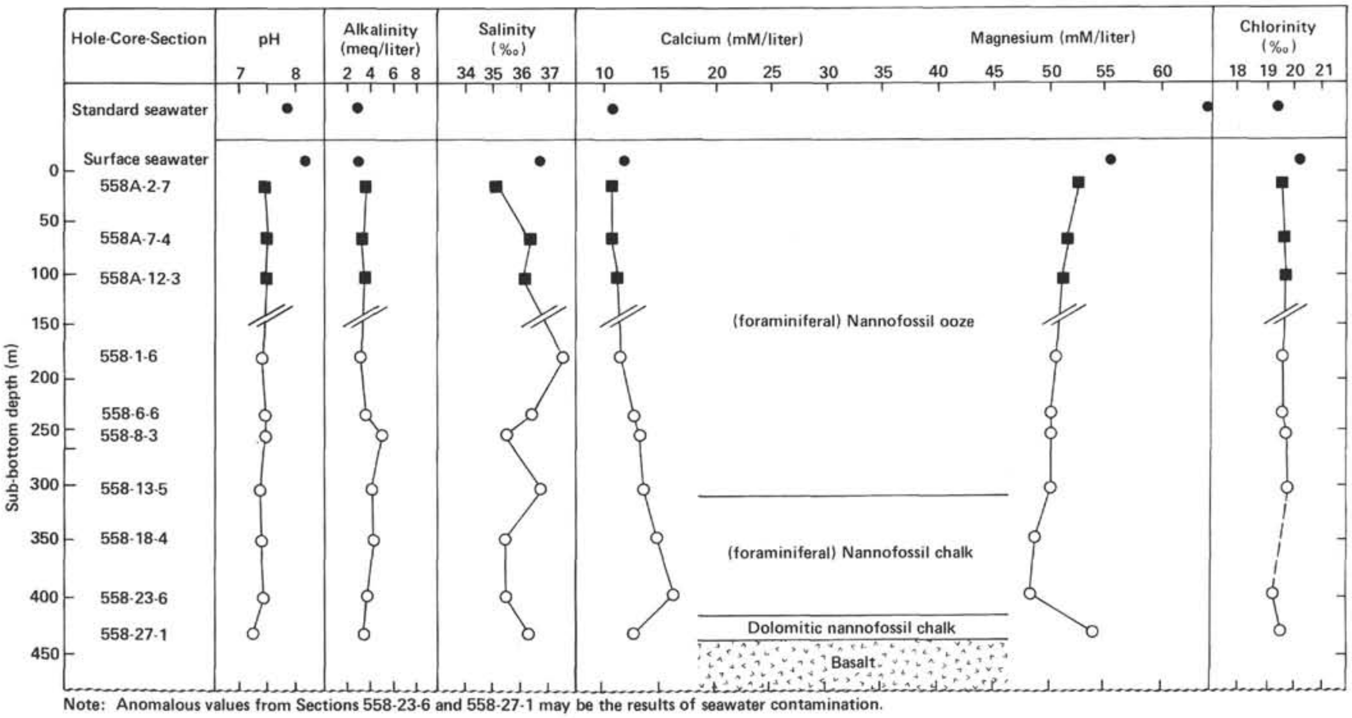

Figure 8. Pore water chemistry water profile, Site 558. Hole 558 results are open circles; Hole 558A, squares.

Table 4. Pore water chemistry results, Site 558.

Core-Section (interval in cm)	Sub-bottom depth (m)	pH	Alkalinity (meq/liter)	Salinity (‰)	Calcium (mM/liter)	Magnesium (mM/liter)	Chlorinity (‰)
Hole 588A							
2-7, 12-19	10.0	7.43	3.47	35.1	10.67	52.16	19.55
7-4, 144-150	56.0	7.44	3.19	36.3	10.67	51.40	19.62
12-3, 143-150	92.0	7.42	3.20	36.1	11.02	51.05	19.65
Hole 558							
1-6, 144-150	167.5	7.36	2.99	37.6	11.00	50.71	19.48
6-6, 140-150	215.0	7.43	3.50	36.4	12.13	49.99	19.41
8-3, 110-120	230.0	7.42	4.79	35.3	12.60	50.05	19.58
13-5, 144-150	280.0	7.31	3.92	36.8	13.39	50.15	19.62
18-4, 110-120	325.0	7.34	4.03	35.3	14.08	48.28	
23-6, 140-150	376.5	7.39	3.27	35.3	15.20	47.81	19.04
27-1, 140-150	411.0	7.13	3.00	36.2	12.09	53.27	19.31

Note: The anomalous values from Sections 558-23-6 and 558-27-1 may be the results of seawater contamination.

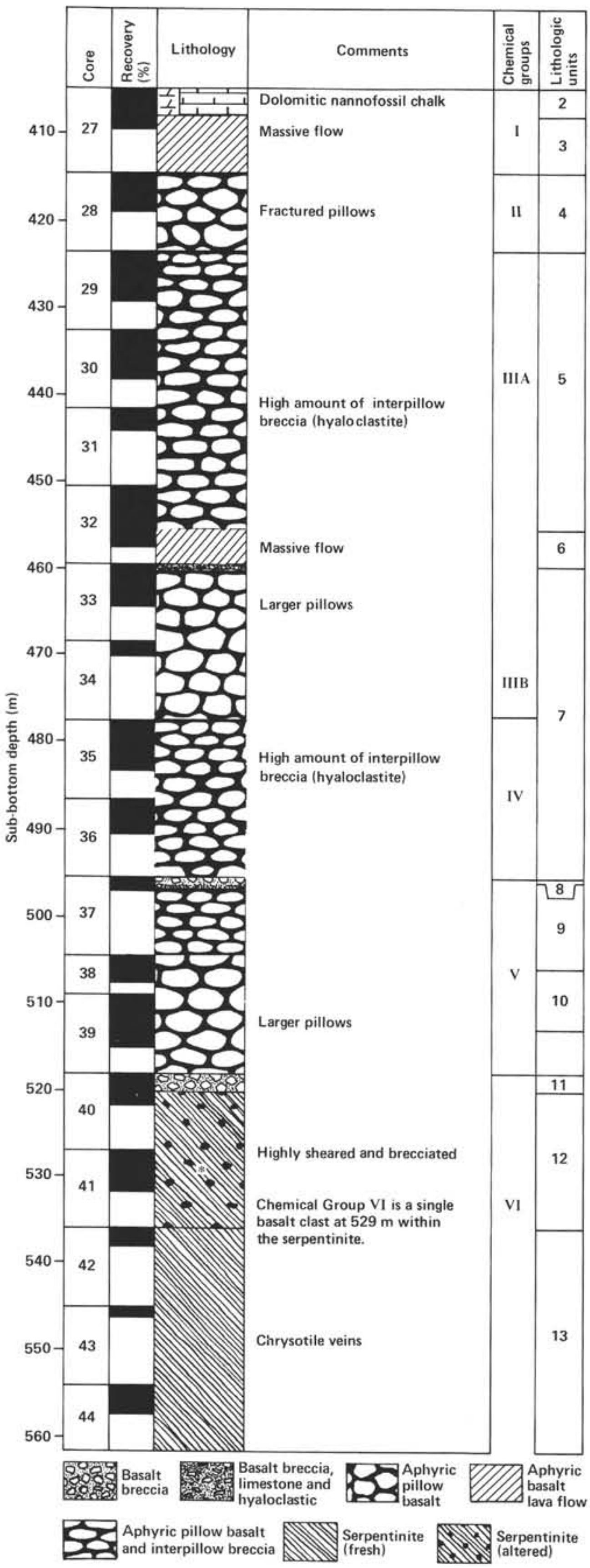

Figure 9. Basement lithology column, Hole 558. See Explanatory Notes (this volume) for lithology symbols.

of the varioles increases downward, ranging from 1 to 6 mm in diameter.

Unit 4 (414.9–423.5 m)

This unit consists of fine-grained aphyric basalt pillows, which are sometimes separated by multiple chilled glass margins. It is overlain by a thin hyaloclastite layer containing flat, angular pieces of glass altered to palagonite at their rims and aligned parallel to one another within a limestone matrix. The whole pillow sequence is highly fractured and contains strongly weathered zones close to the fractures. The remainder of the rock appears fresh to slightly weathered. Pillow thickness, about 60 cm in the upper part of the unit, increases slightly towards the bottom.

Unit 5 (423.5–455.5 m)

This unit consists of approximately 32 m of aphyric basalt pillows with abundant interpillow breccia. The fine-grained pillow interiors appear to be fresh to moderately altered and grade outwards through an altered variolitic zone to fresh aphanitic basalt close to cooling margins. Basalt glass usually occurs as a rind around the pillows. Interpillow hyaloclastite breccias consist of glass pieces with minor basalt clasts in a limestone matrix or calcite cement. Glass clasts smaller than 5 mm are mostly completely altered to palagonite, whereas the larger clasts are only rimmed by alteration products. Roughly 30 pillows were recovered in this unit, ranging in drilled thickness from about 30 cm to approximately 1 m.

Unit 6 (455.5–459.5 m)

Unit 6 consists of fine-grained aphyric massive basalt. A vertical fracture filled with calcite extends along the length of the cored section. Weathered areas extend 0.5 cm on either side of the fracture. Vesicles are rare; they are small (less than 2 mm), round, and clay filled.

Unit 7 (459.5–495.5 m)

This unit strongly resembles Unit 5. It consists of about 36 m of fine-grained aphyric basalt pillows, nearly all of which are separated by fresh glass margins. The amount of interpillow breccia, although less than in Unit 5, increases down the unit. Altered variolitic transition zones commonly separate fresh or moderately altered, fine-grained pillow interiors from fresh aphanitic to glassy outer zones. Calcite-filled veinlets and fractures occur throughout this unit.

Unit 8 (495.5–496.2 m)

This 70-cm-thick unit consists mainly of limestone with interbedded altered basalt breccia and hyaloclastite layers. Smaller clasts (less than 1 cm) are mostly altered to palagonite, whereas the larger clasts are fresh with narrow palagonite rims. The limestone contains a dendritic pattern of black oxides. In places, cavities are filled with calcite cement.

Unit 9 (496.2–505.0 m)

Unit 9 consists of fresh to moderately altered fine-grained aphyric basalt, occurring as pillows and interpil-

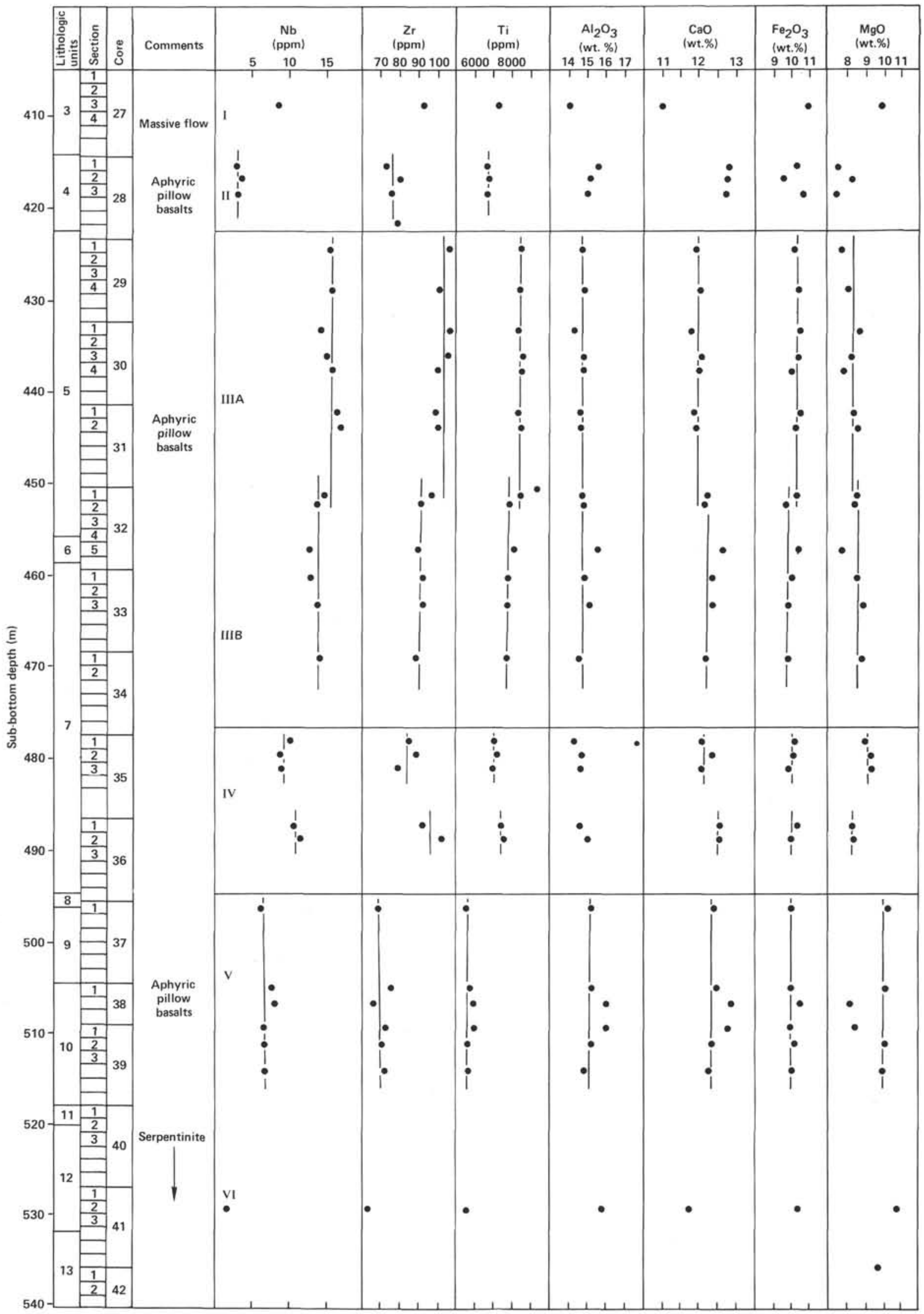

Figure 10. Downhole variations in chemical abundances, Hole 558. Chemical groups are designated by Roman numerals.

low breccia. Clasts of glass derived from pillow margins, aphanitic basalt, and variolitic basalt are common in the breccia. The majority of glass shards are approximately 2 to 10 mm long and are slightly altered to palagonite.

Unit 10 (505.0–518.0 m)

Unit 10 consists of moderately altered fine-grained aphyric basalt forming large pillows. Pillow rims are marked by a gradation from fine-grained aphyric basalt through variolitic basalt to aphanitic basalt. The drilled thickness of the pillows ranges from a few tens of centimeters to about 1.5 m; most pillows are less than 80 cm. Clay-filled or calcite-filled fractures and calcite veinlets are common throughout the section.

Unit 11 (518.0–520.0 m)

This unit is a basalt breccia composed of angular to subrounded aphyric, fine-grained to aphanitic basalt clasts. Clast size ranges from a few millimeters to a few centimeters. The matrix is mainly limestone accompanied by some sparry calcite cement.

Unit 12 (520.0–531.5 m)

Unit 12 consists of brown altered serpentinite and serpentinite breccia (often described as sheared gabbro in visual core descriptions) and mylonite with minor, less strongly serpentinized, anorthosite veins. The serpentinite is highly altered gabbro with rare relict pyroxenes 1–5 mm in size. The serpentinite breccia consists of clasts of serpentinite in a matrix of clay minerals, talc, and additional serpentine. The clasts range in size from approximately 1 mm to several centimeters. Two meters above the bottom of Unit 12, the mylonite zone contains angular, moderately altered basalt clasts, including one large basalt clast at 529.9 m.

Unit 13 (531.5–561.5 m)

Unit 13 is composed of strongly sheared blue green serpentinite mylonite containing clasts of serpentinite up to 1 m in drilled thickness. Serpentinite clasts are dark green to black, and weakly to moderately sheared, with sinuous, white, chrysotile veinlets varying in abundance from 2–20% and ranging from 0.1 to 20 mm in thickness.

Petrographic and Chemical Groups

Basalts from Site 558 can be divided into six groups on the basis of chemical analysis (Tables 5 and 6). Chemical group boundaries do not always coincide with lithologic unit boundaries described in the previous section. Samples from each chemical group are also petrographically similar regardless of lithologic unit, but not all groups are petrographically distinct (Groups I, IV, and V are very similar).

All basalts from this site are aphyric and few are holocrystalline; the majority of samples examined display intersertal textures, with more glass-rich textures occurring closer to pillow margins. Weathering is pervasive throughout Site 558; most samples show at least some brownish discoloration in hand specimen, and orange brown iron hydroxides are present in varying amounts in virtually all thin sections. Brown discoloration is strongly developed in variolitic zones throughout the hole.

Table 5. Average analyses for the six chemical groups from Hole 558.

Chemical group	I	II	III	IV	V	VI
N	1	3	13	5	6	1
Major elements (wt.%)						
SiO_2	50.67	50.86	50.70	50.19	49.37	48.71
TiO_2	1.22	1.12	1.38	1.22	0.96	0.92
Al_2O_3	14.10	15.11	14.82	14.65	15.49	15.81
Fe_2O_3	10.92	10.08	10.17	10.98	10.17	10.73
MnO	0.16	0.15	0.15	0.16	0.16	0.16
MgO	9.87	7.69	8.33	8.90	9.48	10.55
CaO	10.55	12.23	11.64	11.90	12.06	11.56
K_2O	0.18	0.18	0.30	0.30	0.20	0.10
P_2O_5	0.14	0.12	0.18	0.13	0.12	0.07
Trace elements (ppm)						
Ti	7320	6720	8280	7308	5780	5520
V	207	255	275	266	224	194
Sr	128	92	175	144	115	107
Y	27.0	29.7	28.7	28.1	22.9	23.0
Zr	83	66	88	80	61	51
Nb	8.6	3.2	14.8	10.5	7.3	2.0
Mg′	67	63	65	65	68	69
Al_2O_3/TiO_2	11.6	13.5	10.8	12.0	16.1	17.2
Ti/Zr	88	102	94	92	96	108

Note: N is the number of samples on which the mean is based. Mg′ is the atomic ratio of $100 \times Mg/(Mg + Fe^{2+})$, calculated using an assumed Fe_2O_3/FeO ratio of 0.15. Averages are calculated from data listed in Table 6.

Twenty-eight samples from Site 558 were analyzed for major and trace elements. The data are shown in Tables 5 and 6, and in Figure 10, depth is plotted versus each of the following elements: Zr, TiO_2, Al_2O_3, CaO, Fe_2O_3, and MgO.

Chemical Group I is defined by a single sample from Section 558-27-3. It is clear from Table 5 and Figure 10 that this sample has a unique chemistry compared to the other chemical groups. The CaO content of this sample (10.7 wt.%) is very low compared to that of the other groups.

Chemical Group IV consists of five samples from Cores 558-35 and 558-36. There may be a minor subdivision in this group between the samples from Cores 558-35 and 558-36. The two samples from Core 558-36 have lower MgO and Mg-numbers than Core 558-35 samples, and higher concentrations of TiO_2, Zr, and Nb. As a group, however, the Zr/Nb ratio is consistent at values of 7–8.3. This is greater than the Zr/Nb ratio value exhibited by chemical Group III but less than for Groups I and II, reflecting the slightly enriched nature of this group, which shows up on the extended Coryell-Masuda diagram (Fig. 11).

Chemical Group V consists of six analyzed samples from Cores 558-37 to 558-39. In terms of most of the major and trace elements, this group is chemically homogeneous with the apparent exception of the two samples from Sections 558-38-2, and 558-39-1, which have low MgO contents (8.2–8.4%) and Mg numbers (63–65) compared to the other basalts in this group (MgO, 10%; Mg-number, 69). Basalts of this group display relatively enriched Coryell-Masuda patterns, similar to those of Groups I and IV (Fig. 11), but with somewhat lower ab-

Table 6. Analyses of major elements (wt.%) and trace elements (ppm) from Hole 558 basalts.

Core-Section (interval in cm) (piece number)	Sub-bottom depth (m)	Chemical group	SiO_2	TiO_2	Al_2O_3	Fe_2O_3	MnO	MgO	CaO	K_2O	P_2O_5	Total	Mg'	Ti	V	Sr	Y	Zr	Nb
27-3, 74-77 (8)	408.9	I	50.67	1.22	14.10	10.92	0.16	9.87	10.55	0.18	0.14	97.81	67	7320	207	128	27.0	83	8.6
28-1, 91-94 (9)	415.4		50.95	1.12	15.14	10.22	0.15	7.51	12.28	0.21	0.12	97.70	62	6720	256	93	29.3	63	2.8
28-2, 121-125 (15)	417.3	II	51.00	1.13	15.15	9.48	0.16	8.22	12.24	0.11	0.13	97.62	66	6780	257	96	29.7	69	3.5
28-3, 60-64 (7)	418.2		50.62	1.11	15.03	10.55	0.15	7.35	12.18	0.21	0.10	97.30	61	6660	253	88	30.2	65	3.2
29-1, 120-125 (7D)	424.8		52.17	1.43	14.76	10.12	0.14	7.68	11.42	0.43	0.19	98.34	63	8580	277	176	30.2	97	15.3
29-4, 71-76 (6)	428.7		50.88	1.41	14.83	10.37	0.15	8.08	11.53	0.39	0.21	97.85	64	8460	273	171	29.6	91	15.7
30-1, 60-64 (8A)	433.1		50.30	1.39	14.34	10.47	0.18	8.66	11.30	0.26	0.18	97.08	65	8340	281	165	29.8	97	14.3
30-3, 99-103 (10B)	436.5		50.28	1.43	14.84	10.35	0.15	8.31	11.60	0.34	0.19	97.49	64	8580	278	173	30.2	96	15.2
30-4, 55-59 (4C)	437.5		51.57	1.42	14.77	10.07	0.14	7.78	11.50	0.23	0.20	97.68	63	8520	268	172	28.8	90	16.0
31-1, 62-64 (5C)	442.2		51.07	1.39	14.61	10.44	0.15	8.32	11.37	0.29	0.19	97.83	64	8340	277	174	31.1	89	16.4
31-2, 128-130 (9)	444.3	III	51.27	1.41	14.64	10.21	0.15	8.52	11.44	0.28	0.19	98.11	65	8460	280	172	28.9	90	17.2
32-1, 106-110 (8A)	451.5		50.33	1.42	14.76	10.28	0.15	8.49	11.74	0.35	0.19	97.71	65	8520	280	171	30.5	87	15.0
32-3, 63-67 (4C)	454.1		50.09	1.32	14.89	9.64	0.13	8.44	11.68	0.26	0.18	96.63	66	7920	274	173	26.2	81	13.9
32-5, 66-70 (2B)	456.2		49.73	1.36	15.68	10.39	0.15	7.81	12.31	0.30	0.19	97.92	63	8160	291	187	27.3	80	12.9
33-1, 77-80 (9A)	460.2		50.05	1.31	14.88	10.09	0.14	8.49	11.80	0.24	0.16	97.16	65	7860	267	180	28.0	82	13.0
33-3, 142-145 (9D)	463.9		50.70	1.30	15.12	9.87	0.14	8.94	11.90	0.28	0.17	98.42	67	7800	274	183	25.7	83	13.9
34-1, 34-38 (3B)	468.8		50.62	1.29	14.62	9.92	0.14	8.77	11.72	0.21	0.17	97.46	67	7740	255	177	26.5	79	14.2
35-1, 128-131 (11C)	478.8		50.24	1.19	14.37	10.29	0.16	9.06	11.65	0.33	0.16	97.45	66	7140	261	146	27.7	75	10.4
35-2, 97-102 (6A)	480.0		50.08	1.21	14.75	10.22	0.15	9.28	11.92	0.25	0.15	98.01	67	7260	273	146	26.5	79	9.3
35-3, 100-102 (8B)	481.6	IV	50.25	1.18	14.38	9.98	0.15	9.41	11.61	0.30	0.13	97.39	68	7080	250	141	26.6	69	9.4
36-1, 62-65 (5)	487.2		49.94	1.24	14.69	10.36	0.16	8.30	12.09	0.28	0.16	97.22	64	7440	284	139	29.9	83	11.5
36-2, 107-110 (5E)	489.1		50.45	1.27	15.06	10.07	0.16	8.43	12.21	0.33	0.17	98.15	65	7620	265	149	30.0	93	12.1
37-1, 137-141 (19A)	496.9		49.18	0.94	15.35	10.12	0.15	10.19	11.95	0.21	0.09	98.18	69	5640	243	113	22.7	58	6.4
38-1, 126-130 (16)	505.8		48.82	0.96	15.33	10.02	0.16	10.01	12.02	0.15	0.11	97.58	69	5760	222	113	22.5	65	7.8
38-2, 84-88 (5B)	506.8		49.85	1.00	16.02	10.55	0.16	8.17	12.42	0.20	0.13	98.50	63	6000	235	117	23.2	56	8.4
39-1, 83-87 (5G)	509.8	V	49.64	1.00	16.01	9.99	0.17	8.43	12.29	0.19	0.13	97.85	65	6000	223	115	23.7	62	6.9
39-2, 35-38 (3A)	510.9		49.77	0.94	15.27	10.21	0.17	10.10	11.87	0.22	0.12	98.67	69	5640	218	112	23.1	61	6.9
39-4, 131-135 (6)	514.8		48.97	0.94	14.93	10.11	0.15	9.95	11.79	0.20	0.11	97.15	69	5640	204	121	22.4	62	7.1
41-2, 143-146 (6F)	529.9	VI	48.71	0.92	15.81	10.73	0.16	10.55	11.56	0.10	0.07	98.61	69	5520	194	107	23.0	51	2.0

Note: Measurements were made on board using ignited samples. On-shore analyses have shown the loss on ignition to be less than 1%. The concentrations listed in the tables of compiled data (Appendix at the end of this volume) include volatile contents. Mg' is the atomic ratio of $100 \times Mg/(Mg + Fe^{2+})$, calculated using an assumed Fe_2O_3/FeO ratio of 0.15.

solute abundances. The variation of chemical composition between the higher and lower MgO members of Group V could possibly be explained by subtraction of a small proportion (few percent) of olivine.

Basalts of Groups I, IV, and V are composed of 30–40% hollow, elongate plagioclase laths up to 0.5 mm long, often arranged in parallel or slightly radiating bundles; different bundles have random orientations. Euhedral-shaped, diamond-shaped, lantern-shaped, or prism-shaped olivine (5–10%) ranges from completely altered (to green brown clay) to less than 50% altered with fresh, clear cores. The remainder of each rock is made up of about 20% granular clinopyroxene and 30–40% dark mesostasis. Depending on the degree to which each sample has crystallized, this mesostasis may be composed of fine granular of sheaflike clinopyroxene and dark brown devitrified glass in almost any proportion. Associated with the mesostasis is about 5% fine granular or skeletal magnetite. An unusual feature of some of the rocks in these groups is the presence, in plagioclase, of numerous, tiny dark brown octahedra of spinel.

Chemical Group II comprises the three analyzed samples from Core 558-28. In terms of both major and trace elements, this group is homogeneous, except for a higher MgO content (and consequently higher Mg-number) in the sample from Section 558-28-2. In comparison to Group I, the aphyric basalts of Group II are notably lower in TiO_2, MgO, Fe_2O_3, Sr, Zr, and Nb but have greater abundances of Al_2O_3 (Table 5 and Fig. 10). Although both Zr and Nb are lower in Group II basalts with respect to Group I, Nb is more strongly depleted than Zr, as is shown by the extended Coryell-Masuda plot for the Group II average in Figure 11.

Group II basalts are almost olivine free, containing at most 2–3% small diamond-shaped olivine euhedra. They contain 30–40% randomly oriented hollow plagioclase laths, 30–40% granular clinopyroxene, and 20–30% dark brown devitrified glass with approximately 5% skeletal magnetite.

Chemical Group III encompasses Lithologic Units 5, 6, and part of 7. Thirteen analyzed samples from Cores 558-28 to 558-34 compose chemical Group III, which has been subdivided into two homogeneous subgroups denoted IIIA and IIIB, encompassing, respectively, samples above and below Section 558-32-2 (Fig. 9).

Although there is no obvious lithologic or petrographic break between these subgroups, the chemical distinction is quite clear (Table 6 and Fig. 10): IIIB has lower TiO_2, Zr, and Nb and slightly greater Sr, Al_2O_3, and CaO. Both groups have similar Fe_2O_3, MgO, and, hence, Mg-numbers. Section 558-32-5 is slightly different from Group IIIB; there is a marked change in CaO, TiO_2, and MgO. The general chemical coherency of this group is demonstrated by the constant Zr/Nb ratio, which reflects the enriched nature of this group when plotted on an extended Coryell-Masuda diagram (Fig. 11). This contrasts markedly with the patterns exhibited by chemical Groups I and II.

Group III basalts contain unusually large amounts of olivine. Glassy rocks adjacent to pillow rims are characterized by up to 10% diamond-shaped and lantern-shaped microphenocrysts as well as abundant chains, branching aggregates, and other skeletal forms of olivine. Plagioclase is present in such samples only in variolites. More-crystalline members of this group contain as much as 20% olivine as small (less than 0.3 mm) diamond-shaped or prism-shaped euhedra, largely altered to clay or, in some cases, to colorless high birefringent aggregates of talc. In these rocks, plagioclase (25–30%) is subordinate to clinopyroxene (30–40%). Granular to skeletal magnetite is unusually abundant (about 10%).

Because these rocks contain twice the amount of olivine usually observed, a high Mg-number is predicted; this, however, is not the case here. The absolute amount of olivine is offset by a larger absolute amount of opaque minerals. This relative abundance of magnetite explains the small difference in MgO content between this and other less olivine-rich groups.

Finally, chemical Group VI consists of a single basalt clast from the serpentinite breccia of Unit 12 (Section 558-41-2). This sample is depleted on an extended Coryell-Masuda diagram (Fig. 11). It is quite different in nature and chemical composition from the depleted samples of chemical Group II (Table 6, Fig. 10).

Geochemistry

The normalized magmaphile element concentrations for the five chemical groups recognized in Site 558 are plotted in Figure 11. Depleted (Nb with respect to Zr), flat, and significantly enriched distributions in the most magmaphile elements within the same hole compose the major results and striking characteristics of Site 558.

Interpreting the Nb/Zr ratio, of the five chemical groups, in respect to the mantle source characteristics, leads to the conclusion that the basalts recovered from Site 558 have a complex origin. At least three different sources appear to have contributed to the basaltic layer. However, the relative enrichment or depletion of the most magmaphile elements (e.g., Nb) with respect to the least magmaphile elements (e.g., Zr) is a function of both the chemical "fingerprint" of the mantle source and of the extent and method of melting. Thus, onshore measurements of rare earth elements, Ta/La (or Nb/La) ratios and Pb, Sr, and Nd isotopic ratios are necessary before distinct mantle sources can be confirmed.

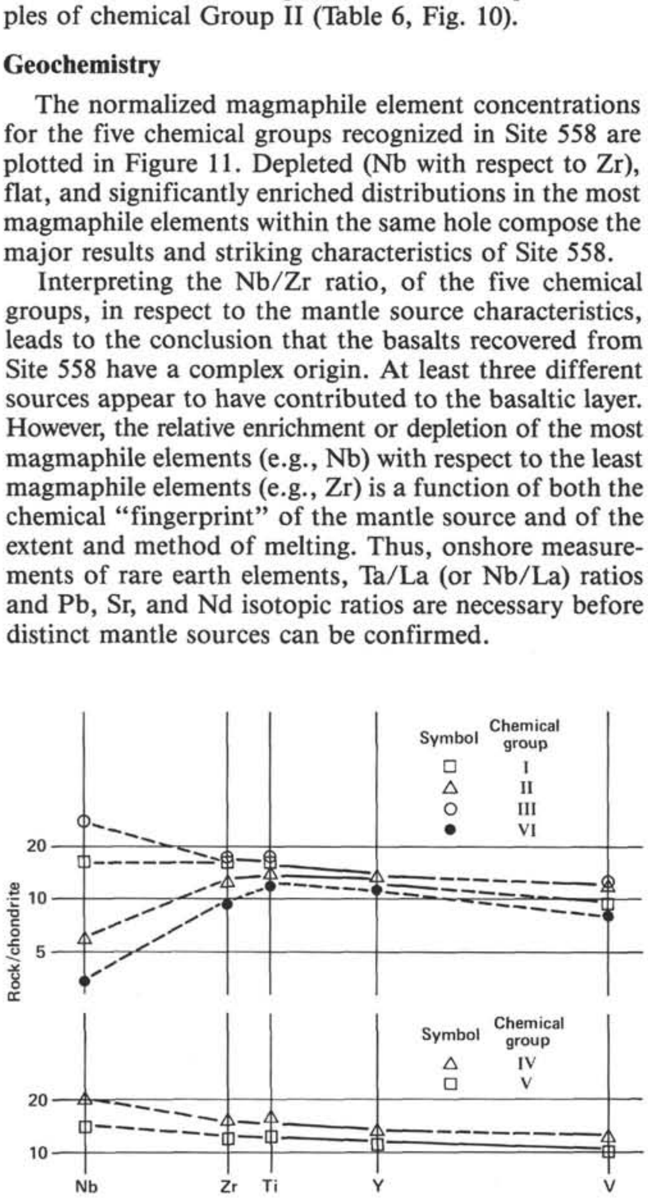

Figure 11. Extended Coryell-Masuda diagram for averages of chemical Groups I–VI, Hole 558.

In Figure 12 normalized Ta concentrations (which are the same as normalized Nb concentrations) are plotted against normalized La for basalts from a variety of localities. All analyses are from the laboratory of P. Sue of CNRS (Treuil et al., 1973).

In general, all samples presenting flat to enriched Coryell-Masuda diagrams have a chondritic $(Ta/La)_{ch}$ ratio (1, by definition) (e.g., Mid-Atlantic Ridge from Azores Triple Junction to Hayes Fracture Zone; Leg 37 and 49 samples from near the FAMOUS area; continental alkali basalt [El Azzouzi, 1981]; basalt from seamounts [Cambon et al, 1980]).

Samples with depleted patterns such as basalts from Site 395 at 22°N on the Mid-Atlantic Ridge and Site 483 on the East Pacific Rise have $(Ta/La)_{Ch}$ ratios close to 0.5. Exceptions to both generalizations do occur. Basalt from Site 409 on the Reykjanes Ridge have $(Ta/La)_{Ch}$ of 1 and slightly depleted patterns (Figs. 12 and 13), whereas basalts from Walvis Ridge (Fig. 12) and dolerite from Morocco (Figs. 12 and 14) have enriched patterns with $(Ta/La)_{Ch}$ of 0.5.

Chondritic $(Ta/La)_{Ch}$ ratios (1.0 by definition) are thought to reflect an initial property of the mantle and are characteristic of most alkalic and transitional basalts (Bougault, 1980). $(Ta/La)_{Ch}$ values of 0.5 may be characteristic of depleted mantle or they may be attributable to fractionation of Ta and La (Nb and La) despite the similarity of their physico-chemical properties (reflected by the constancy of these element ratios over a wide concentration range). Such fractionation could only result from very high degrees of partial melting or from specific melting processes such as dynamic melting (Langmuir et al., 1977) or step melting (Bougault et al., 1979).

In either case, it is clear that the range of extended Coryell-Masuda plots observed at Site 558 will be better understood when isotopic data are available; both extended Coryell-Masuda plots and isotopic data will contribute to the understanding of the variations of the Ta/La ratios and the cause of these variations.

Independently of the geodynamic-geochemical target of Leg 82 (to try to obtain a perspective in space and time of mantle heterogeneities), the results obtained at Site 558 are interesting from the purely fundamental point of view of geochemistry. Using these results in conjunction with isotopic data, we may be able to answer questions such as the following: (1) what are the relative contribution(s) of the "fingerprint" of mantle source(s), and (2) what is the effect of melting on the distribution of magmaphile elements, according to an extended Coryell-Masuda plot?

The relative contributions of mantle source and melting effects could not be resolved on board, but the extent of fractional crystallization and magma chamber processes can be determined. Within chemical Group V, low MgO samples from Sections 558-38-2, and 558-39-1, may be derived from the subgroup of the four remaining samples by removal of 5% olivine. However, major and minor element contents suggest that it is not possible for the different chemical units to be derived from one an-

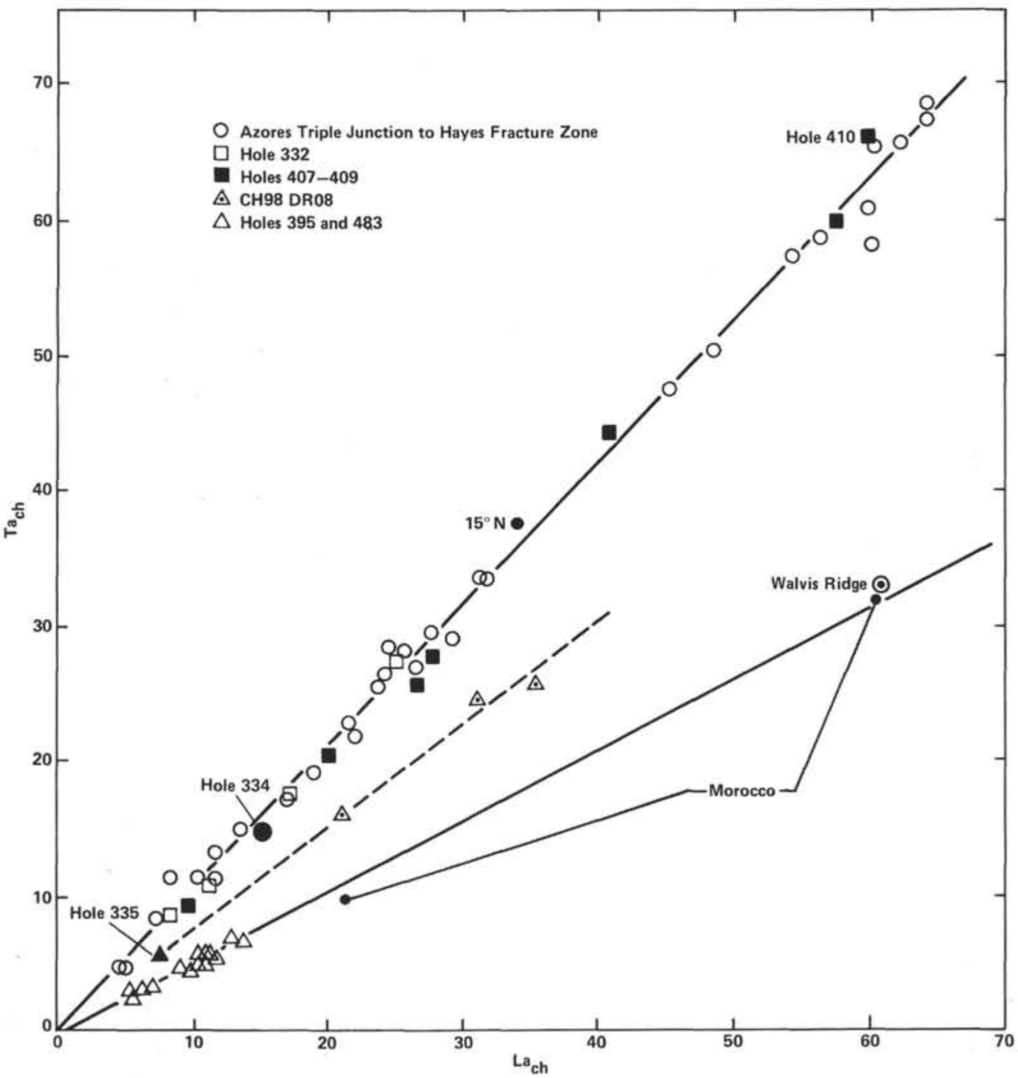

Figure 12. Plot of Ta versus La concentrations normalized to chondrites for basalts from various, worldwide locations.

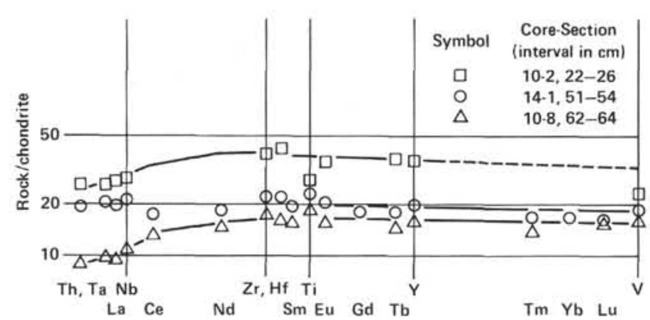

Figure 13. Extended Coryell-Masuda diagram for basalts from Hole 409.

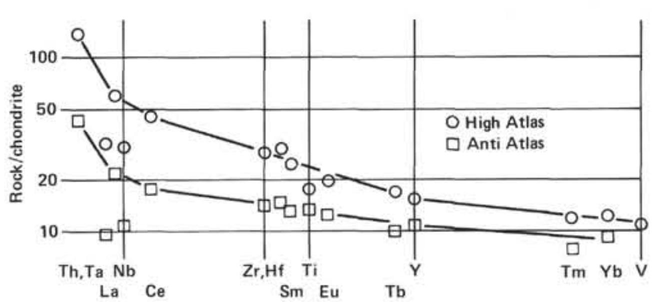

Figure 14. Extended Coryell-Masuda diagram for Moroccan dolerites (Bertrand et al., 1981).

other, solely by fractional crystallization. In addition, the large differences in their extended Coryell-Masuda plots make it highly unlikely that the parental liquids of the different units could have resided in the same magma chamber, or that magma mixing could account for the observed geochemistry. The results obtained at Site 558 fit much more easily with the hypothesis of magma batches from different short-lived magma reservoirs.

MAGNETICS

Basalt Paleomagnetism

After 158 m of sediments were washed down and 256.5 m of sediments were cored, 114 m of basalts were cored. Twenty-six minicores were collected from basalts in Cores 558-28 through 558-39. The intensity of natural remanent magnetization (NRM) and other paleomagnetic properties are given in Table 7. Samples from Sections 558-28-1, 558-28-3 and 558-29-2 are weakly magnetized compared to the samples from the rest of the cores. This may be the result of alteration of titanomagnetite or a different grain size of the same mineral. Demagnetization was not done on board so that additional properties could be studied on shore.

Based on NRM inclination values, two groups were identified. The samples with negative inclination are dominant and suggest that the site is located between Anomalies 13 and 15, whereas the samples with positive inclination suggest either a later time of intrusion or acquisition of secondary magnetization caused by the present magnetic field of the earth. However, some of the samples with positive inclination may not be *in situ;* they were collected between brecciated layers.

Inclination values are much shallower than the expected dipole inclination for the latitude of this site (37°46′); this suggests tectonic rotation since the acquisition of remanence.

Sediment Paleomagnetism-Magnetostratigraphy

We cored 256.5 m of sediments before hitting the basement basalts. Using small plastic cubes, we collected oriented samples at intervals of 25 cm. However, because of the varying degree of compactness of the sediments, some of the samples were collected at 40–50 cm intervals, and other samples were taken at intervals of 10–15 cm.

The samples from Cores 558-1 through 558-14 were very weakly magnetized (0.001–0.01 μG). Their intensity was very close to or even below the noise level (0.01 μG) of the Digico spinner magnetometer and the measurements were not reliable. Therefore, the samples from Cores 558-1 through 558-14 were collected for onshore studies at Lamont-Doherty Geological Observatory, where a cryogenic magnetometer is available.

The intensity and directions of NRM for samples from Core 558-15 through Section 558-27-2 were measured on board. Only 7 of 191 samples had reversed polarity. A few samples were selected for progressive alternating-field (AF) demagnetization to see if the remanence directions were stable or not. A typical result of AF demagnetization is shown in Figure 15. Most of the samples had a secondary component of magnetization caused by the present-day earth's magnetic field, but the secondary component is removed after AF demagnetization at 50–75 Oe. An AF of 100 Oe was selected as an optimum field to remove this secondary component of magnetization. Therefore, all samples from Core 558-15 through Section 558-27-2 were demagnetized at a single step of 100 Oe. The stable directions of inclination and corresponding polarities are plotted in Figure 16.

A brief look at the paleontologic ages assigned to sediments from these cores suggested that (1) the Oligocene/Miocene boundary was in Core 558-18, (2) Core 558-15 was older than 15 Ma, and (3) Section 558-25-2 was 34–35 Ma old (for details, see Sedimentology and Biostratigraphy section). Based on these observations, we compared the correlation of the observed magnetic polarity reversal sequence with the Magnetic Polarity Time Scale (MPTS) of Lowrie and Alvarez (1981). The long normal in Core 558-16 is correlated with Anomaly 6, the long reversal in the upper part of Core 558-19 with the reversal between Anomalies 6C and 7, the long normal at the top of Core 558-15 with Anomaly 5C, and the long reversal in Cores 558-25 and 558-26 with the long reversal between Anomalies 12 and 13. After this,

Table 7. Paleomagnetic properties, Hole 558.

Core-Section (interval in cm)	J_{NRM} ($\times 10^{-3}$ emu/cm^3)	Dec. NRM (°)	Inc. NRM (°)	χ ($\times 10^{-6}$ emu/cm^3 Oe)	Q (= $J_{NRM}/0.45\chi$)
28-1, 52–54	0.29	101.0	−10.2	53	12.07
28-3, 2–4	0.25	130.7	3.3	95	5.74
29-1, 126–128	2.65	240.0	−21.7	84	70.21
29-2, 124–126	0.76	325.9	52.4	71	23.70
29-3, 7–9	2.76	91.7	57.0	147	41.79
29-3, 101–103	2.74	72.6	−1.3	93	65.55
29-4, 3–5	4.17	355.1	−33.8	112	82.75
30-1, 72–79	3.80	357.3	−39.1	110	76.70
30-2, 12–14	1.22	81.1	−46.0	100	16.06
30-3, 81–83	2.25	189.7	−41.8	84	59.65
30-4, 65–67	2.96	206.2	−30.5	81	81.31
31-1, 56–58	3.26	270.8	−35.7	66	109.75
31-2, 97–99	4.87	271.2	38.9	76	141.83
32-1, 15–17	1.55	5.7	−35.3	65	52.81
32-3, 4–6	5.04	355.9	−40.1	105	106.76
32-4, 120–122	2.41	207.0	−24.5	90	59.40
32-5, 36–38	1.85	104.2	−43.3	80	51.32
33-1, 46–48	4.31	314.0	−32.0	84	113.93
33-2, 2–4	4.99	231.8	−28.2	95	116.70
33-3, 120–122	6.59	27.3	−34.4	126	116.27
34-1, 23–25	7.01	325.2	−28.7	266	58.58
38-2, 28–30	3.71	264.7	37.5	68	121.29
39-1, 127–129	2.28	14.9	−27.2	77	65.70
39-2, 15–17	4.28	278.1	−16.5	100	95.15

Note: J_{NRM} is the intensity of the natural remanent magnetization; Dec. is declination; Inc. = inclination; χ = susceptibility; Q = Königsberger ratio.

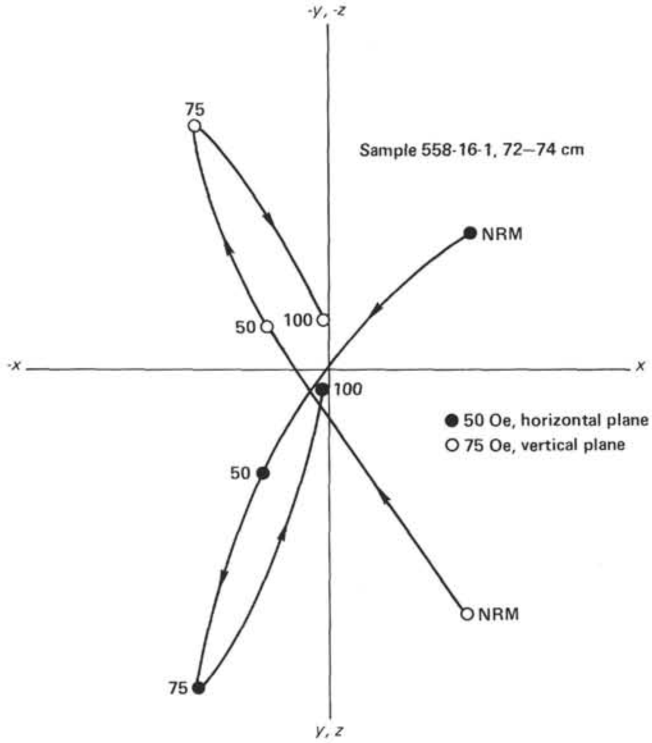

Figure 15. Vector diagram showing the results of alternating field demagnetization. NRM = natural remanent magnetization.

the rest of the correlation is checked and compared with the standard MPTS. The correlation chart given in Figure 16 suggests that an almost complete sequence of magnetic polarity reversals is recorded in these sediments and that a precise age can be assigned to the sedimentary sequence using magnetostratigraphic studies. See Khan and others (this volume) for the results of magnetostratigraphic studies for Cores 558-1 through 558-14 and for Hole 558A cores.

After the observed magnetic polarity reversal sequence was correlated with the standard MPTS, the sediment accumulation rate was calculated by plotting age versus sediment depth (Fig. 17). A very steady sediment accumulation rate of 0.47 cm/ky was calculated for Core 558-15 through Section 558-22-2, whereas a higher rate of 1.0 cm/ky was calculated for Sections 558-22-3 through 558-27-2. Although no drastic change is observed at this break, it does correspond to a slight change in lithology from CB5 (nannofossil chalk) to CB7 (nannofossil-foraminiferal chalk). For details, see Sedimentology and Biostratigraphy section. Based on the depth versus age curve of Figure 17, an age of 36 Ma is calculated for the basement basalt, which agrees with the location of this site between Magnetic Anomalies 13 and 15 (close to 13).

In conclusion, the sediments in Core 558-15 through 558-27-2 range in age from 16.2 to 36 Ma and record an almost complete sequence of magnetic polarity reversal of earth's magnetic field for this span of time. The sediment accumulation rate calculated for Sections 558-22-3 through 558-27-2 is twice the rate calculated for Core 558-15 through Section 558-22-2.

PHYSICAL PROPERTIES

Sediments

Combination of the cores from Holes 558 and 558A gives an almost continuously cored section with good recovery. Measurement of seismic velocity, density, and thermal conductivity was made systematically with all core sections being run through the continuous GRAPE system. The preliminary results are shown in Table 8 and Figure 18.

The density data are rather sparse in this report because of the difficulty of taking discrete undeformed samples from the soft sediments. When the continuous GRAPE data are processed, a complete record will be available. Data shown in Figure 18 are a combination of 2-minute GRAPE on rock chunks and cylinder samples, as well as some points from the continuous GRAPE analog records.

Velocity data above 330 m sub-bottom were measured on core halves in liners and are hence measured horizontally, parallel to any bedding traces. Below this depth, the rock was sufficiently lithified to be cut into discrete samples and measurements were made parallel to the core axis, normal to bedding. Because sediments of this type typically show velocity anisotropy of around 5%, we would expect values for sediments below 330 m to be systematically lower by this percentage. Such an offset is apparent in Figure 18. All measured velocities are low compared to those recorded by the Schlumberger sonic log (see Downhole Measurements section). This could be due either to drying of the cores to undersaturation by pore water before measurement, or to the removal of the cores from their *in situ* confining pressures. Because care was taken to sample core material as soon as possible after splitting, and the data are consistently lower than the downhole values, we deduce that the major factor in reducing sample velocity is release of confining pressure.

The thermal conductivity data were measured by the routine needle-probe technique and show an increase in conductivity with depth. Units used in Table 8 and Figure 18 are in mcal $cm^{-1}\ s^{-1}\ {}^{\circ}C^{-1}$. Accuracy of values is about $\pm 8\%$. One surprising feature of the conductivity measurements is their lack of dependence on the degree of deformation of the core. Because measurements were made on unsplit cores, occasionally, when the core was split, the measured volume was shown to be significantly deformed. Such positions are noted in the righthand column of Table 8. The data from these points are included in Figure 18 and do not show values significantly different from those of undeformed core, so are not separately identified on Figure 18.

Vane shear strength measurements were made on all sediments sampled down to 270 m sub-bottom, after which the state of lithification precluded measurements. Apart from showing an increase in shear strength with depth, and a high dependence on the state of deformation of the core, the data are unremarkable and are not plotted in Figure 18.

The variation of physical properties with depth shown in Figure 18 reveals only one major feature. There is a

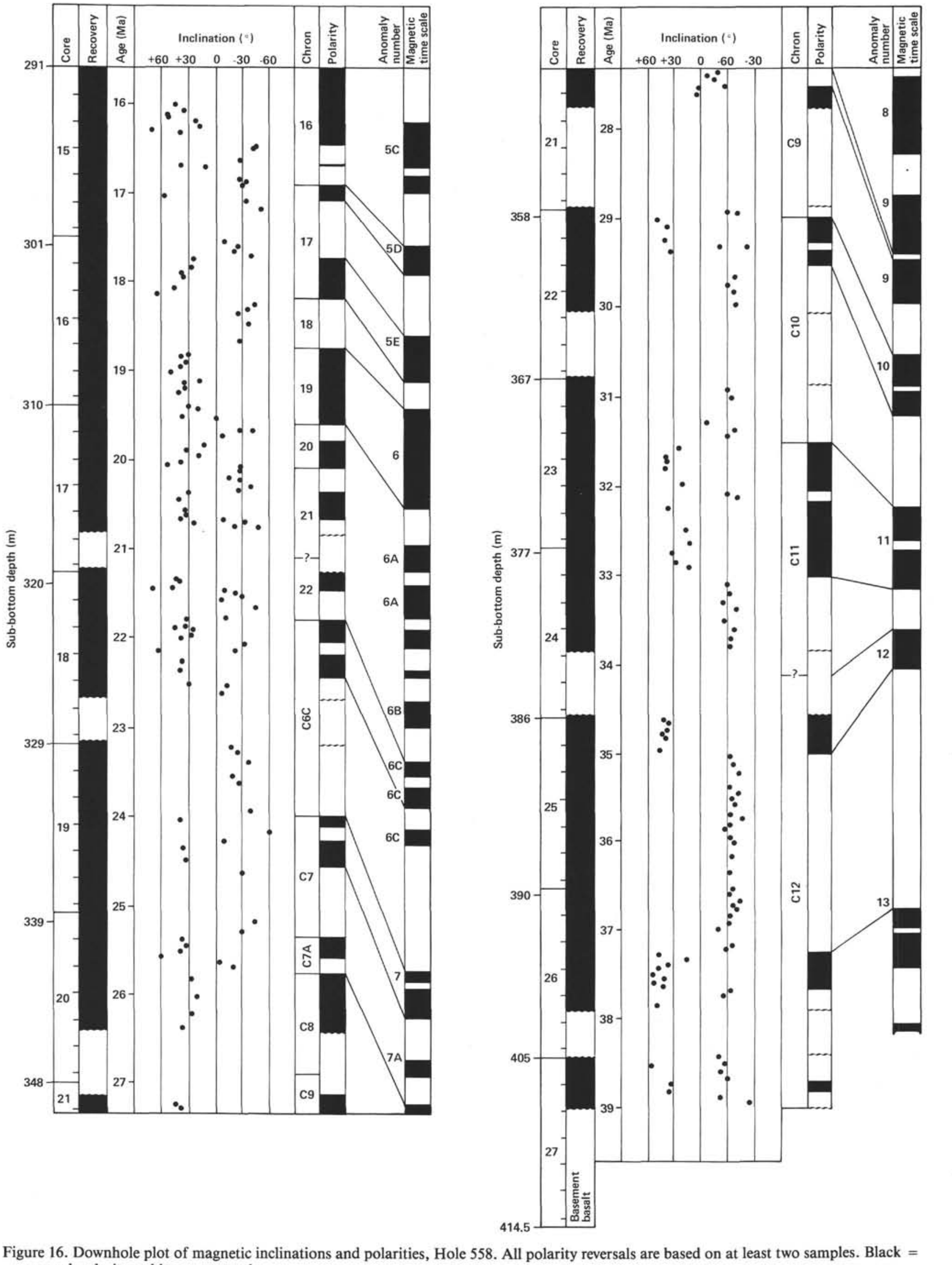

Figure 16. Downhole plot of magnetic inclinations and polarities, Hole 558. All polarity reversals are based on at least two samples. Black = normal polarity; white = reversed.

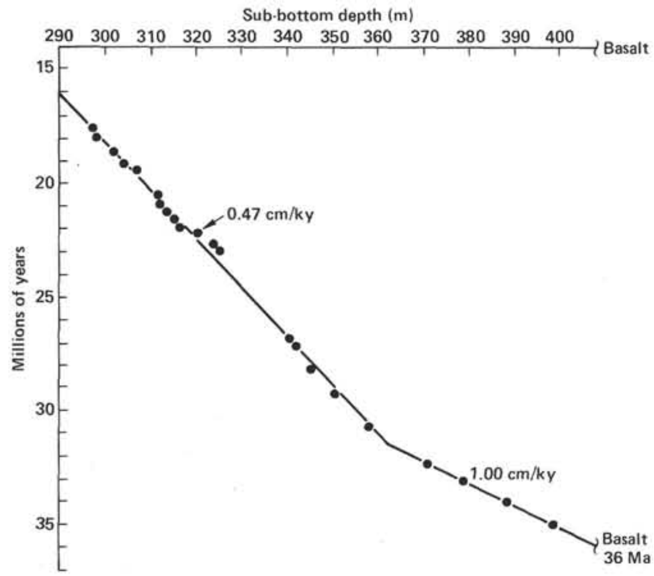

Figure 17. Sediment accumulation rates based on paleomagnetic data, Site 558.

gradational but fairly rapid increase in density and seismic velocity, and a rather poorly defined increase in thermal conductivity between 280 and 300 m sub-bottom, centered on 290 m sub-bottom. This feature is far greater in amplitude than progressive compaction effects and must represent a change in the composition of the sediment or a sudden increase in age (disconformity). This feature correlates with a change in accumulation rate detected by nannofossils and foraminifers and with a decrease in carbonate content of the sediment.

The change in density and sonic velocity at 290 m sub-bottom results in a marked change in acoustic impedance, which is gradational over a depth interval of 30 m and correlates with the similar features seen in the log curves for Site 556.

The underway profiling data near both Site 556 and Site 558 show no continuous reflector, which presumably indicates that the transition in physical properties is a gradation as shown by the physical property measurements and the downhole logs, rather than a sharp boundary. This would in turn suggest that the boundary represents a compositional change in the sediment rather than a disconformity.

At the base of the sedimentary section, the two last velocity measurements show a rise in velocity, then a sharp decrease. The feature is due to a dolomitized horizon in the sediments and the velocity change is clearly seen in the sonic downhole log (Fig. 21) just above the basement interface.

Basement Section

Within the basement section of the hole, sampling for physical property measurement was difficult because of the friable nature of the altered basalts and gabbros. Measurements are hence strongly biased towards fresh specimens of each lithology. The values measured are unremarkable and are mainly of use as a control on the wireline log data.

DOWNHOLE MEASUREMENTS

Logging

Operations

Logging of Hole 558 was made difficult by extremely bad hole conditions. After the bit was dropped, the drill string was pulled to a sub-bottom depth of 127 m by 1600 hr. 9 October, and the sonic log was run first. On the first run (recording velocity), it reached a depth of 546 m, but on the second run (for waveform recording), the hole was blocked at 452 m sub-bottom. The recorded data are very noisy, and the depth scale is distorted by repeated jamming of the tool in the hole, which had closed in places to a diameter of 4 in. These runs were completed at 2300 hr.

An attempt was made to run a temperature log (small diameter tool) that only reached 189 m sub-bottom. We decided to wash down the hole to total depth, then flush with 100 barrels of gel mud. This operation was performed between 0400 and 0915 hr. 10 October.

The laterolog was run to nearly total depth, 544 m sub-bottom, but during the attempt to repeat the section, the tool hit a blockage at 444 m sub-bottom, indicating very rapid deterioration of the hole. This operation was completed at 1500 hr. Density and porosity logs were lowered with great difficulty to 445 m and the caliper was broken in spudding the tool during attempts to penetrate further.

A second attempt to run the temperature log was started at 2045 hr. Because of the low tool weight and large heave motion of the ship, the tool was overrun and the cable became knotted. Fortunately, the cable and tool were successfully recovered through the drill pipe. Total depth reached by the tool is uncertain but probably about 200 m sub-bottom. Logging operations were concluded at 0300 hr. 11 October. Total logging operations required 37 hr. The operations are summarized in Table 9.

Sediment Section

Figure 19 shows the density, sonic velocity, and resistivity, and natural gamma-ray logs for Hole 558. The data generally are of good quality. An exception to this is the density log (shown dashed) and the porosity log (which is not shown). Throughout the sediment section, the hole is washed to a diameter greater than the span of the excentralizer on the density and porosity tools. The result of this is that the tools make poor wall contact and read erroneously low density and high porosity.

The logs show that the sediments below the drill pipe can be divided into two units with a gradational boundary at about 290 m sub-bottom. The density increases from 1.8 to 1.95 $g \cdot cm^{-3}$, the sonic velocity from 1.9 to 2.1 $km \cdot s^{-1}$, and the resistivity from 0.9 ohm-m to 1.3 ohm-m. These changes are also apparent in the physical properties measurements (Fig. 18). The boundary at 290 m separates geophysical Units I and II. These correlate with Lithologic Units 1 and 2, and the boundary is a change of carbonate content from 90 to 50%. Within each unit, the logs show small-scale variability that is above the noise level of the logs, but the interpretation of which is uncertain.

Table 8. Physical properties measurements, Site 558.

Core-Section (interval or depth in section in cm)	Sub-bottom depth (m)	Sonic velocity (km/s)		Temperature (°C)	Thermal conductivity (mcal/[cm·deg·s])	GRAPE density (g/cm³)		Gravimetric density			Acoustic impedance (g/[cm·s])	Vane shear strength (g/cm²)	Lithology or remarks
		V.	H.			V.	H.	Wet-bulk density (g/cm³)	Water content (%)	ϕ (%)			
Hole 558													
1-2, 30	159.8	2.05*		21.0								2300	Nannofossil ooze *Sample deformed during velocity measurements
1-2, 57	160.1	2.18*		21.0								1400	
1-2, 115	160.6	2.22*		20.0					31			900	
1-6, 84	166.3	2.10*		21.0								1400	
2-2, 66	169.7	1.59		21.0	3.38				35			1000	
2-2, 135	170.4	1.57		21.0								700	
2-4, 138	173.4	1.67		21.0								1200	
3-3, 16	180.2	1.59		21.0								800	
3-3, 85	180.9	1.59		21.0								700	
3-5, 12	183.1	1.57		21.0								500	
4-2, 76	188.8	1.57		21.0	3.38							2000	
4-2, 138	189.4	1.56		21.0								1700	
4-5, 57	193.1	1.54		21.0					34			700	
4-5, 141	193.9	1.58		21.0								800	
5-2, 79	198.3	1.58		21.0	3.80							1100	
5-2, 139	198.9	1.58		21.0								1100	
5-5, 37	202.4	1.58		21.0					33			1500	Nannofossil ooze
5-5, 130	203.3	1.60		21.0								750	
6-2, 12	207.1	1.56		22.0								1700	
6-2, 131	208.3	1.56		22.0	3.52							1200	
8-1, 14	224.6	1.58		22.0								1900	
8-1, 120	225.7	1.59		22.0								1500	
8-2, 111	227.1				3.60								
9-2, 15	235.7	1.54		22.0								2300	Slight green color
9-2, 119	236.7	1.56		22.0								2400	
11-2, 15	254.6	1.57		22.0								1000	Shear strength underestimated
11-2, 44	254.9	1.67		22.0								1500	
12-2, 18	264.2	1.59		22.0								1600	
12-2, 135	265.4	1.62		22.0	3.82							2000	
12-4, 14	267.1	1.59		22.0								2200	
12-4, 98	268.0	1.65		22.0								1800	
13-2, 15	273.6	1.62		22.0									Nonlithified sediment crumbles, does not shear.
13-2, 98	274.5	1.58		22.0	3.59								Nannofossil ooze
13-4, 12	276.6	1.60		22.0									
13-4, 132	277.8	1.63		22.0									
15-2, 12	292.6	1.74		22.0									
15-2, 86	293.4	1.75		22.0	4.62								
16-2, 22	302.2	1.67		21.0									Velocity low because of poor condition (deformed)
16-2, 146	303.5	1.73		21.0									
17-2, 14	311.6	1.80		21.0									
17-2, 81	312.3	1.72		21.0	4.44								
18-2, 35	321.4			22.0	4.12								
18-2, 136–139	322.4	1.71		22.0			1.94				3.3		
19-2, 29–33	330.7		1.66	22.0	4.10		2.00				3.3		
19-2, 80–84	331.3		1.67	22.0			1.99				3.3		
20-2, 28–31	340.3		1.67	22.0			1.96				3.3		
20-2, 107	341.1				3.92								
21-2, 89–92	350.4		1.64	22.0			1.94				3.2		
21-2, 137	350.9				4.20								Nannofossil ooze
22-2, 26–31	359.3		1.67	22.0			1.93				3.2		
22-2, 132	360.3				4.0								
23-2, 8–12	368.6		1.65	22.0			1.81				3.0		
23-2, 103	369.5				4.02								
24-2, 65–69	378.7		1.63	22.0			1.97				3.2		
25-2, 57–61	388.1		1.66	22.0			1.92				3.2		
25-2, 133	388.8				4.22								
26-2, 46–50	397.5		1.66	22.0			2.02				3.3		
27-1, 16–20	405.2		1.74	22.0			2.11	2.0	21.2	42.5	3.6		
27-2, 113–118	407.7		1.64	22.0			2.08				3.4		Dolomite rich
28-3, 4–14	417.6		5.39	22.0									Basalt
29-4, 15–25	428.2	4.45		22.0		2.63					11.7		Glassy margin of pillow basalt
30-3, 19–30	435.7		5.36	22.0	3.99		2.79				15.0		Basalt
33-1, 86–96	460.4	4.90		22.0		2.71					13.3		Slightly altered basalt
34-1, 20–34	468.8		5.45	22.0	3.99		2.79				15.2		Basalt
35-3, 122–127	481.7		4.91	22.0									Altered basalt
36-1, 5–20	486.6		4.75	22.0			2.70				12.8		Basalt
38-2, 71–78	506.7	5.30		22.0		2.82					14.9		Basalt
39-4, 114–115	508.7							2.7	5.0	13.2			
40-1, 123–129	519.3	3.79		22.0	2.78	2.20					8.3		Breccia
40-3, 109–110	520.6							2.4	7.6	18.4			

Table 8. (Continued).

Core-Section (interval or depth in section in cm)	Sub-bottom depth (m)	Sonic velocity (km/s) V.	Sonic velocity (km/s) H.	Temperature (°C)	Thermal conductivity (mcal/[cm·deg·s])	GRAPE density (g/cm^3) V.	GRAPE density (g/cm^3) H.	Gravimetric density: Wet-bulk density (g/cm^3)	Gravimetric density: Water content (%)	ϕ (%)	Acoustic impedance (g/[cm·s])	Vane shear strength (g/cm^2)	Lithology or remarks
Hole 558 (Cont.)													
41-1, 60–63	527.6	3.58		22.0		2.44					8.7		Serpentinized gabbro
41-3, 8–9	528.6							2.8	1.8	5.0			
43-1, 40–50	545.4	3.26		22.0		2.35					7.7		Altered gabbro
44-1, 22–31	554.3	3.55		22.0	6.08	2.49					8.8		Altered gabbro
Hole 558A													
2-2, 35	2.3	1.58		23.0								600	Nannofossil ooze
2-2, 113–115	3.1	1.56		23.0	2.43	1.63					2.5	400	
2-5, 77	7.3	1.57		23.0					42			600	
2-5, 136	7.9	1.57		23.0								700	
3-2, 19	11.7	1.54		23.0								600	
3-2, 114	12.6	1.55		23.0	2.79	1.81					2.8	1000	
3-5, 14–16	16.2	1.55		23.0					44			2000	
3-5, 140–142	17.4	1.56		23.0								1700	
4-2, 23	21.2	1.59		23.0								1000	
4-2, 123	22.2	1.59		23.0	2.71	1.77					2.8	800	
4-5, 35	25.8	1.59		23.0								2000	
4-5, 134	26.8	1.59		23.0								1200	
5-2, 17	30.7	1.61		23.0								1400	
5-2, 133	31.8	1.58		23.0	3.11	1.82					2.9	1300	
5-5, 17	35.2	1.58		23.0								2300	
5-5, 137	36.4	1.60		23.0					37			2400	
6-2, 35	40.3	1.61		23.0								1600	Nannofossil ooze
6-2, 131	41.3	1.60		23.0	3.15	1.84					2.9	1900	
6-5, 20–23	44.7	1.60		23.0								1800	
6-5, 132–135	45.8	1.62		23.0								2600	
7-2, 66	50.2	1.60		23.0								1500	Very deformed
7-2, 130	50.8	1.58		23.0	3.28							1400	Very deformed
7-5, 18–20	54.2	1.61		23.0					36		3.1	2000	
7-5, 135–137	55.4	1.61		23.0								1900	
8-3, 18–20	60.7	1.59		23.0								2000	
8-3, 130	61.8	1.59		23.0	3.37	1.91					3.0	2200	
8-5, 20–22	63.7	1.59		23.0					37			1800	
8-5, 124–126	64.8	1.62		23.0								1300	
9-2, 132	69.8				3.36								Very deformed
9-3, 104–106	71.0	1.61		23.0		1.93			36		3.1	1500	
10-2, 15–17	75.7	1.58		23.0					33			1000	
10-2, 116–120	76.7	1.60		23.0								750	
11-2, 131	79.8	1.59		23.0	3.62							700	Very deformed
11-5, 21–23	83.2	1.62		23.0					33			1600	
11-5, 135–137	84.4	1.62		23.0		2.07					3.4	2750	
12-2, 26–28	88.3	1.57		23.0								700	Deformed
12-2, 128	89.3	1.57		23.0	3.75							1300	Deformed
12-5, 20–22	92.7	1.58		23.0		1.94			33		3.1	1300	
12-5, 140–143	93.9	1.59		23.0								1600	
13-2, 15–17	97.7	1.58		23.0								1100	
13-2, 129	98.8	1.58		23.0	3.66	1.97					3.1	2700	
13-5, 27–29	102.3	1.60		23.0					31			2200	
14-5, 24–26	109.2	1.58		23.0					33			2100	
14-5, 130	110.3	1.59		23.0	3.75	1.92					3.0	2500	
15-2, 14–16	114.2	1.58		23.0								2500	
15-2, 129	115.3	1.57		23.0		1.96					3.1	2400	
15-5, 13–15	118.6	1.58		23.0					32			2500	
15-5, 134–137	119.9	1.59		23.0								2900	
16-2, 10–12	123.6	1.56		23.0								1500	Nannofossil ooze
16-2, 136–138	124.9	1.58		23.0	3.62							3000	
16-5, 15–17	128.2	1.56		23.0	3.62				33			2600	
16-5, 137–140	129.4	1.58		23.0		1.94					3.1	3800	

Note: V. = vertical, H. = horizontal; water content is corrected; ϕ = porosity. All values measured at laboratory temperature and pressure. For details of techniques, see Explanatory Notes, this volume.

Figure 20 shows the equivalent logs from Hole 556 where no sediment cores were taken. The correspondence between the logs is remarkable; not only does a major change in physical properties occur in Hole 556 at a proportional depth in the sediment section, but minor variations in the logs are correlatable from Site 556 to Site 558. It is inferred that the sediment lithology and depositional history of the two sites, which are on the same isochron and at similar water depths, were the same.

The change in density and sonic velocity between chemical Units I and II generates the only appreciable acoustic impedance contrast within the sediments. It may be expected that this horizon could be traced through the area between the sites on seismic profiler records. Initial study of underway data shows several weak reflectors, which are geographically discontinuous within the lower part of the sediments. The quality of reflection at the Unit I/Unit II boundary will be strongly related to the

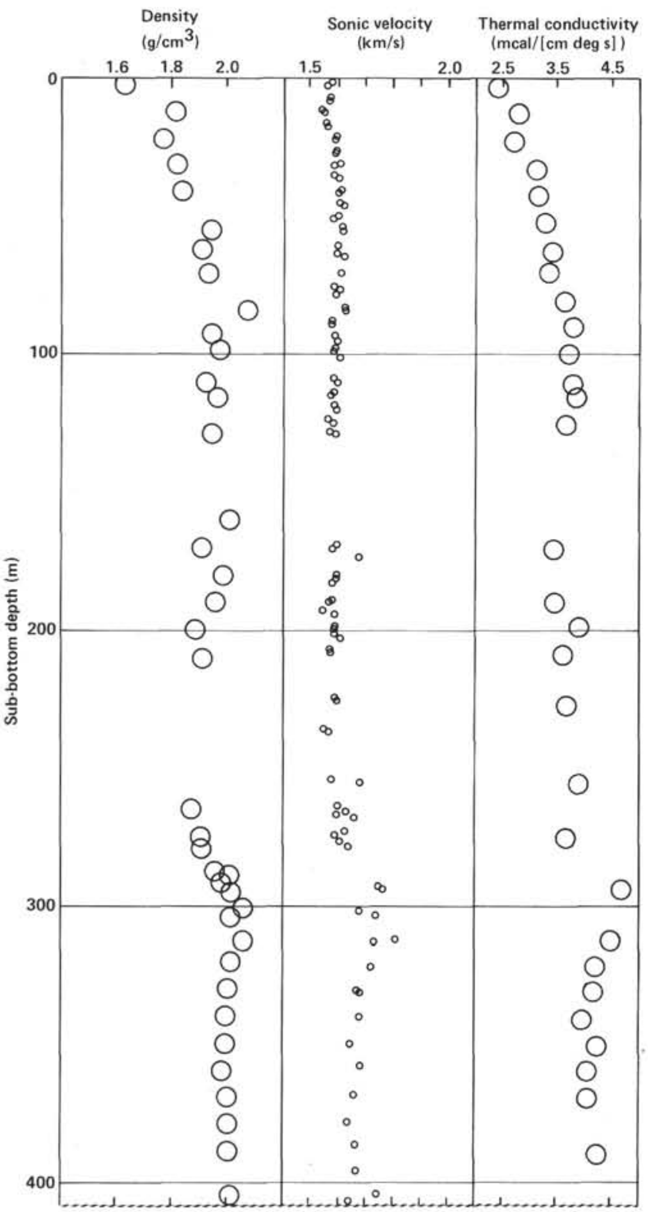

Figure 18. Physical property variations in the sediment section of Holes 558 and 588A. Symbol diameter shows the measurement error of that physical property. Density values above 320 m sub-bottom depth are taken from analog GRAPE records and do not appear in Table 8.

sharpness of that boundary, and this may well vary geographically.

Basement Section

The poor hole condition resulted in data that were generally poor in quality. The laterolog was the only tool that reached the bottom of the hole and provided good data, although this tool had a broken caliper. The sonic log also reached near-bottom on the velocity run, but the data are very noisy, probably because of wall contact. The sonic caliper log contained spikes because of tool malfunction (which also occurred during the logging of Hole 556). Both sonic and resistivity logs have distorted depth scales because the tools became

Table 9. Schedule of logging runs.

Run 1. Sonic velocity (DDBHC), natural gamma ray (GR) caliper (CAL)
Pass 1: sonic velocity
Logger on bottom 1830 10/9; maximum sub-bottom depth = 546 m
Pass 2: waveform recording
Logger on bottom 2030 10/9; maximum sub-bottom depth = 452 m
Run 2. High resolution temperature (HRT)
Logger on bottom 0300 10/10; maximum sub-bottom depth = 189 m
0400–0915 10/10:
Wash to total depth; flush hole with mud
Circulation stopped 0815 10/10
Run 3. Dual laterolog, GR, self potential (SP)
Logger on bottom 1130 10/10; maximum sub-bottom depth = 544 m
Run 4. Gamma ray density (FDC), neutron porosity (CNL), GR
Logger on bottom 1800 10/10; maximum sub-bottom depth = 445 m
Run 5. HRT
Logger on bottom 2300 10/10; maximum sub-bottom depth = 200 m

Note: Circulation stopped: 1400 hr. 9 October.

jammed in the lower part of the hole, but these can be recognized by steps in the tension log that are part of the original records. The porosity and density logs appear to be of good quality but only extend to 37 m below the basement interface.

As at Site 556, the basement section has been divided into geophysical units in the lower part of the hole based primarily on the resistivity log. These units are shown in Figure 21 and Table 10. Comparison with the lithologic column shows that the pillow basalt units and altered gabbros give a similar log response to that seen at Hole 556. However, the interpretation of the interval from 405 to 425 m reveals complexity that is not apparent in the lithologic column.

The density log shows a progressive increase in density down through the dolomitic nannofossil ooze, with a sharp decrease just above the basalt at 408 m sub-bottom. These changes can also been seen in physical property measurements (Fig. 18) and are reflected in the sonic and porosity logs. The basalt, Lithologic Unit 3, can be clearly identified by its high velocity, resistivity, density, and low porosity and is shown to be only 2 m thick. Below this is a unit of variable density around 2.2 g/cm^3, low porosity, high resistivity, and high but variable sonic velocity (about 4.7 km/s). This is interpreted as a sedimentary unit; however, it is difficult to reconcile the low density with the high sonic velocity. Using a Schlumberger sonic-density crossplot diagram, we can see that the porosity and velocity are appropriate for a limestone, but the low density requires a lower grain density such as that of gypsum. No material was recovered from this unit, possibly because of a blockage of the drill bit as indicated by the slow drilling rate. This unit is 6 m thick.

Below this, pillow basalts occur in the lithologic column and are shown by high resistivity and high, variable sonic velocity as was detected at Hole 556. Within the pillow basalts, a lower unit from 497 to 522 m sub-bottom is distinguished by a high and relatively constant resistivity of 250 ohm-m. This unit corresponds to Lithologic Units 9 and 10 and Chemical Unit V. Although the sonic velocity is also high and steady at 5.2 km/s in this unit above 514 m sub-bottom, the sonic log is extremely noisy below this depth.

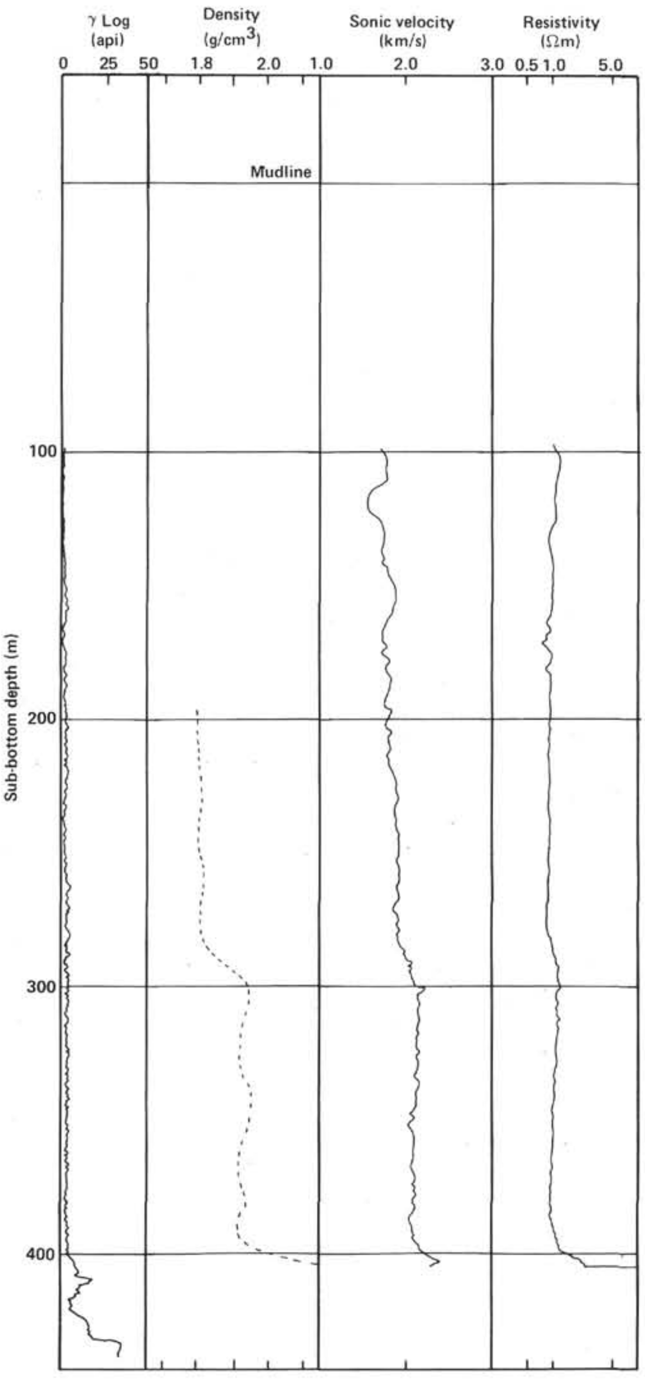

Figure 19. Wireline log curves for sedimentary section of Hole 558. Density curve drawn with dashed line to indicate the poor quality of the data.

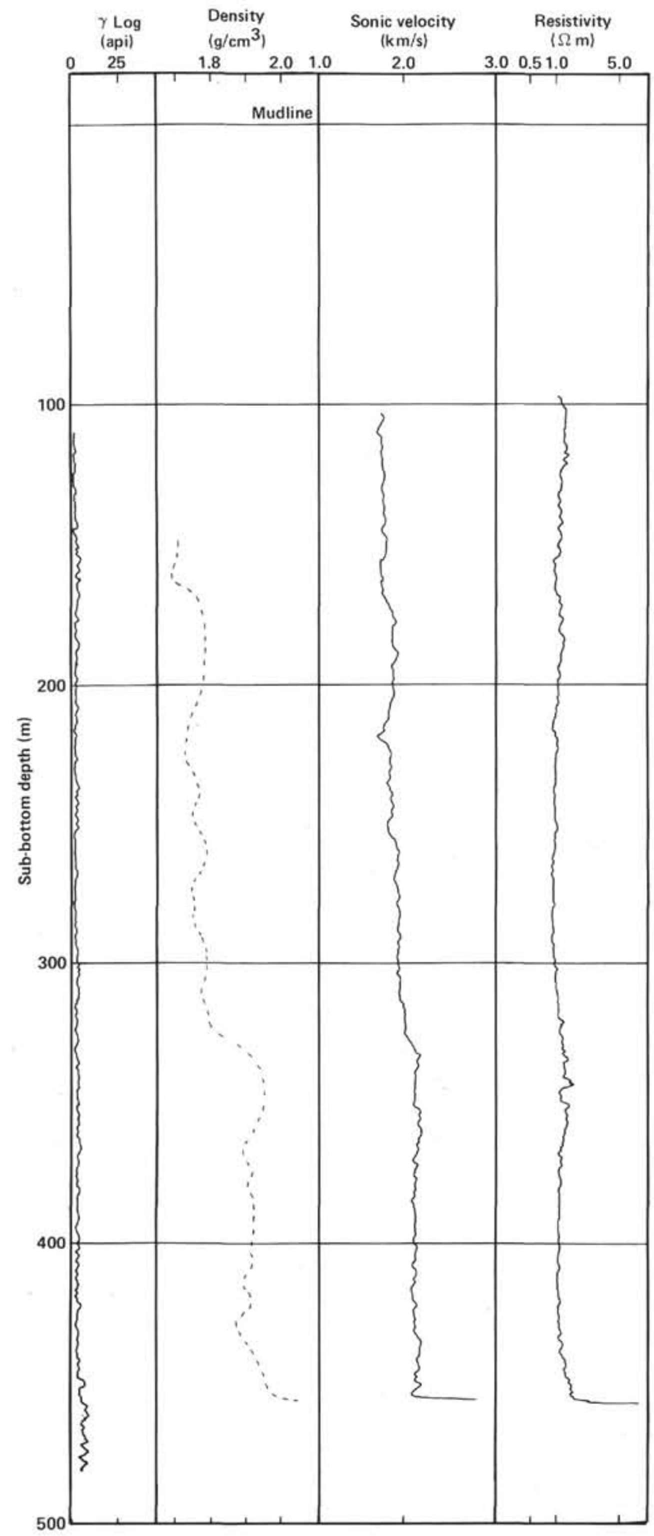

Figure 20. Wireline log curves for the sedimentary section of Hole 556. Density curve drawn with dashed line to indicate the poor quality of the data.

Below 522 m, the resistivity and sonic velocity fall to lower values in the serpentinite, Lithologic Units 12 and 13. It is not clear whether the basalt breccia, Lithologic Unit 11, occurs above or below the logging boundary at 522 m.

Downhole Temperatures

Because of the poor hole conditions, no temperature measurements were made in the basement section of the hole or in the lower sedimentary unit (Unit 2). The available data from the mudline to a depth of 234 m sub-bottom are shown in Figure 22. Two depth profiles are available from the two attempts to run a temperature log. For a depth of some 100 m below the mudline, the logs

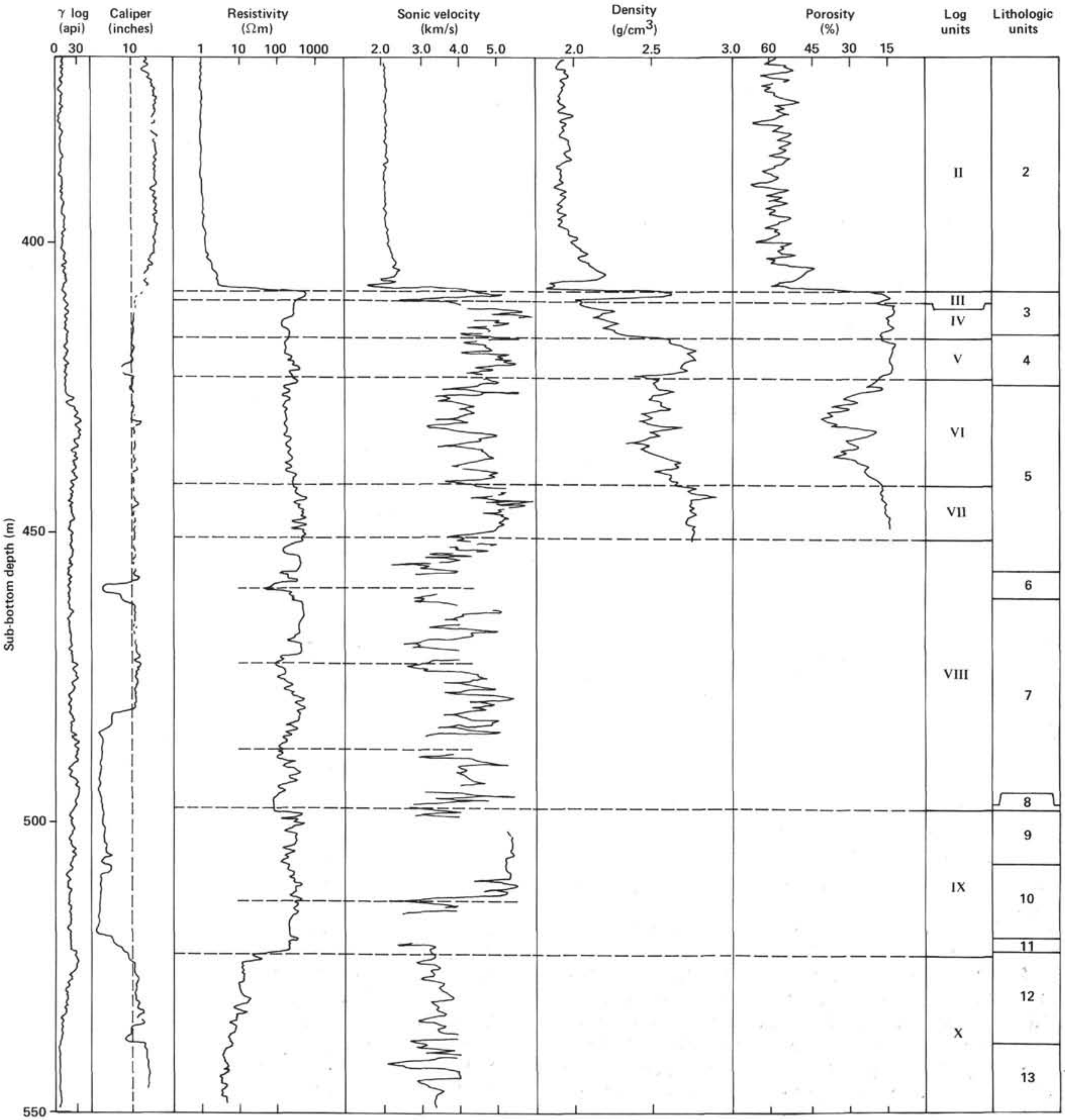

Figure 21. Wireline log curves for basement section of Hole 558. Curves have been redrawn omitting noise spikes. Gaps indicates intervals where noise obscures data.

were run inside the drill pipe, and the minor rise in temperature at 3820 m below rig floor may be a feature of the drill string or of contact between the drill string and the sidewall of the hole.

The rise in temperature with depth over the short interval logged is taken as evidence that there is no large-scale water flow in the hole and that the hole is reequilibrating. Because the hole was blocked below the logged depth, this result is not totally unexpected. The lower temperature gradient in the upper part of the hole may be due to the pumping action of the drill string caused by the heave of the ship.

The mudline temperature of 0.5°C is lower than expected, and a temperature log was made of the ocean water as the log was raised through the drill string after pass 2. The results are shown in Figure 23. The temperature tool was accurately calibrated in the interval between logging Hole 556 and 558, and temperatures at

Table 10. Geophysical units identified by logging measurements, Hole 558.

Unit	Depth range (m sub-bottom)	Resistivity (ohm m)	Sonic velocity (km/s)	Density (g/cm^3)	Porosity (%)	Lithology	Remarks
I	0–290	0.9	1.9	1.8	[a]	Nannofossil ooze	Carbonate content = 90% 0–17 Ma
II	290–408	1.3	2.1	1.95	[a]	Nannofossil ooze	Carbonate content = 50% 17–34 Ma
III	408–410	500	4.5	2.6	15	Massive pillow basalt	Tight constraint on layer thickness
IV	410–416	200	4.7	2.2	15	Unknown: limestone?	Inferred sedimentary layer
V	416–423	200	4.7	2.7	15	Fractured pillow basalt	Very uniform properties
VI	423–441	150	4.4	2.5	30	Pillow basalt and interpillow breccia	High gamma-ray value
VII	441–450	400	5.1	2.75	17		Very uniform properties
VIII	450–497	100–400	3.7–4.6				Broad (15-m wavelength) variations in sonic velocity and resistivity; X-ray peaks at 474, 488, and 494 m
IX	497–522	250	5.1				Very uniform resistivity throughout; uniform sonic velocity above 514 m; poor sonic return below
X	522–581	3–10	3.4			Fresh and altered serpentinite	Resistivity decreases toward bottom; gamma-ray peak at 524 m

Note: Top of basement taken to be 4170 m on resistivity log and 4172 m on sonic velocity and porosity/density logs.
[a] Data unreliable because of poor sidewall contact.

558 should be accurate to ±0.2°C. It is hoped that the information in Figure 23 may be useful to physical oceanographers; depth profiles such as this are simple to obtain and incur neither financial nor time cost at any hole that is logged.

SUMMARY AND CONCLUSIONS

Site 558 is located between Anomalies 13 and 15 on a flow line passing through the FAMOUS area and sites drilled during Legs 37 (332, 333, 334, 335) and 49 (411, 412, 413). We decided to have a complete program of coring basement and sediment and logging because of the large amount of data already available near and at the ridge crest.

The upper part of the basement drilled at Site 558 comprises nine lithologic units of aphyric basalt. Most of these units are composed of pillow basalt with variable amounts of interpillow breccia or of basaltic breccia. Fresh glass is very common at the margin of the pillows throughout the basaltic layer and is usually embedded in neoformed calcite filling cracks and interpillow spaces. The lower part of the basement comprises two lithologic units of altered serpentinite, serpentinite breccia, and mylonite. A basalt clast was found in one of these units.

The chemical analyses of 29 samples of the basaltic layer define six homogeneous chemical groups whose average major and trace element concentrations are given in Table 6. Five percent of olivine fractionation can account for the small compositional variations observed in Unit V. There is no cogenetic relationship between the different homogeneous groups. The most striking result obtained at Site 558 is the occurrence of depleted ($[Nb/Zr]_{Ch}$ = 0.4), flat ($[Nb/Zr]_{Ch}$ = 1), and enriched ($[Nb/Zr]_{Ch}$ = 1.6) patterns of magmaphile elements presented in Figure 11. After Holes 413 (Leg 49) and 504B (Leg 69–70), Site 558 is the third site presenting this feature. Isotope data and other trace elements are necessary to go further in interpretation in terms of mantle sources and petrogenetic processes.

The entire sedimentary layer (408 m) was cored through a combination of piston coring (Hole 558A) (0 to 131.5 m) and rotary coring (158 to 408 m). The recovered lower Oligocene through Pleistocene pelagic calcareous sediments provide a more complete stratigraphic section than has yet been obtained from the North Atlantic. The age of oldest sediment (34–37 Ma—as determined from the nannofossils found in basalt breccia at the top of basement—and 36 Ma—as determined by magnetostratigraphic studies) is in agreement with the position of the hole between Magnetic Anomalies 13 and 15. A major change in the sediment lithology at a depth of 300 m (approximately at the boundary between lower and middle Miocene) corresponds to a change of carbonate content (90% in the upper part, 50% below) and in the accumulation rate (16 m/Ma in the upper part and 8 m/Ma in the lower part). The well-defined magnetic polarity stratigraphy in the lower part of the section should provide reliable limits on the ages of biostratigraphic zones.

A complete set of logs was attempted; because of poor hole conditions, the attempt was not entirely successful. However, the major lithologic boundary in the sediment is clearly evident within density, sonic, and resistivity logs. A similar change in these logs was noted at an equivalent depth at Site 556, implying that this li-

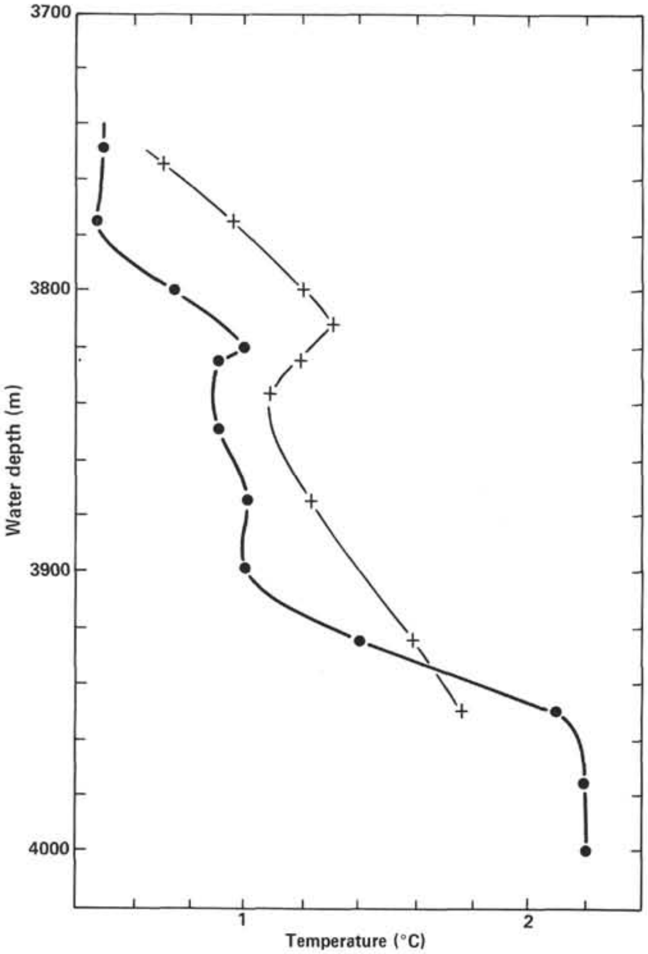

Figure 22. High-resolution temperature (HRT) log curves for Hole 558. The curve joining X data points represents HRT Run 1 (circulation stopped: 1400 Oct. 9; log on bottom: 0130 Oct. 10; elapsed time: 11.5 hr.). The curve joining ● data points represents HRT Run 2 (circulation stopped; 0815 Oct. 10; log on bottom: 2300 Oct. 10; elapsed time: 14.75 hr.). Mudline depth = 3766 m; Units 1/2 boundary = 4056 m; sediment/basement boundary = 4171 m.

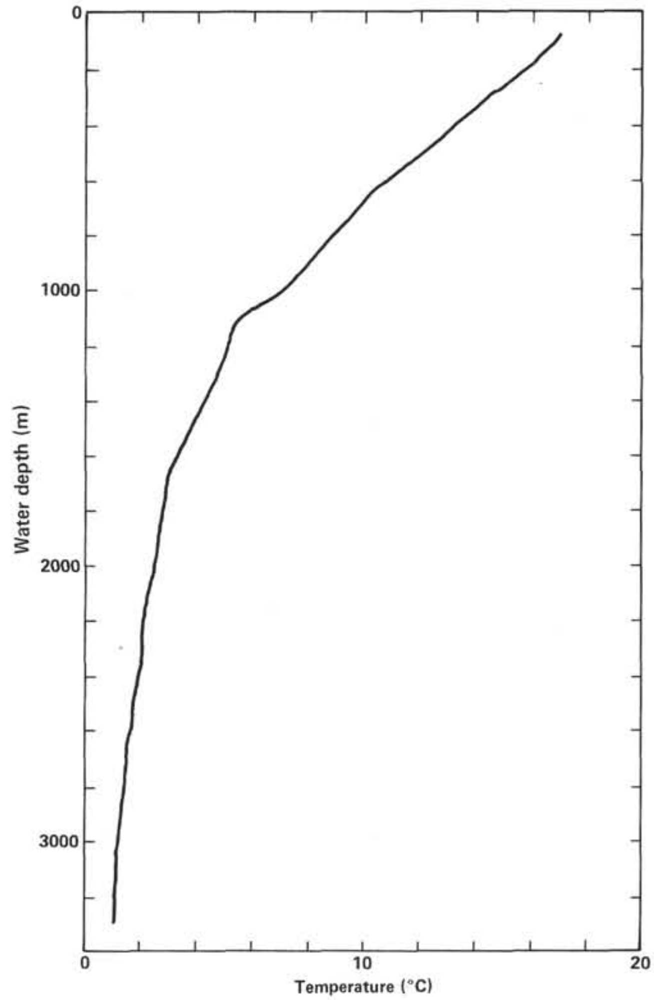

Figure 23. Ocean temperature profile recorded by high-resolution temperature log within drill pipe.

thology change is probably a broad regional feature. Other minor changes within the sets of logs at Sites 556 and 558 also appear to coincide.

REFERENCES

Aumento, F., Melson, W. G., et al., 1977. *Init. Repts. DSDP*, 37: Washington (U.S. Govt. Printing Office).

Berger, W. H, and von Rad, U., 1972. Cretaceous and Cenozoic sediments from the Atlantic ocean. *In* Hayes, D. E., Pimm, A. C., et al., *Init. Repts. DSDP*, 14: Washington (U.S. Govt. Printing Office), 787-954.

Bertrand, H., Dostal, J., and Dupuy, C., 1982. Geochemistry of early Mesozoic tholeiites from Morocco. *Earth Planet. Sci. Lett.*, 58: 225-239.

Blow, W. H., 1969. Late middle Eocene to Recent planktonic foraminiferal biostratigraphy. *In* Brönnimann, P., and Renz, H. H. (Eds.), *Proc. First Int. conf. Plankt. Microfossils:* Leiden (E. J. Brill), 1: 199-422.

Bougault, H., 1980. Contribution des éléments de transition à la compréhension de la genèse des basaltes océaniques. Analyse des éléments traces dans les roche par spectrométrie de fluorescence X [Thèse]. Université Paris VII, Paris, France.

Bougault, H., Cambon, P., Corre, O., Joron, J. L., and Treuil, M., 1979. Evidence for variability of magmatic processes and upper mantle heterogeneity in the axial region of the Mid-Atlantic Ridge near 22° and 36°N. *Tectonophysics* 55:11-34.

Cambon, P., Joron, J. L., Bougault, H., and Treuil, M., 1980. Leg 55 Emperor Seamounts: trace elements in transitional tholeiites, alkali basalts and hawaiites—mantle homogeneity or heterogeneity and magmatic processes. *In* Jackson, E. D., Koizumi, I., et al., *Init. Repts. DSDP*, 55: Washington (U.S. Govt. Printing Office), 585-598.

El Azzouzi, M., 1981. Géochimie comparee de quelques éléments hygromagmaphiles dans des roches volcaniques de contextes geódynamiques variés [Thèse de 3eme cycle]. Université de Bretagne Occidentale, Brest, France.

Gartner, S., 1977. Calcareous nannofossil biostratigraphy and revised zonation of the Pleistocene. *Mar. Micropaleontol.*, 2:1-25.

Graciansky, P. C. de, Poag, C. W., and Shipboard Scientific Party, in press. Site 550. *In* Graciansky, P. C. de, Poag, C. W., et al., *Init. Repts. DSDP*, 80: Washington (U.S. Govt. Printing Office).

Langmuir, C. H., Bender, J. F., Bence, A. E., Hanson, G. N., and Taylor, S. R., 1977. Petrogenesis of basalts from the FAMOUS area: Mid-Atlantic Ridge. *Earth Planet. Sci. Lett.* 36:133-156.

Lowrie, W., and Alvarez, W., 1981. One hundred million years of geomagnetic polarity history. *Geology*, 9:392-397.

Murray, J. W., 1979. Cenozoic biostratigraphy and paleoecology of Sites 403 to 406 based on the foraminifers. *In* Montadert, L., Roberts, D. G., et al., *Init. Repts. DSDP*, 48: Washington (U.S. Govt. Printing Office), 415-430.

Okada, H., and Bukry, D., 1980. Supplementary modification and introduction of code numbers to the low-latitude coccolith biostratigraphic zonation. *Mar. Micropaleontol.*, 5(3):321-325.

Rögl, F., and Hochuli, P., 1976. The occurrence of *Bolboforma*, a probable algal cyst, in the Antarctic Miocene of DSDP Leg 35. *In* Hollister, C. D., Craddock, C., et al., *Init. Repts. DSDP*, 35: Washington (U.S. Govt. Printing Office), 713-720.

Treuil, M., Jaffrezic, H., Deschamps, N., Derrec, G. F., Joron, J. L., Pelletier, B., Novotny, S., and Courtois, C., 1973. Analyse des lanthanides, du hafnium, du scandium, du chrome, du manganese, du cobalt, du cuivre dans les minéraux et les roches par activation neutronique. *J. Radioanal. Chem.*, 18:55-68.

von Daniels, C. H, and Spiegler, D., 1974. *Bolboforma* n. gen. (Protozoa?) eine neue stratigraphisch wichtige Gattung aus dem Oligozän/Miozän Nordwestdeutschlands. *Palaontol. Z.*, 48:57-76.

SITE 558 HOLE CORE 1 CORED INTERVAL 158.0–167.5 m

TIME-ROCK UNIT	BIOSTRATIGRAPHIC ZONE	FORAMINIFERS	NANNOFOSSILS	RADIOLARIANS	DIATOMS	SECTION	METERS
Miocene						1	0.5, 1.0
						2	
						3	
						4	
	N15 (late Miocene) CN7 (NN9) (middle to late Miocene) *Discoaster hamatus* zone					5	
upper Miocene						6	
middle Miocene? upper Miocene?		AG	AM			7, CC	

GRAPHIC LITHOLOGY

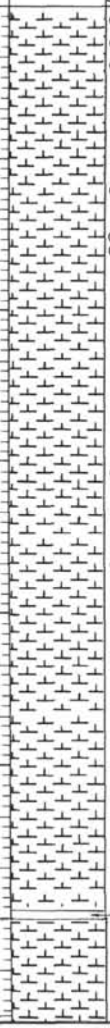

DRILLING DISTURBANCE / SEDIMENTARY STRUCTURES / SAMPLES

2.5Y N8

2.5Y N7

2.5Y N8

2.5Y N7

2.5Y N8

IW

2.5Y N8

2.5Y N8

LITHOLOGIC DESCRIPTION

DOMINANT LITHOLOGY NANNOFOSSIL OOZE

White (2.5Y N8)

Firm

Uniform with no obvious bedding or bioturbation

In Section 2 two faint interbeds of light gray nannofossil ooze, slightly firmer but no change in sediment components can be seen in smear slide examination.

SMEAR SLIDE SUMMARY (%):

	2, 24 M	3, 80	4, 100 D	5, 70
Composition:				
Feldspar	Tr	Tr	Tr	Tr
Clay	6	9	9	9
Pyrite	Tr	–	–	–
Carbonate unspec.	1	1	3	–
Foraminifers	3	10	8	6
Calc. nannofossils	90	80	80	85
Radiolarians	Tr	–	–	–

Carbonate Bomb (%):
3, 80 = 91

SITE 558 HOLE CORE 2 CORED INTERVAL 167.5–177.0 m

TIME-ROCK UNIT	BIOSTRATIGRAPHIC ZONE	FORAMINIFERS	NANNOFOSSILS	RADIOLARIANS	DIATOMS	SECTION	METERS
Miocene						1	0.5, 1.0
						2	
						3	
						4	
	N15 (late Miocene) CN7 (NN9) *Discoaster hamatus* zone (late middle to early late Miocene)					5	
middle to upper Miocene						6	
		AG	AG			7, CC	

GRAPHIC LITHOLOGY

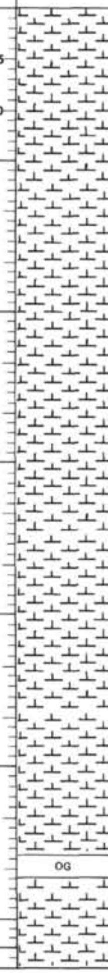

DRILLING DISTURBANCE / SEDIMENTARY STRUCTURES / SAMPLES

2.5Y N8

2.5Y 8/2

2.5Y N8

LITHOLOGIC DESCRIPTION

DOMINANT LITHOLOGY NANNOFOSSIL OOZE

White (2.5Y N8 to 2.5Y 8/2)

Firm

Uniform with no obvious bedding or bioturbation

SMEAR SLIDE SUMMARY (%):

	1, 70 D	3, 70 D	5, 30 M	5, 70 D
Composition:				
Feldspar	Tr	Tr	–	–
Clay	9	9	9	9
Palagonite	–	–	–	Tr
Pyrite	–	–	Tr	–
Carbonate unspec.	1	2	Tr	2
Foraminifers	8	3	5	3
Calc. nannofossils	82	86	85	86

SITE 558 HOLE CORE 3 CORED INTERVAL 177.0–186.5 m

TIME–ROCK UNIT	BIOSTRATIGRAPHIC ZONE	SECTION	METERS	DRILLING DISTURBANCE / SEDIMENTARY STRUCTURES / SAMPLES
Miocene; middle to upper Miocene	N15 (early late Miocene) CN7 (NN9) (see Core 2) late middle to early late Miocene	1, 2, 3, 4, 5, 6, 7, CC	0.5, 1.0	samples * in Sections 3 and 6

FOSSIL CHARACTER: FORAMINIFERS, NANNOFOSSILS, RADIOLARIANS, DIATOMS

GRAPHIC LITHOLOGY

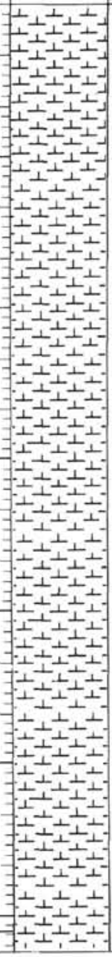

varies very gradually between 2.5Y N8 to 2.5Y 8/2

LITHOLOGIC DESCRIPTION

DOMINANT LITHOLOGY NANNOFOSSIL OOZE

White (2.5Y N8 to 2.5Y 8/2)

Firm

No obvious bedding or bioturbation

SMEAR SLIDE SUMMARY (%):

	3, 75	6, 75
Composition:		
Clay	9	9
Palagonite	Tr	–
Pyrite	Tr	–
Carbonate unspec.	2	5
Foraminifers	2	2
Calc. nannofossils	87	84

SITE 558 HOLE CORE 4 CORED INTERVAL 186.5–196.0 m

TIME–ROCK UNIT	BIOSTRATIGRAPHIC ZONE	SECTION	METERS	DRILLING DISTURBANCE / SEDIMENTARY STRUCTURES / SAMPLES
Miocene; middle to upper Miocene	N15 late N14 (<12 ma) (earliest late Miocene) CN6 (NN8) *Catinaster coalitus* zone (middle Miocene)	1, 2, 3, 4, 5, 6, 7, CC	0.5, 1.0	samples * in Sections 3 and 6

FOSSIL CHARACTER: FORAMINIFERS AG, NANNOFOSSILS AG, RADIOLARIANS, DIATOMS

GRAPHIC LITHOLOGY

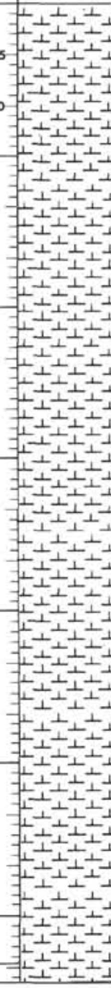

2.5Y N8

2.5Y N8

LITHOLOGIC DESCRIPTION

DOMINANT LITHOLOGY NANNOFOSSIL OOZE

White (2.5Y N8)

Firm

No obvious bedding or bioturbation

SMEAR SLIDE SUMMARY (%):

	3, 75	6, 75
	D	D
Composition:		
Feldspar	1	Tr
Clay	6	9
Carbonate unspec.	2	2
Foraminifers	4	2
Calc. nannofossils	87	87

Carbonate Bomb (%):
3, 110 = 93

SITE 558 HOLE CORE 5 CORED INTERVAL 196.0–205.5 m

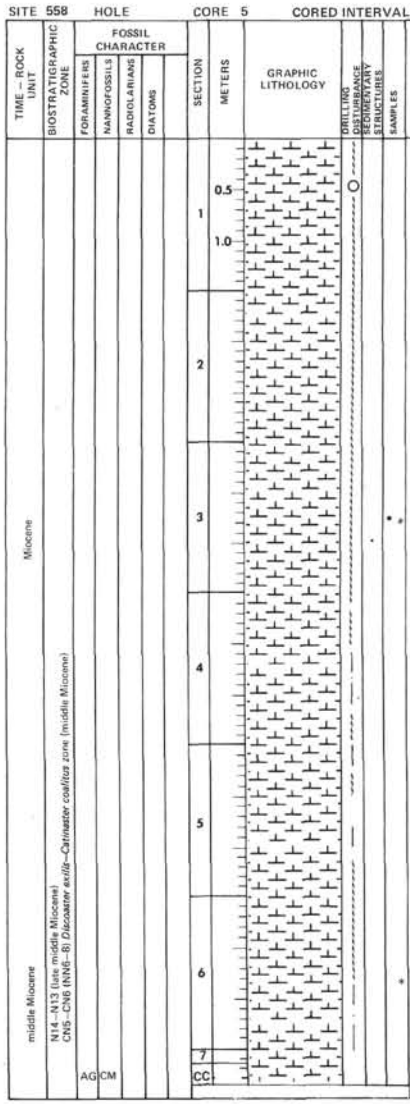

LITHOLOGIC DESCRIPTION

2.5Y N8

DOMINANT LITHOLOGY NANNOFOSSIL OOZE

White (2.5Y N8)

Firm

No obvious bioturbation or bedding

Occasional faint gray streaks

SMEAR SLIDE SUMMARY (%):

	3, 80	6, 80
	D	D
Composition:		
Feldspar	–	1
Clay	10	10
Palagonite	Tr	Tr
Carbonate unspec.	2	3
Foraminifers	2	Tr
Calc. nannofossils	86	86

Carbonate Bomb (%):
3, 80 = 89

SITE 558 HOLE CORE 6 CORED INTERVAL 205.5–215.0 m

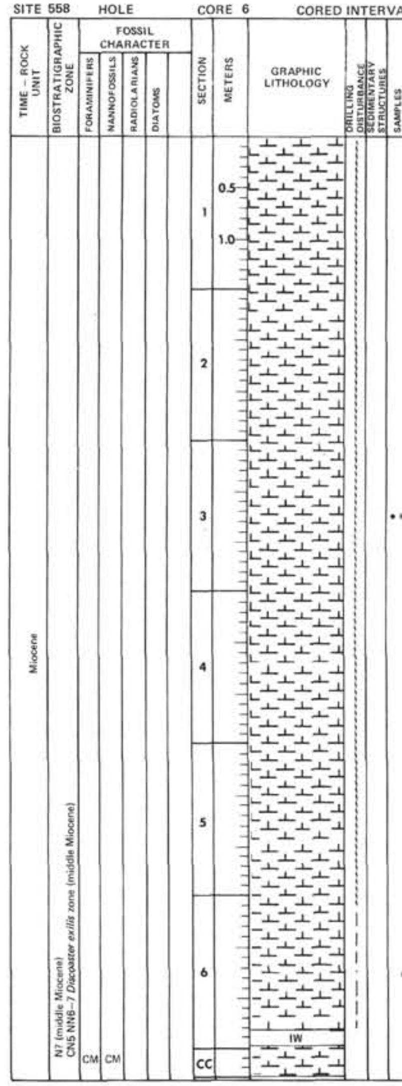

LITHOLOGIC DESCRIPTION

2.5Y N8

DOMINANT LITHOLOGY NANNOFOSSIL OOZE

White (2.5Y N8)

Firm

No obvious bedding or bioturbation

SMEAR SLIDE SUMMARY (%):

	3, 80	6, 80
Composition:		
Feldspar	Tr	Tr
Mica	Tr?	Tr?
Heavy minerals	–	Tr
Clay	10	10
Volcanic glass	Tr	–
Palagonite	Tr	–
Carbonate unspec.	4	3
Calc. nannofossils	84	86
Radiolarians	Tr?	–

Carbonate Bomb (%):
3, 80 = 88

SITE 558 HOLE CORE 7 CORED INTERVAL 215.0–224.5 m

TIME – ROCK UNIT	BIOSTRATIGRAPHIC ZONE	FORAMINIFERS	NANNOFOSSILS	SECTION
middle Miocene Miocene	N13 (middle Miocene) CN5 (NN6–7) *Discoaster exilis* zone (middle Miocene)	CM	CM	1, CC

Meters: 0.5, 1.0

Colors: 5Y 8/1 → 2.5Y N8

LITHOLOGIC DESCRIPTION

DOMINANT LITHOLOGY NANNOFOSSIL OOZE

White (5Y 8/1 to 2.5Y N8)

Firm to soft

No obvious bedding or bioturbation

SMEAR SLIDE SUMMARY (%):

	1, 80	CC
		D
Composition:		
Feldspar	Tr	Tr
Clay	90	10
Opaques	Tr	Tr
Carbonate unspec.	1	8
Foraminifers	1	1
Calc. nannofossils	88	80
Other	–	Tr

SITE 558 HOLE CORE 8 CORED INTERVAL 224.5–234.0 m

TIME – ROCK UNIT	BIOSTRATIGRAPHIC ZONE	FORAMINIFERS	NANNOFOSSILS	SECTION
Miocene; middle Miocene	CN5 (NN6–7) *D. exilis* zone	CM	AM	1, 2, 3, 4, CC

Meters: 0.5, 1.0

Graphic lithology: IW, OG

Colors: 7.5YR 8 (Section 2); 7.5YR 8 (Section 4)

LITHOLOGIC DESCRIPTION

DOMINANT LITHOLOGY NANNOFOSSIL OOZE

White (7.5YR 8)

Firm

No obvious bedding

Possibly very faint white mottling but no obvious bioturbation

SMEAR SLIDE SUMMARY (%):

	3, 75	CC
	D	M
Composition:		
Feldspar	Tr	Tr
Heavy minerals	–	2
Clay	8	10
Palagonite	–	Tr
Opaques	Tr	2
Carbonate unspec.	5	5
Foraminifers	5	10
Calc. nannofossils	80	70
Other	Tr	–

Carbonate Bomb (%):
3, 70 = 91

SITE 558 HOLE CORE 9 CORED INTERVAL 234.0–243.5 m

TIME – ROCK UNIT	BIOSTRATIGRAPHIC ZONE	FORAMINIFERS	SECTION
middle Miocene	N11–N9 (early middle Miocene) CN5 (NN6–7) *D. exilis* zone	CM	1, 2, 3, CC

Meters: 0.5, 1.0

Colors: 2.5Y N8 (Section 1); 7.5YR N8 (Section 2)

LITHOLOGIC DESCRIPTION

DOMINANT LITHOLOGY NANNOFOSSIL OOZE

Soupy to firm; very firm at Section 2, 10 cm

White (2.5Y N8 to 7.5YR N8)

No obvious bedding or bioturbation; faint mottling, 0.2 cm thick layer
At Section 2, 10–12 cm – more firm than rest of Sections 2 and 3.

Possible burrow in Section 3 and CC.

Minor lithologies:
(1) Foram-nanno ooze in Section 1.

Soupy, white

(2) Nanno ooze with micronodules

Same as dominant litho. but has darker streaks and mottles

SMEAR SLIDE SUMMARY (%):

	1, 68	2, 10	CC
	M	D	M
Composition:			
Feldspar	Tr	Tr	Tr
Heavy minerals	–	–	Tr
Clay	10	10	9
Opaques	–	Tr	–
Micronodules	–	–	1?
Carbonate unspec.	2	3	3
Foraminifers	10	1	1
Calc. nannofossils	78	85	85
Fish remains	–	Tr?	–
Other	–	Tr	–

Carbonate Bomb (%):
1, 70 = 90

SITE 558 HOLE CORE 10 CORED INTERVAL 243.5–253.0 m

TIME – ROCK UNIT	BIOSTRATIGRAPHIC ZONE	FORAMINIFERS	NANNOFOSSILS	RADIOLARIANS	DIATOMS	SECTION	METERS
middle Miocene	N7 (middle Miocene) CN5 (NN6–7) *D. exilis* zone (middle Miocene)	AG	AG			1	0.5, 1.0
						CC	

GRAPHIC LITHOLOGY

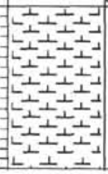

DRILLING DISTURBANCE / SEDIMENTARY STRUCTURES / SAMPLES

LITHOLOGIC DESCRIPTION

2.5Y N8
to
7.5YR N8

DOMINANT LITHOLOGY NANNOFOSSIL OOZE

Soft to firm

White (2.5Y N8–7.5YR N8)

No bedding or bioturbation obvious; faint mottling in bottom of Section 1.

SMEAR SLIDE SUMMARY (%):

	1, 135
	D
Composition:	
Feldspar	Tr
Clay	10
Carbonate unspec.	8
Foraminifers	1
Calc. nannofossils	80
Sponge spicules	Tr
Other	Tr

Carbonate Bomb (%):
1, 70 = 89

SITE 558 HOLE CORE 11 CORED INTERVAL 253.0–262.5 m

TIME – ROCK UNIT	BIOSTRATIGRAPHIC ZONE	FORAMINIFERS	NANNOFOSSILS	RADIOLARIANS	DIATOMS	SECTION	METERS
middle Miocene	N7 (middle Miocene) CN5 (NN6–7) 9m (middle Miocene) *D. exilis* zone	CM	AG			1	0.5, 1.0
						2	
						3	
						CC	

GRAPHIC LITHOLOGY

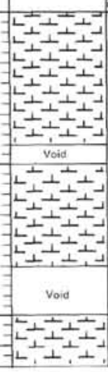

DRILLING DISTURBANCE / SEDIMENTARY STRUCTURES / SAMPLES

LITHOLOGIC DESCRIPTION

7.5YR N8
to
2.5Y N8

DOMINANT LITHOLOGY NANNOFOSSIL OOZE

White (7.5YR N8–2.5Y N8)

Soft to soupy to firm

No obvious bedding or any bioturbation

SMEAR SLIDE SUMMARY (%):

	1, 74	3, 25
Composition:		
Feldspar	1	Tr
Clay	3	9
Volcanic glass	Tr	–
Zeolite	Tr	Tr?
Carbonate unspec.	3	5
Foraminifers	2	1
Calc. nannofossils	90	84

Carbonate Bomb (%):
1, 70 = 95

SITE 558 HOLE CORE 12 CORED INTERVAL 262.5–272.0 m

TIME – ROCK UNIT	BIOSTRATIGRAPHIC ZONE	FORAMINIFERS	NANNOFOSSILS	RADIOLARIANS	DIATOMS	SECTION	METERS
Miocene; lower?/middle? Miocene	N9–N8 (base of middle Miocene) CN4 (NN5) *Sphenolithus heteromorphus* zone (middle Miocene)	CM	AG			1	0.5, 1.0
						2	
						3	
						4	
						5	
						6	
						CC	

GRAPHIC LITHOLOGY

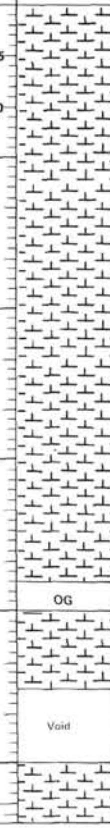

DRILLING DISTURBANCE / SEDIMENTARY STRUCTURES / SAMPLES

LITHOLOGIC DESCRIPTION

2.5Y N8
to
7.5YR N8

DOMINANT LITHOLOGY NANNOFOSSIL OOZE

White (2.5Y N8)

Firm, except soupy in Section 5

No obvious bedding or bioturbation except faint mottling at Section 1, 80 cm and possible faint color mottling randomly distributed. Dark streak at Section 2, 120 cm.

SMEAR SLIDE SUMMARY (%)

	1, 80	2, 120	3, 63	3, 90	6, 30
	M	M	D	D	D
Composition:					
Feldspar	Tr	Tr	Tr	Tr	Tr
Heavy minerals	–	–	–	–	Tr
Clay	8	8	7	6	8
Palagonite	–	Tr	–	–	–
Opaques	Tr	Tr	Tr	–	–
Micronodules	Tr–1	1	–	–	–
Carbonate unspec.	5	3	2	2	–
Foraminifers	5	5	10	1	1
Calc. nannofossils	80	80	80	90	90
Diatoms	Tr	Tr	–	–	–
Sponge spicules	Tr	Tr	Tr	Tr	Tr
Other	Tr	Tr	Tr	Tr	–

Carbonate Bomb (%):
1, 70 = 90

SITE 558 HOLE CORE 13 CORED INTERVAL 272.0–281.5 m

TIME – ROCK UNIT: Miocene; lower? middle? Miocene

BIOSTRATIGRAPHIC ZONE: N8 late early Miocene; CN4 (NN5) *Sphenolithus heteromorphus* zone (middle Miocene)

FOSSIL CHARACTER: Foraminifers AM; Nannofossils AM

SECTION: 1, 2, 3, 4, 5, 6, CC

METERS: 0.5, 1.0

GRAPHIC LITHOLOGY

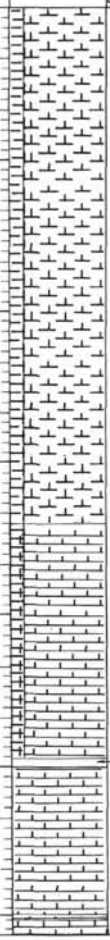

Colors: 2.5Y N8; 2.5Y N8; 10YR 8/1; 2.5Y N8; 2.5Y N8; 7.5YR 8/2 to 7.5YR 7/2; IW; 5YR 8/2; 5YR 8/2

LITHOLOGIC DESCRIPTION

DOMINANT LITHOLOGY NANNOFOSSIL OOZE TO NANNOFOSSIL CHALK

White (2.5Y N8) to pinkish white (10YR N8 and 7.5YR 8/2) to pinkish gray (7.5YR 7/2) to pinkish white (5YR 8/2).

Firm to very firm.

No obvious bedding or bioturbation

Minor lithology:
Foram-nanno ooze, similar to above with >10% forams

At top of Section 3 – slight color change pinkish chalk ooze.

At 60 cm of Section 4 – marked color change to pinkish white chalk.

SMEAR SLIDE SUMMARY (%):

	2, 45	3, 25	4, 55	4, 105	5, 90	6, 85
	M	D	D	D	M	D
Composition:						
Feldspar	Tr	Tr	Tr	Tr	1	Tr
Heavy minerals	Tr	Tr	Tr	1	Tr	–
Clay	10	12	20	10	10	10
Volcanic glass	–	Tr	–	–	–	–
Opaques	–	Tr	–	–	–	–
Carbonate unspec.	5	5	16	15	17	16
Foraminifers	15	2	3	1	10	2
Calc. nannofossils	70	80	60	70	60	70
Diatoms	–	–	Tr	–	1	Tr
Radiolarians	Tr	Tr	Tr	Tr	–	Tr
Sponge spicules	Tr	Tr	Tr	1	Tr	Tr
Silicoflagellates	Tr	–	Tr	1	–	Tr
Other	–	–	–	Tr	–	–

Carbonate Bomb (%):
3, 70 = 87

SITE 558 HOLE CORE 14 CORED INTERVAL 281.5–291.0 m

TIME – ROCK UNIT: Miocene; lower? middle? Miocene

BIOSTRATIGRAPHIC ZONE: N7–N5 (early Miocene); CN4 (NN5) *S. heteromorphus* zone (middle Miocene)

FOSSIL CHARACTER: Foraminifers AG

SECTION: 1, 2, 3, 4, 5, 6, 7, CC

METERS: 0.5, 1.0

GRAPHIC LITHOLOGY

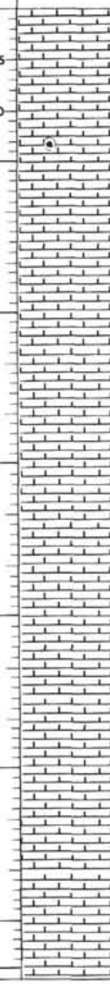

Colors: 10YR 8/3; 7.5YR 8/2; 10YR 8/3; 7.5YR 8/2; 10YR 8/3; 7.5YR 8/2; 10YR 8/3; 7.5YR 8/2; 10YR 8/3; 7.5YR 8/2; 10YR 8/3; 7.5YR 8/2

LITHOLOGIC DESCRIPTION

DOMINANT LITHOLOGY NANNOFOSSIL CHALK

Very pale brown (10YR 8/3) grades to the dominant color of pinkish white (7.5YR 8/2)

Occasional black streaks (nodules?)

Chalk are usually fractured by drilling with ocassionally soupy zones

No obvious bedding

SMEAR SLIDE SUMMARY (%):

	1, 95	3, 5	4, 110	5, 35	6, 40
	D	M			
Composition:					
Feldspar	Tr	Tr	Tr	Tr	Tr
Clay	15	15	10	14	10
Micronodules	Tr	1	Tr	Tr	Tr
Carbonate unspec.	1	1	8	1	10
Foraminifers	3	2	10	5	3
Calc. nannofossils	80	80	70	80	75
Diatoms	Tr	–	Tr	Tr	Tr
Radiolarians	Tr	Tr	Tr	Tr	Tr
Sponge spicules	Tr	Tr	Tr	Tr	Tr
Silicoflagellates	Tr	Tr	Tr	Tr	–

Carbonate Bomb (%):
1, 5 = 70 6, 2 = 74
1, 42 = 88 6, 38 = 88

SITE 558 HOLE CORE 15 CORED INTERVAL 291.0–300.5 m

TIME – ROCK UNIT	BIOSTRATIGRAPHIC ZONE	FOSSIL CHARACTER: FORAMINIFERS	NANNOFOSSILS	RADIOLARIANS	DIATOMS	SECTION	METERS
Miocene / lower Miocene	N7–N5 (early Miocene) CN3 (NN3–4) *Helicosphaera ampliaperta* zone (late early Miocene)	AG	AG			1, 2, 3, 4, 5, 6	0.5, 1.0

GRAPHIC LITHOLOGY

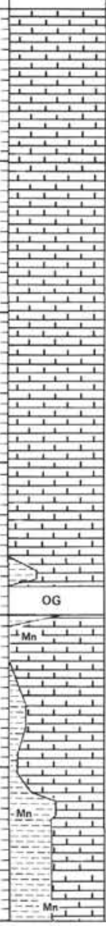

DRILLING DISTURBANCE / SEDIMENTARY STRUCTURES / SAMPLES

LITHOLOGIC DESCRIPTION

7.5YR 8/2
10YR 8/1
10YR 8/2
10YR 8/1
10YR 8/2
2.5Y N7
10YR 8/2
10YR 6/2
10YR 8/2
10YR 6/2
10YR 5/2
10YR 8/2
10YR 6/2
10YR 8/2
10YR 6/3
10YR 6/2

DOMINANT LITHOLOGIES:

(1) NANNOFOSSIL CHALK

The dominant color changes from pinkish white (7.5 YR 8/2) to light brownish gray (10YR 6/2), these colors grade to white (10YR 8/1–10YR 8/2) and occasionally to grayish brown (10YR 5/2) and light gray (2.5Y N7).

Fractured by drilling

Mottled by bioturbation to lighter color than surrounding sediment

No obvious bedding

(2) MARLY NANNOFOSSIL CHALK

Section 4, 105–112 cm and Section 6 – light brownish gray (10YR 6/2) to pale brown (10YR 6/3).

Occasional nodules (manganese?) are scattered throughout Sections 5 and 6.

SMEAR SLIDE SUMMARY (%):

	1, 75	2, 140	4, 57	5, 100	6, 40
	D	M	D	D	M
Composition:					
Feldspar	Tr	5	Tr	Tr	Tr
Heavy minerals	Tr	–	Tr	Tr	Tr
Clay	10	60	15	10	12
Volcanic glass	Tr	Tr	Tr	–	Tr
Micronodules	Tr	–	Tr	1	Tr
Carbonate unspec.	16	10	8	7	5
Foraminifers	2	–	5	2	1
Calc. nannofossils	70	25	70	79	82
Diatoms	Tr	–	Tr	–	Tr
Radiolarians	Tr	–	Tr	Tr	Tr
Sponge spicules	Tr	–	Tr	Tr	Tr
Silicoflagellates	Tr	–	Tr	Tr	Tr

Carbonate Bomb (%):
1, 122 = 88
6, 50 = 86

SITE 558 HOLE CORE 16 CORED INTERVAL 300.5–310.0 m

TIME – ROCK UNIT	BIOSTRATIGRAPHIC ZONE	FOSSIL CHARACTER: FORAMINIFERS	NANNOFOSSILS	RADIOLARIANS	DIATOMS	SECTION	METERS
Miocene / lower Miocene	N5? (early Miocene) CN2–≈NN2 *Sphenolithus belemnos* zone (late early Miocene)	AG	AM			1, 2, 3, 4, 5, 6, 7, CC	0.5, 1.0

GRAPHIC LITHOLOGY

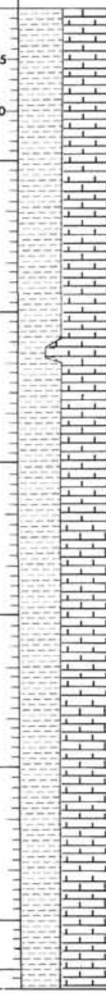

DRILLING DISTURBANCE / SEDIMENTARY STRUCTURES / SAMPLES

LITHOLOGIC DESCRIPTION

10YR 6/2
10YR 6/4
10YR 6/2
10YR 6/4
10YR 6/2
10YR N8
10YR 6/3
10YR 6/4
10YR 6/3
10YR 6/4
10YR 6/3

DOMINANT LITHOLOGY MARLY NANNOFOSSIL OOZE

Light brownish gray to light yellowish brown in alternating vague cycles; some dark micronodules

This color change is associated with reduction of carbonate to 50% (see below).

Firm to hard, very slightly deformed, friable

Bioturbated to highly bioturbated; halo burrows common; nodules. Massive bedding with vague color changes. Small fractures or slickensided faults with very minor offset (penecontemporaneous deformation).

SMEAR SLIDE SUMMARY (%):

	3, 40	3, 80	6, 80
Composition:			
Feldspar	Tr	Tr	Tr
Heavy minerals	Tr	Tr	Tr
Clay	18	45	45
Volcanic glass	–	Tr	–
Micronodules	1	1	–
Zeolite	–	–	1?
Carbonate unspec.	2	1	7
Foraminifers	1	9	8
Calc. nannofossils	78	40	42
Diatoms	Tr	1	Tr
Radiolarians	Tr	2	Tr
Sponge spicules	–	Tr	2
Silicoflagellates	–	Tr	Tr

Carbonate Bomb (%):
3, 70 = 50

SITE 558 HOLE CORE 17 CORED INTERVAL 310.0–319.5 m

TIME – ROCK UNIT: Oligocene?/Miocene

BIOSTRATIGRAPHIC ZONE: N4 (earliest Miocene) CN1–≈NN1 *Triquetrorhabdulus carinatus* zone (earliest Miocene)

FOSSIL CHARACTER: FORAMINIFERS AG; NANNOFOSSILS AM; RADIOLARIANS; DIATOMS

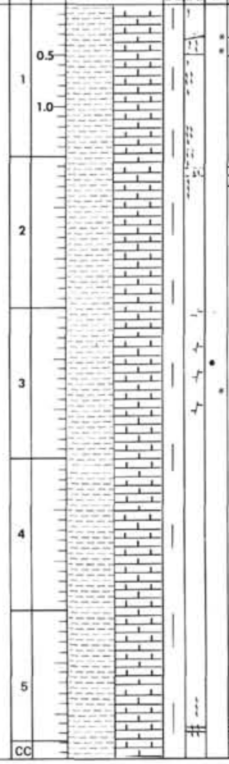

10YR 6/3
10YR 8/1
10YR 7/3
10YR 6/3
10YR 8/1
10YR 8/1
10YR 7/2
10YR 6/3
10YR 8/1
10YR 6/3

LITHOLOGIC DESCRIPTION

DOMINANT LITHOLOGY MARLY NANNOFOSSIL CHALK

Pale brown (10YR 6/3) with thin interbeds of white (10YR 8/1)

Firm to hard, but commonly fractured by drilling

Massive bedding except for thin white interbeds

Mottled throughout core

Microfaults are common in Sections 1, 2, and 3.

Nodules (manganese?) are scattered throughout Sections 1 and 2.

The white interbeds are more highly bioturbated. (Are these oxidized boundaries between cycles?)

SMEAR SLIDE SUMMARY (%):

	1, 31	1, 43	3, 80
	M	M	D
Composition:			
Feldspar	–	Tr	Tr
Heavy minerals	–	1	Tr
Clay	–	40	45
Volcanic glass	10?	Tr	Tr
Palagonite	–	–	Tr
Nodule frag.	6–10?	3	1
Carbonate unspec.	10	–	–
Foraminifers	–	1	2
Calc. nannfoossils	20	54	50
Diatoms	–	–	Tr
Radiolarians	–	–	1
Sponge spicules	–	?	Tr

Carbonate Bomb (%):
3, 58 = 50

SITE 558 HOLE CORE 18 CORED INTERVAL 319.5–329.0 m

TIME – ROCK UNIT: Oligocene? Miocene?

BIOSTRATIGRAPHIC ZONE: N4–P22 (Oligocene–Miocene) CN1–≈NN1 *T. carinatus* zone (latest Oligocene to earliest Miocene)

FOSSIL CHARACTER: FORAMINIFERS AG; NANNOFOSSILS AM; RADIOLARIANS; DIATOMS

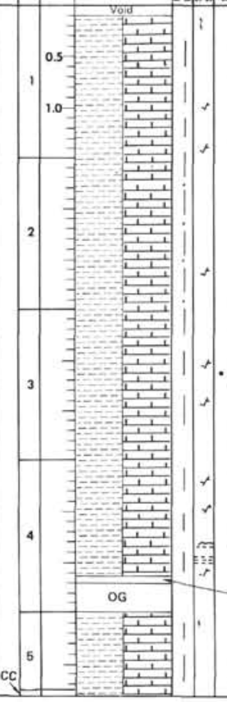

10YR 6/3
10YR 8/1
10YR 8/3
10YR 6/3
10YR 8/1
IW
10YR 6/3

LITHOLOGIC DESCRIPTION

DOMINANT LITHOLOGY MARLY NANNOFOSSIL CHALK

Pale brown (10YR 6/3) with a small layer of lighter colors in Section 4.

Firm to hard, but commonly fractured by drilling

Massive bedding except for Section 4, 80–100 cm.

Mottled throughout core

Microfaults are common throughout core

SMEAR SLIDE SUMMARY (%):

	3, 80	4, 87
	D	M
Composition:		
Feldspar	Tr	Tr
Heavy minerals	Tr	Tr
Clay	43	4
Volcanic glass	–	Tr
Palagonite	–	Tr
Opaques	Tr	–
Micronodules	1	2
Zeolite	Tr	Tr
Foraminifers	5	5
Calc. nannofossils	44	5
Diatoms	Tr	Tr
Radiolarians	2	2
Sponge spicules	Tr	Tr
Silicoflagellates	Tr	–

Carbonate Bomb (%):
3, 68 = 49

SITE 558 HOLE CORE 19 CORED INTERVAL 329.0–338.5 m

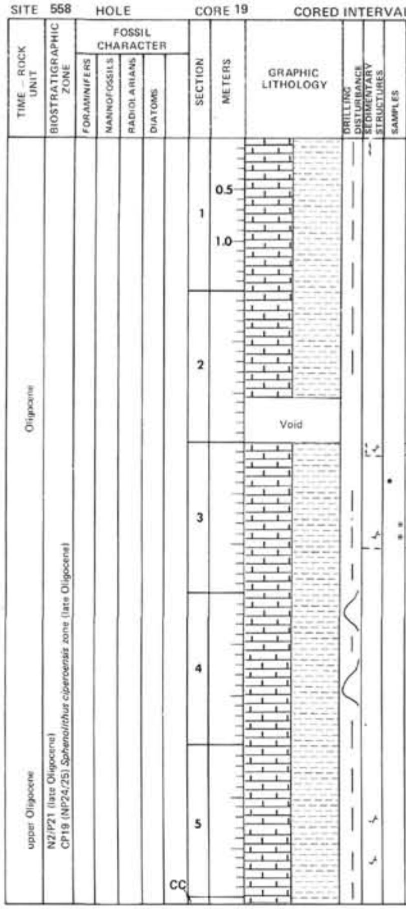

10YR 6/4
10YR 6/4
10YR 5/4
10YR 6/4
10YR 5/4
10YR 6/4
10YR 6/4

LITHOLOGIC DESCRIPTION

DOMINANT LITHOLOGY MARLY NANNOFOSSIL CHALK

Light yellowish brown (10YR 6/4) grading to yellowish brown (10YR 5/4)

Firm to hard but commonly fractured by drilling

Massive bedding with fine, irregular laminations of darker sediment. Darker seams or laminations may be dissolution boundaries – i.e. bedding planes with clay residue.

Mottled throughout core (bioturbation).

Microfaults are common in Sections 3 and 5.

SMEAR SLIDE SUMMARY (%):

	3, 80	3, 92
	D	D
Composition:		
Feldspar	Tr	Tr
Heavy minerals	Tr	Tr
Clay	46	45
Volcanic glass	Tr	Tr
Palagonite	–	Tr
Micronodules	1	–
Zeolite	–	2?
Foraminifers	3	1
Calc. nannofossils	45	48
Diatoms	Tr	–
Radiolarians	2	2
Sponge spicules	Tr	Tr
Silicoflagellates	Tr	–

Carbonate Bomb (%):
3, 40 = 48

SITE 558 HOLE CORE 20 CORED INTERVAL 338.5–348.0 m

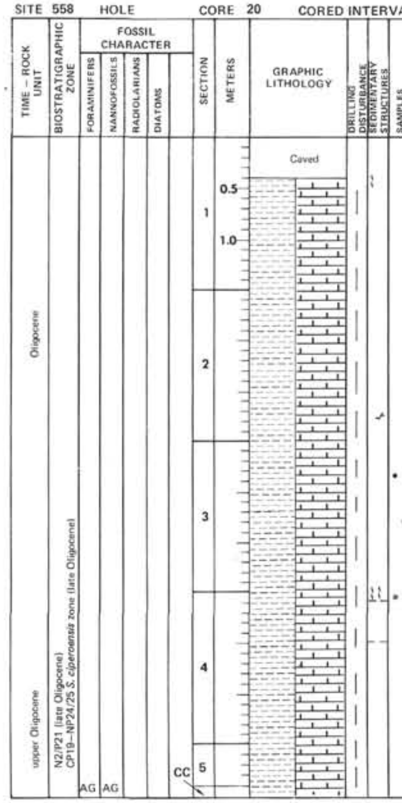

10YR 6/4
10YR 5/4
10YR 6/4
10YR 5/4
10YR 6/4
10YR 6/4

LITHOLOGIC DESCRIPTION

DOMINANT LITHOLOGY MARLY NANNOFOSSIL CHALK

Light yellowish brown (10YR 6/4) grading to yellowish brown (10YR 5/4)

Firm to hard, but commonly fractured by drilling

Massive bedding with occasional fine, darker laminations

Mottled throughout core

Microfaults in Section 2

Trace of dolomite crystals

SMEAR SLIDE SUMMARY (%):

	3, 80	4, 8
Composition:		
Feldspar	Tr	Tr
Heavy minerals	Tr	Tr
Clay	50	49
Volcanic glass	Tr	–
Micronodules	Tr–1	1
Zeolite	Tr–1	2
Foraminifers	5	1
Calc. nannofossils	41	45
Diatoms	1	–
Radiolarians	1	1
Sponge spicules	–	1?
Dolomite	Tr	–

Carbonate Bomb (%):
3, 40 = 46

SITE 558 HOLE CORE 21 CORED INTERVAL 348.0–357.5 m

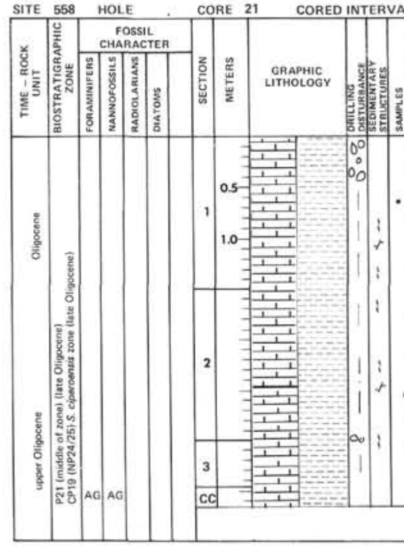

cavings

10YR 6/4
to
10YR 6/3

LITHOLOGIC DESCRIPTION

DOMINANT LITHOLOGY MARLY NANNOFOSSIL CHALK

Soupy to hard, drilling fractures

Light yellowish brown (10YR 6/4 to 10YR 6/3)

Faint mottling and bioturbation; burrows

Massive bedding

SMEAR SLIDE SUMMARY (%):

	2, 105
Composition:	
Feldspar	Tr
Heavy minerals	Tr
Clay	52
Micronodules	Tr
Zeolite	Tr
Carbonate unspec.	2
Foraminifers	8
Calc. nannofossils	37
Radiolarians	Tr

Carbonate Bomb (%):
1, 70 = 47

SITE 558 HOLE CORE 22 CORED INTERVAL 357.5–367.0 m

TIME-ROCK UNIT	BIOSTRATIGRAPHIC ZONE	FORAMINIFERS	NANNOFOSSILS	RADIOLARIANS	DIATOMS	SECTION	METERS
upper Oligocene / Oligocene	P21 (lower part of zone) (late Oligocene) CP19a–NP24 *S. ciperoensis* zone–*Cyclicargolithus floridanus* subzone (late Oligocene)	AG	AG			1, 2, 3, 4	0.5, 1.0

GRAPHIC LITHOLOGY / DRILLING DISTURBANCE / SEDIMENTARY STRUCTURES / SAMPLES

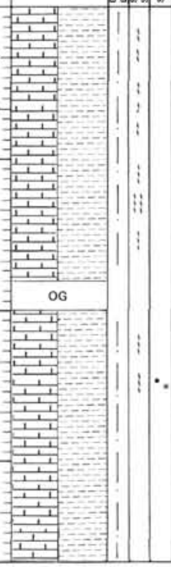

LITHOLOGIC DESCRIPTION

10YR 6/4

10YR 6/4

DOMINANT LITHOLOGY MARLY NANNOFOSSIL CHALK

Soft to hard, fractured by drilling

Light yellowish brown (10YR 6/4)

Burrows, 10YR 8/4

Massive bedding with faint mottling and bioturbation

SMEAR SLIDE SUMMARY (%):

	3, 80
Composition:	
Feldspar	Tr
Heavy minerals	Tr
Clay	52
Zeolite	Tr
Carbonate unspec.	2
Foraminifers	8
Calc. nannofossils	36
Radiolarians	1

Carbonate Bomb (%):
3, 70 = 46

SITE 558 HOLE CORE 23 CORED INTERVAL 367.0–376.5 m

TIME-ROCK UNIT	BIOSTRATIGRAPHIC ZONE	FORAMINIFERS	NANNOFOSSILS	RADIOLARIANS	DIATOMS	SECTION	METERS
upper Oligocene / Oligocene	P21 (late Oligocene) CP19a–NP24 (late Oligocene)	AG	AM			1, 2, 3, 4, 5, 6, 7	0.5, 1.0

GRAPHIC LITHOLOGY / DRILLING DISTURBANCE / SEDIMENTARY STRUCTURES / SAMPLES

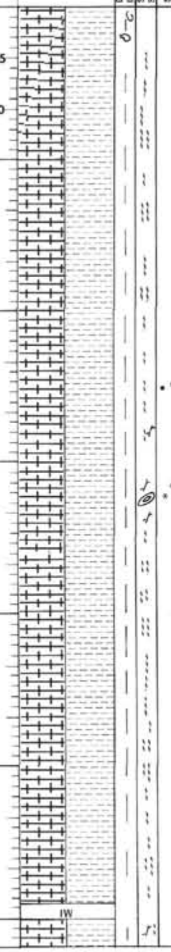

LITHOLOGIC DESCRIPTION

10YR 6/4

smear slide in burrow

burrow

DOMINANT LITHOLOGY MARLY FORAM NANNOFOSSIL CHALK

Light yellowish brown (10YR 6/4)

Fractured by drilling, firm to hard

Faint mottling bioturbation and burrows of very pale brown (10YR 8/3) material, otherwise massive bedding

Faint darker streaks and darker brown (10YR 5/4) mottling at Section 5, 5 cm.

SMEAR SLIDE SUMMARY (%):

	3, 80 D	4, 28 M	4, 33 M	5, 5 M
Composition:				
Feldspar	Tr	Tr	Tr	Tr
Heavy minerals	Tr	Tr	Tr	Tr
Clay	51	46	46	48
Volcanic glass	–	–	Tr	Tr
Palagonite	–	–	Tr	–
Micronodules	Tr	1	Tr	Tr
Zeolite	Tr	1	2	Tr
Carbonate unspec.	–	–	–	3
Foraminifers	2	10	10	2
Calc. nannofossils	43	40	40	44
Radiolarians	Tr	1	Tr	Tr
Sponge spicules	–	–	–	1
Silicoflagellates	Tr	Tr	–	–
Dolomite	–	Tr	–	Tr

Carbonate Bomb (%):
3, 80 = 47

SITE 558 HOLE CORE 24 CORED INTERVAL 376.5–386.0 m

TIME – ROCK UNIT	BIOSTRATIGRAPHIC ZONE	FORAMINIFERS	NANNOFOSSILS	RADIOLARIANS	DIATOMS	SECTION	METERS
upper Oligocene	P20–P19 (boundary between early and late Oligocene) CP18–NP23 (early late Oligocene)	AG	AM			1, 2, 3, 4	0.5, 1.0

GRAPHIC LITHOLOGY / DRILLING DISTURBANCE / SEDIMENTARY STRUCTURES / SAMPLES

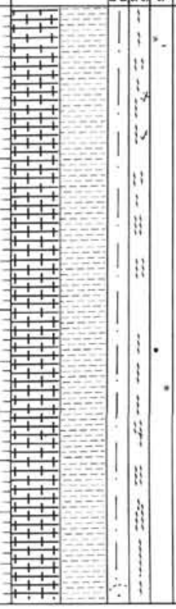

LITHOLOGIC DESCRIPTION

10YR 6/4

DOMINANT LITHOLOGY MARLY FORAM NANNOFOSSIL CHALK

Light yellowish brown (10YR 6/4)

Firm to hard, drilling fracture

Massive bedding

Numerous burrows (elliptical parallel bedding plane) surrounded by 10YR 8/3 (light). Faint mottling – bioturbation.

SMEAR SLIDE SUMMARY (%):

	1, 32	3, 80
	M	D
Composition:		
Feldspar	Tr	Tr
Heavy minerals	Tr	Tr
Clay	45	50
Volcanic glass	Tr	–
Micronodules	Tr	1
Zeolite	Tr	Tr
Carbonate unspec.	2	2
Foraminifers	10	10
Calc. nannofossils	40	33
Diatoms	–	Tr
Radiolarians	1	Tr
Dolomite	Tr	–

Carbonate Bomb (%):
3, 45 = 45

SITE 558 HOLE CORE 25 CORED INTERVAL 386.0–395.5 m

TIME – ROCK UNIT	BIOSTRATIGRAPHIC ZONE	FORAMINIFERS	NANNOFOSSILS	RADIOLARIANS	DIATOMS	SECTION	METERS
lower? upper? Oligocene	*Sphenolithus predistentus* zone (early late to late early Oligocene); P19 (late early Oligocene) CP17 (NP23)	AM	AM			1, 2, 3, 4, 5, 6, CC	0.5, 1.0

GRAPHIC LITHOLOGY / DRILLING DISTURBANCE / SEDIMENTARY STRUCTURES / SAMPLES

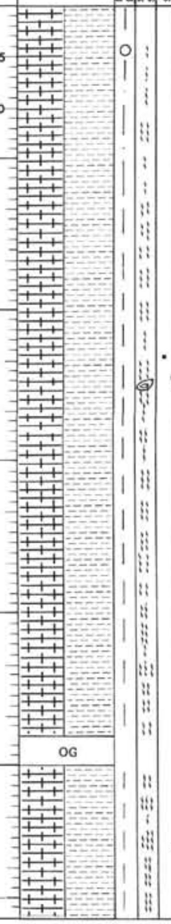

LITHOLOGIC DESCRIPTION

10YR 6/4

DOMINANT LITHOLOGY MARLY FORAM NANNOFOSSIL CHALK

Light yellowish brown (10YR 6/4)

Hard with soft to firm intervals

Massive bedding

Faint mottling – bioturbation. Intense burrowing; burrows filled with very pale brown (10YR 8/3); round or elliptical

Drilling fracture

SMEAR SLIDE SUMMARY (%):

	3, 70	3, 80	6, 80
	M	D	D
Composition:			
Feldspar	Tr	Tr	Tr
Heavy minerals	Tr	Tr	Tr
Clay	45	47	46
Volcanic glass	–	Tr	Tr
Micronodules	Tr	1	Tr
Zeolite	Tr	Tr	2
Foraminifers	10	10	8
Calc. nannofossils	40	36	37
Radiolarians	1	1	1
Dolomite	3	5	10

Carbonate Bomb (%):
3, 80 = 47

base

SITE 558 HOLE CORE 26 CORED INTERVAL 395.5–405.0 m

TIME – ROCK UNIT	BIOSTRATIGRAPHIC ZONE	FORAMINIFERS	NANNOFOSSILS	RADIOLARIANS	DIATOMS	SECTION	METERS
lower Oligocene	P18 (early Oligocene) CP16b, c (NP22–21) early Oligocene	AM	AM			1, 2, 3, 4, 5, CC	0.5, 1.0

GRAPHIC LITHOLOGY

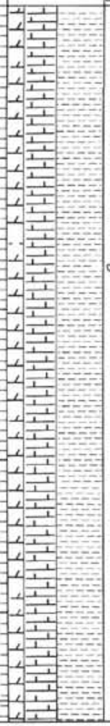

caving

10YR 6/4

10YR 5/4

10YR 5/4

LITHOLOGIC DESCRIPTION

DOMINANT LITHOLOGY MARLY DOLOMITIC NANNO CHALK

Brown (10YR 6/4 to 10YR 5/4) becoming darker towards base of core

Darker (10YR 5/4) at bottom of Section 5

Firm to hard

Intense bioturbation, massive bedding

Drilling fracture

The presence of authigenic dolomite rhombs increases in this core from the small percentages seen in Core 25.

SMEAR SLIDE SUMMARY (%):

	1, 100 D	2, 5 D	3, 80 D	4, 60 D	4, 110	5, 75
Composition:						
Feldspar	Tr	Tr	Tr	Tr	Tr?	Tr
Heavy minerals	Tr	Tr	Tr	Tr	Tr	–
Clay	50	51	49	50	50	51
Volcanic glass	Tr	Tr	Tr	–	–	Tr
Palagonite	–	–	Tr	–	–	–
Micronodules	1	Tr	Tr	1	1	Tr
Carbonate unspec.	1	1	1	2	1	–
Foraminifers	2	5	2	2	3	2
Calc. nannofossils	20	20	15	20	0	7
Radiolarians	?	2	2	Tr	Tr	1
Silicoflagellates	–	–	–	Tr	Tr	–
Dolomite	25	20	30	25	25	10

Carbonate Bomb (%):
3, 79 = 47

SITE 558 HOLE CORE 27 CORED INTERVAL 405.0–414.5 m

TIME – ROCK UNIT	BIOSTRATIGRAPHIC ZONE	FORAMINIFERS	NANNOFOSSILS	RADIOLARIANS	DIATOMS	SECTION	METERS
lower Oligocene	CP16 (NP21) *Helicosphaera reticulata* zone *Coccolithus subdistinctus* subzone (early Oligocene)		AM			1, 2, 3	0.5, 1.0

GRAPHIC LITHOLOGY

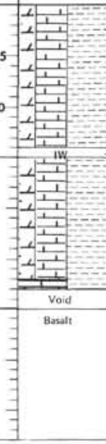

10YR 5/4

10YR 5/3

10YR 4/4

10YR 5/3

IW

10YR 8/6

LITHOLOGIC DESCRIPTION

DOMINANT LITHOLOGY MARLY DOLOMITIC NANNO CHALK

Firm to hard

Brown (10YR 5/4) to yellowish brown (10YR 5/3)

Mottled and bioturbated throughout, with dark specks in bioturbated sections

Bioturbation increases downward and color also darkens from 10YR 5/4 to 10YR 5/6.

Intense bioturbation in Section 2.

Authigenic dolomite rhombs present throughout (15–20%).

Minor lithology:
Marly nannofossil limestone

Pale yellowish brown, as broken pieces just above basalt. It is altered limestone.

SMEAR SLIDE SUMMARY (%):

	1, 40 D	1, 120 M	1, 135 D	2, 20	2, 80	2, 120 D
Composition:						
Feldspar	Tr	Tr	Tr	Tr	Tr	Tr
Heavy minerals	Tr	Tr	Tr	Tr	Tr	Tr
Clay	48	57	56	56	56	56
Volcanic glass	–	Tr	–	–	Tr	–
Palagonite	–	Tr	Tr	Tr	–	1
Micronodules	1	1	1	Tr	Tr	Tr
Zeolite	Tr	–	–	Tr	–	Tr
Foraminifers	1	1	1	2	2	2
Calc. nannofossils	25	20	20	20	20	30
Radiolarians	–	–	1	1	1	Tr
Sponge spicules	–	Tr	–	–	–	–
Silicoflagellates	–	–	–	–	Tr	–
Dolomite	15	20	20	20	20	10

Carbonate Bomb (%):
1, 78 = 41

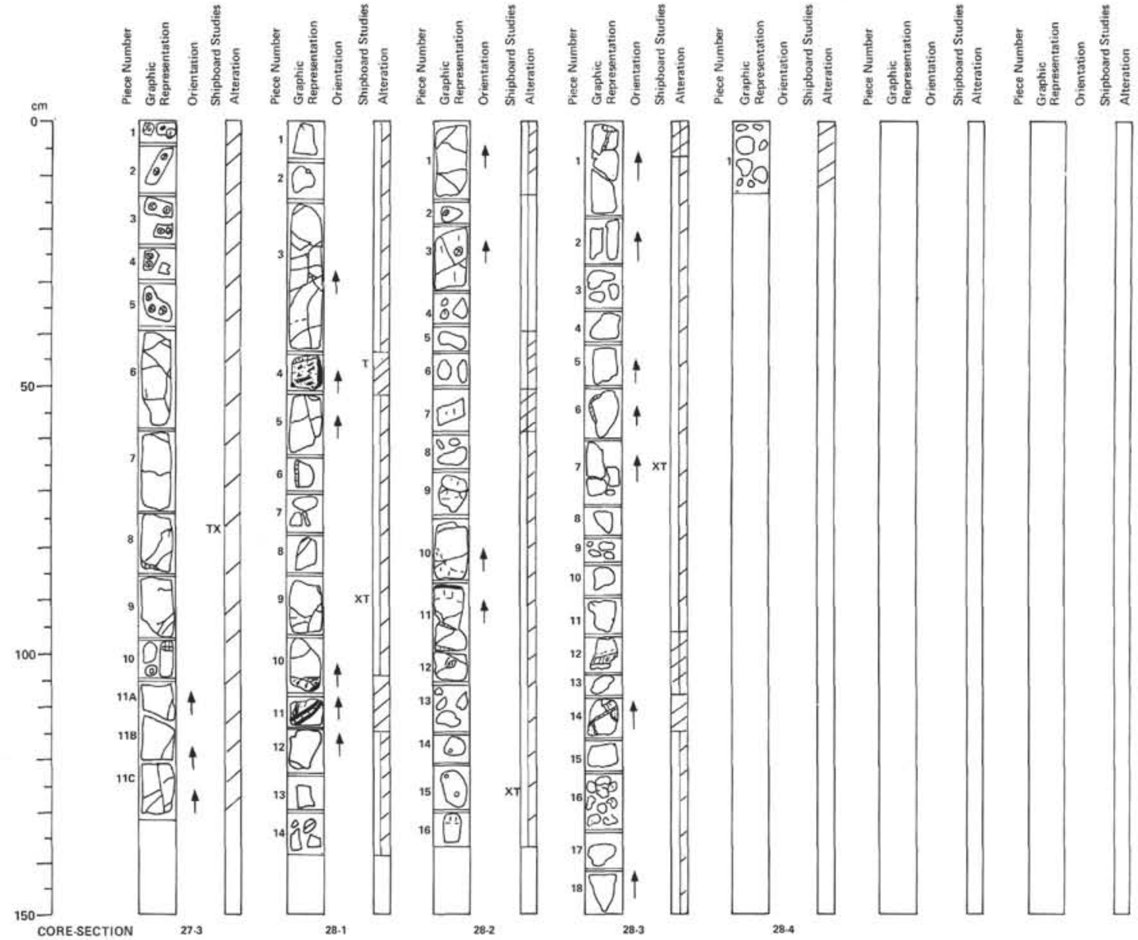

SITE 558, CORE 27 Depth 405.0–414.5 m

SECTION 3

0–105 cm: The pieces in the interval are of questionable order.

Pieces 1–5: Variolitic texture. The varioles range from 1–6 mm in diameter. The varioles range from dark brown in the center to light brown at the edges. Some pockets of devitrified glass (gray) lie between the varioles.

Piece 6–9: Fine grained dark gray (2.5YR N4/0) aphyric basalt. There are many irregular and undulating fractures filled with calcite. Alteration is more extensive in the basalt along the fractures. Vesicles (< 1 mm) are rare and filled.

Piece 10: Badly altered aphyric basalt with calcite filled fractures. One edge has zoned calcite sedimentation: 1) brick red fine grained calcite with mixed layer clay mineral (XRD determinates) , 2) transparent sparry calcite, and 3) fine grained white calcite.

Piece 11: Has the same description as Pieces 6–9 of this section (3).

SITE 558, CORE 28 Depth 414.5–423.5 m

SECTION 1

HIGHLY FRACTURED APHYRIC PILLOW BASALTS

Pieces 1–3: Fine grained aphyric basalt; color ranges from dark gray (7.5YR N4/0) in Pieces 1 and 2 to gray (7.5YR N5/0) in Piece 3. Piece 3 appears strongly fractured – some small veins are filled with calcite cement. Vesicles are rare; in Piece 2 are some round vesicles filled with clay (size ~ 2.0–2.5 mm) some are empty (size <0.5 mm).

Piece 4: Hyaloclastite interpillow breccia (basalt-glass-breccia). Elongated glass pieces (size 1–30 mm) are aligned horizontally and are fresh. Only their rims and some very small breccia pieces are altered to brown clay. One vertical oriented glass piece shows multiple glass rinds separated from one another by clay. At the top of this piece occurs transparent calcite cement. Matrix of breccia is limestone.

Pieces 5–14: Fine-grained aphyric basalt; color gray (7.5YR N5/0). Fractures are common. Vesicles are very rare and sometimes filled with clay. Piece 9 shows transition from vitric basalt at the top to tachylitic(?) devitrified basalt. At the bottom of Pieces 10 and 11 occur pillow rinds of fresh glass – the rind of Piece 11 is a multiple one; the glass is separated by clay and calcite.

SECTION 2

FRACTURED APHYRIC PILLOW BASALTS

Light gray (7.5YR 6/0), mottled brown alteration along some broken and fractured surfaces. Scattered vesicles partially filled by white or gray(?) zeolites.

16–36 and 82–88 cm: mottled gray–light brown (10YR 6/4) variolitic basalt (close to pillow margins).

Thin Section at 122–124 cm: Aphyric basalt, intersertal texture, fine grained, 35% plagioclase (0.1–0.4 mm) skeletal to accicular, 20% granular clinopyroxene (0.01–0.05 mm), 3% granular magnetite (0.01–0.04 mm), 5% devitrified glass, 36% mesostasis, 1% vesicles.

SECTION 3

FRACTURED APHYRIC BASALT (PILLOWS?)

Light gray (7.5YR N6/0). Calcite veins occasionally found; slight alteration to light gray brown (7.5YR N6/2).

51–59 cm: Slightly altered basalt, slightly brown–gray in color. Small plagioclase crystals 1–2 mm diameter visible (7.5YR N6/2). Some dark patches noted; identification uncertain.

Pieces 3, 9, and 16: Actually collections of small pebble-sized basalt fragments (Similar to Sections 1 and 2).

Thin Section at 61–63 cm: Aphyric to sparsely phyric hyalopilitic, tachylitic basalt.

SECTION 4

FRACTURED APHYRIC BASALT

Weathered brown along fractures.

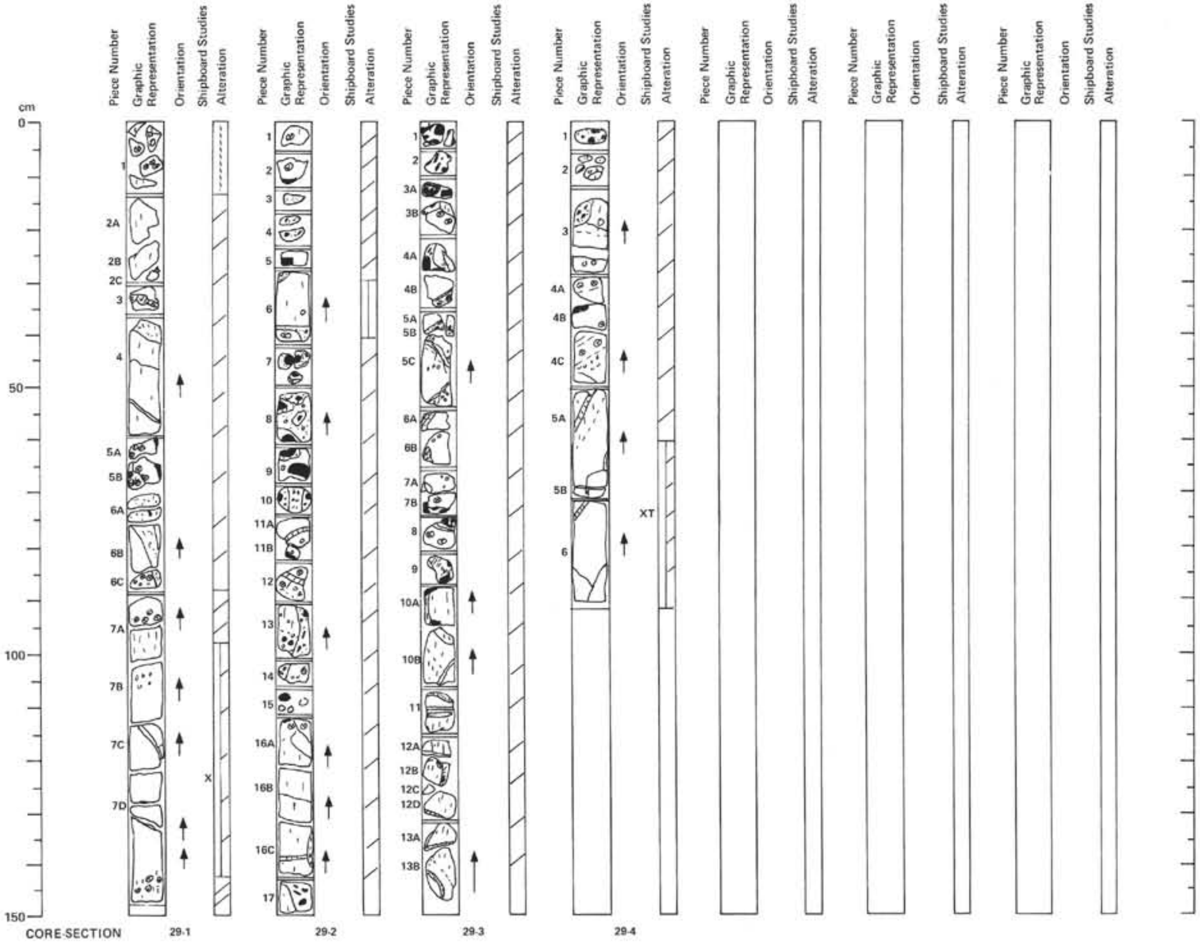

SITE 558, CORE 29 Depth 423.5–432.5 m

SECTION 1

APHYRIC PILLOW BASALT

0–13 cm: Strongly altered variolitic basalt.

13–87 cm: Moderately altered variolitic basalt with limestone fillings in fractures ( ). Fine grained brownish gray (2.5Y 5/2).

87–146 cm: Single pillow with gray brown (10YR 5/2) variolitic edges (top 89–92 cm, bottom 140–146 cm), fine grained, gray (1.5Y N5).

94–96 cm: ~5% vesicles filled with black clay.

SECTION 2

APHYRIC PILLOW BASALT AND INTERPILLOW BRECCIA

0–110 and 143–149 cm: Interpillow breccia:

1) Aphanitic, aphyric black basalt clasts, sparsely vesicular, altered gray green at edges. Sometimes grading into 2) (unshaded).

2) Fine grained aphyric basalt , medium gray (2.5Y 5/0) (pillow interior), generally altered mottled gray and light brown (10YR 6/2) (shown by vertical dashes).

3) Smaller (<2 cm) angular glass fragments, largely palagonitized, but most with fresh centers.

4) Limestone matrix (dotted), buff colored (7.5YR 7/2) lithified limestone with small calcite veins (diagonally hatched).

110–140 cm: Pillow of dark gray (5Y 4/0) aphyric basalt with black aphanitic upper margin (minor glass) and narrow (4 cm) gray brown (10YR 4/2) variolitic zone.

SECTION 3

PILLOW BASALT FLOW, WITH INTERSPERSED LIMESTONE CEMENTED INTERPILLOW BRECCIA

As in Sections 1 and 2 (full description Section 2).

42–51 cm, Piece 5C: Aphyric basalt with green (10G N8/2) discolored limestones matrix, glass fragments set within. Vesicles filled with calcite; irregular black patches interspersed.

54–63 cm: Aphyric basalt with a lighter shade of green than above.

SECTION 4

0–32 cm: Interpillow breccia with sparry calcite cement.

33–88 cm: Single aphyric fine grained basalt pillow as in Section 2.

20–27 cm: Occasional large (5–10 mm) calcite filled vesicles.

43–48 cm: Vesicular (~ 5%) zone inside variolitic zone. Vesicles (1–2 mm) either unfilled or calcite filled.

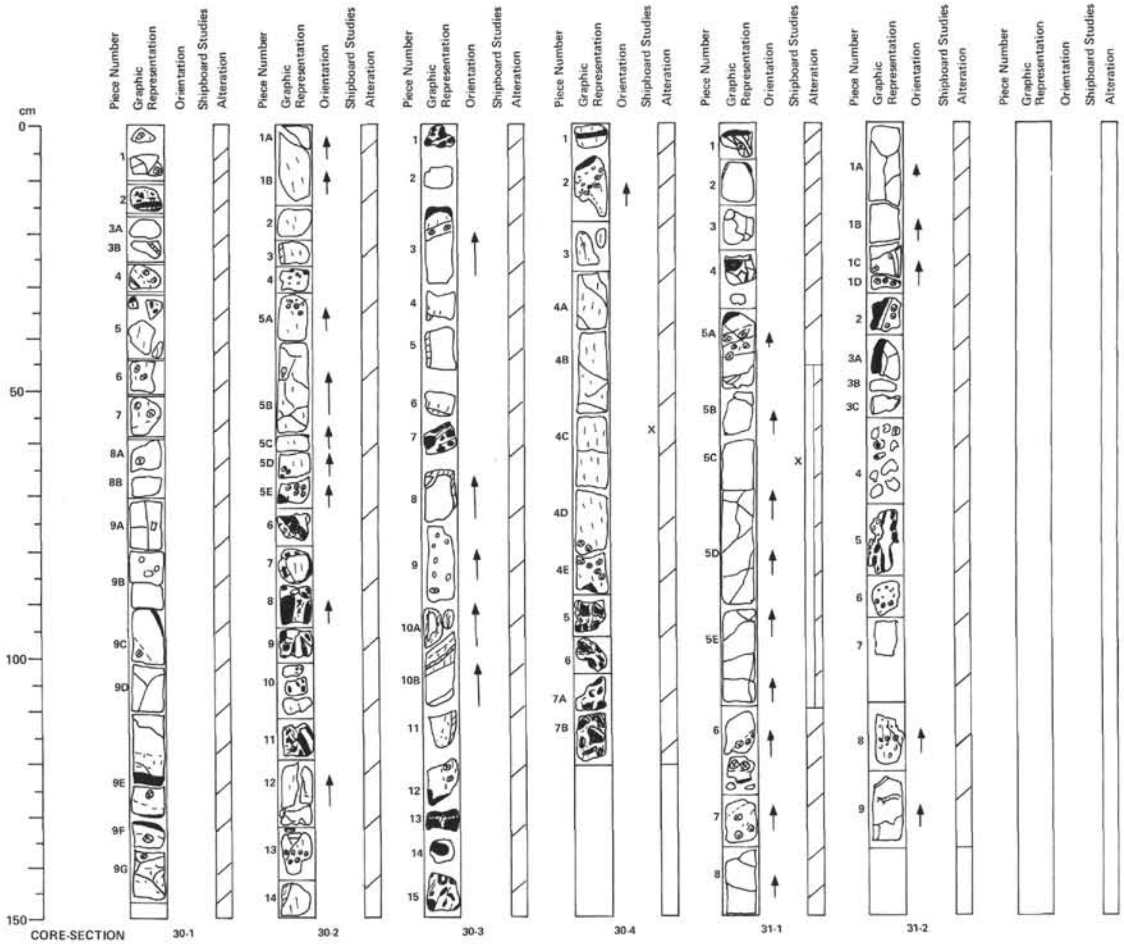

SITE 558, CORE 30 — Depth 432.5–441.5 m

SECTION 1

APHYRIC PILLOW BASALT AND INTERPILLOW BRECCIA

0–64 cm: Black aphyric aphanitic basalt grading to grayish brown (10YR 6/2) variolitic basalt forming broken pillow fragments. Matrix of smaller (<2 cm) angular glass fragments largely palagonitized cemented by clear sparry calcite.

64–145 cm: Fine grained aphyric basalt, dark gray (2.5Y 4/0) altered to gray-brown (10YR 5/2) along fractures. Pillow margins grade through variolitic,and aphanitic zones to glass where shown. Irregular, calcite filled(?, vesicles form ~ 5% of rock from 75–85 cm, scattered elsewhere. Needles of zeolite(?) in calcite.

Note slight darkening (2.5Y 5/0–2.5Y 4/0) of fine grained basalt from Core 29 to Core 30.

SECTION 2

APHYRIC PILLOW BASALT

0–25 cm: Medium gray (7.5YR N5), fine grained basalt with calcite in fractures.

33–77 cm: Medium brownish gray (2.5Y N5) single pillow with yellow brown (2.5Y 6/2) variolitic edges (top 33–38 cm, bottom 66–70 cm) and 5% round empty vesicles (up to 2 mm) at top and calcite in fractures and irregular calcite and green clay filled vesicles (up to 8 mm).

72–79 cm: Interpillow breccia in calcite matrix. Many glass angular clasts, some altered to yellow brown and green clays.

79–146 cm: Fine grained grading down through variolitic zone (136–138 cm) into black aphanitic zone (138–146 cm) with calcite in fractures.

SECTION 3

APHYRIC PILLOW BASALTS AND INTERPILLOW GLASS/CALCITE BRECCIA

As in Sections 1 and 2. Pillows dark gray (2.5Y N4) in color, grading to gray brown (10YR 5/2) along fractures, to black aphanitic aphyric basalt rimmed with glass.

0–20 cm: Glass/calcite breccia (sparry calcite matrix) 2 mm to 1 cm diameter glass fragments.

20–55 cm (pillow unit): glass to variolitic aphanitic aphyric black basalt to variolitic, dark gray brown to gray aphyric basalt; inverse sequence on bottom.

64–122 cm: Single pillow unit; sequence same as for 20–55 cm pillow.

64–88 cm: Irregular vesicles, majority of which appear empty near top of segment to mostly calcite and/or clay filled.

90–120 cm: Calcite rinds on aphyric basalts get thicker and more involved.

120–125 cm: Aphyric basalt grades through variolitic texture to glassy bottom.

125–150 cm: Glass/calcite breccia as in 0–20 cm; fragments are larger, some up to ~4 cm in length.

SECTION 4

APHYRIC PILLOW BASALT

0–5 cm: Glass rim with calcite followed by aphanitic black basalt.

5–30 cm: Glass rim to aphanitic black basalt grading into fine grained medium gray (2.5Y N5) with empty vesicles in aphanitic zone and calcite filled vesicles in fine grained zone.

30–108 cm: Single pillow with no top and variolitic lower edge (79–85 cm).

108–120 cm: Interpillow breccia – fresh glass clasts in calcite matrix with rims altered to yellow brown clay.

SITE 558, CORE 31 — Depth 441,5–450.5 m

SECTION 1

Section comprises aphyric basalt; color dark gray (2.5Y N4); thin mostly calcite filled fractures are common.

Fresh glass in Pieces 1, 2, 4, 5A, and 6 partly altered to palagonite.

Variolitic texture in Pieces 2, 3, 5A, and 6. Variolites are <2 mm. Empty round vesicles occur scattered throughout Pieces 2–4 (size < 2 mm). Round vesicles in Pieces 7 and 8 are filled with calcite and clay (size <2 mm). One large elongated vesicle occurs at the bottom of Piece 8, filled half with green clay and half with calcite (size ~20 x 3 mm). Piece 5–6 is a separated pillow with chilled rinds at the top and bottom; the amount of vesicles decreases downward.

SECTION 2

APHYRIC PILLOW BASALT

0–30 cm: Bottom part of single pillow, medium gray (2.5Y N5), fine grained with medium yellow brown (10YR 6/2) very variolitic lower edge (26–28 cm) and calcite in fractures and in irregular vesicles (1%).

30–73 cm: Isolated pieces of pillow basalt. Piece 2 with variolitic edge (35–37 cm) and Piece 3A with glass rim in calcite matrix.

73–85 cm: Interpillow breccia fresh glass clasts (with yellow/orange rims) in calcite matrix and one large (2 cm) cavity with drusy calcite.

85–133 cm: More isolated pieces of pillow basalt as in 30–73 cm. Piece 6 has variolitic edge at 88–90 cm. Piece 8 has variolitic edge at 111–116 cm, plus empty vesicles (up to 4 mm) below variolitic edge and calcite filled vesicles in interior of pillow.

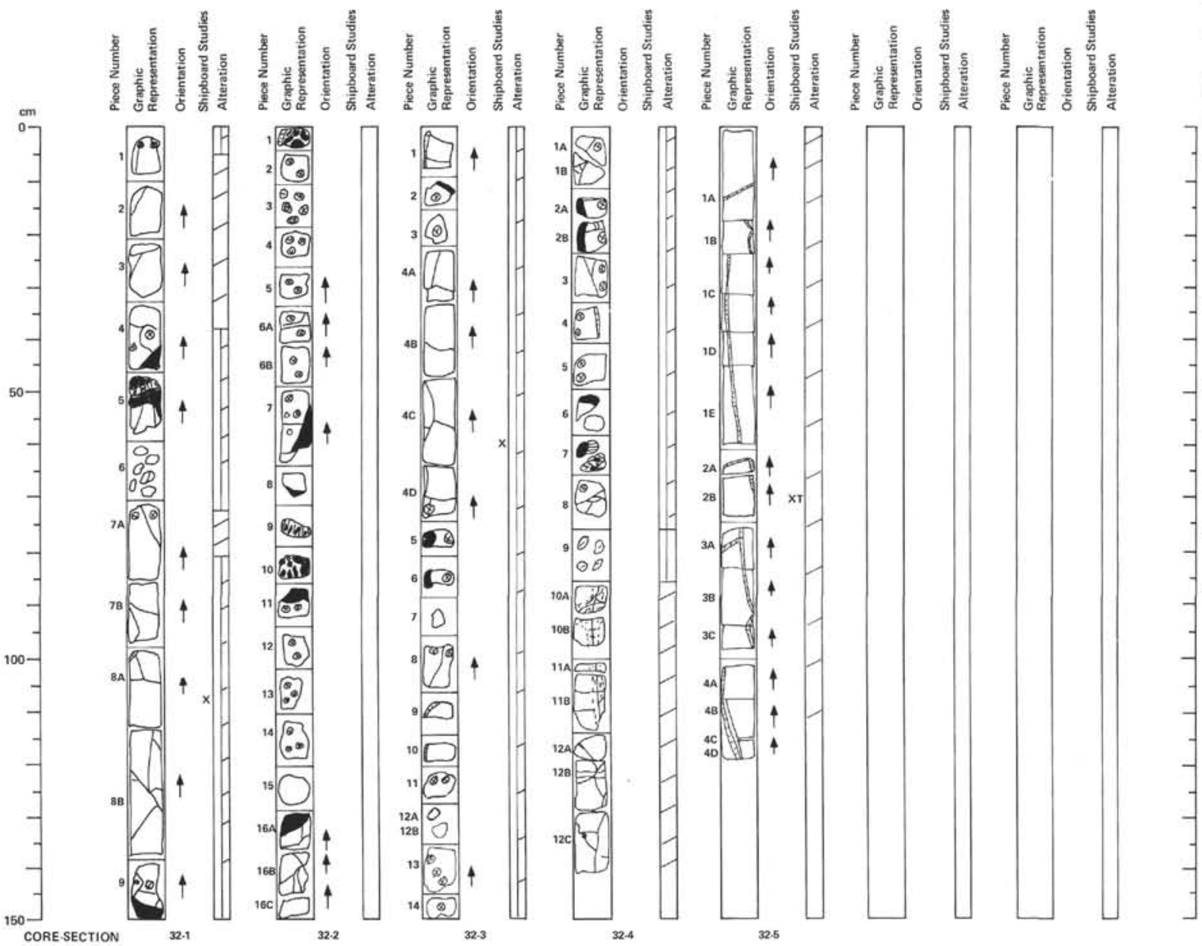

SITE 558, CORE 32 Depth 450.5–459.5 m

SECTION 1

Fresh to moderately altered aphyric pillow basalt; color dark gray (2.5Y N4/0); chilled glass rinds occur in Pieces 4, 5, and 9; close to these rinds to the interior of pillows occurs variolitic transition from vitric to fine grained crystallized basalt.

Vesicles are common and partly round (size $\lesssim$ 2 mm), partly irregular shaped (size $\lesssim$ 8 mm). In the interior of pillow (Piece 7B to upper part of Piece 8B) vesicles are rare. Vesicle filled with calcite and clay.

Fractures and veins are filled with calcite.

SECTION 2

Piece 1 is part of a chill margin with calcite veins.
Pieces 2–15 are variolitic basalt, dark gray (2.5Y N4/0). Varioles are brown.
Pieces 1, 7, 8, 9, 10, and 16A has chilled margins.
Pieces 9 and 10 have calcite between broken pieces of glass.
Pieces 16A, B, and C are fine grained aphyric gray basalt with many calcite filled fractures.
$\lesssim$1 mm calcite filled round vesicles (2%) occur in Pieces 6, 7, and 12.
$\lesssim$1 mm unfilled round vesicles (2%) occur in Pieces 2, 3, 4, 5, 8, 12, 14, and 15.

SECTION 3

Fine grained aphyric gray (7.5YR N5/0) basalt. Round vesicles up to 3.5 mm; irregular vesicles are rare (<5 mm).
Fresh glass (chilled pillow margins) in Pieces 2, 5, and 6 always accompanied by variolitic transition zone.
The whole section is strongly fractured; veins are filled with calcite ( ).

SECTION 4

0–58 cm and 65–75 cm, Pieces 1–8: Aphyric, variolitic pillow basalt with chilled rinds in Pieces 2 and 6; color dark gray (2.5YR N4/0); vesicles are common and round and empty (size $\lesssim$ 1.5 mm).

58–64 cm, Piece 7: Hyaloclastite (calcite cemented glass breccia).

75–140 cm, Pieces 9–12: Fine grained aphyric basalt, color gray (2.5YR N5/0); vesicles are rare, round, and filled (with clay?). This basalt is more altered than the upper one (in Pieces 1–8). Fractures are cemented with calcite and show partly altered zone beside them.

At 75 cm: Break? – end pillow lavas.

SECTION 5

Single flow (continues from Section 4).

Massive fine grained aphyric basalt; color gray (2.5YR N5/0); shows no vesicles; fractures and veins are filled with calcite ( ).

Frequent fine traces (healed fractures?) altered brown and fine mottled brown alteration of mesostasis(?).

Thin Section at 66–70 cm: Hyalopilitic aphyric basalt.

120 cm: End of flow.

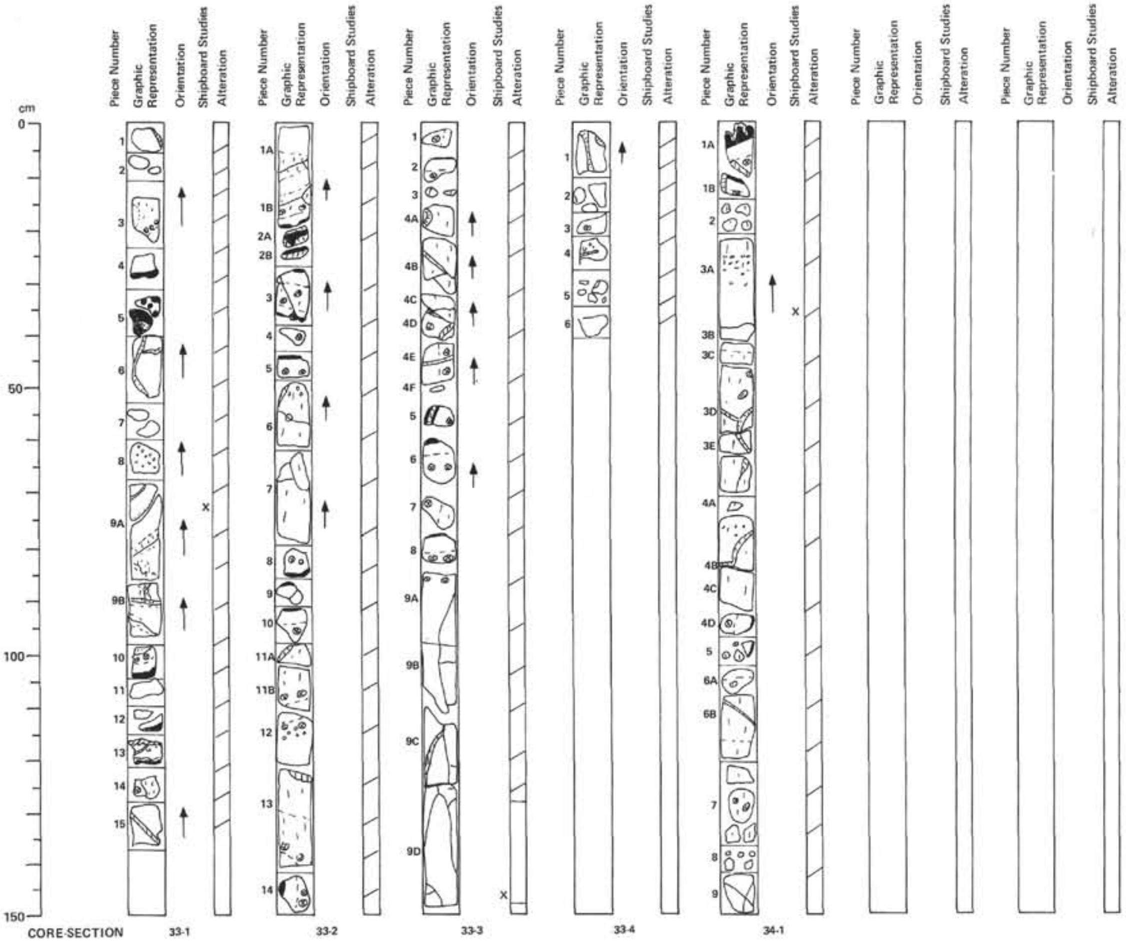

SITE 558, CORE 33 Depth 459.5–468.5 m

SECTION 1

APHYRIC PILLOW BASALT

0–32 cm: Light gray brown (10YR 6/2) aphyric basalt grading through variolitic basalt to black ophanitic aphyric basalt rimmed with glass (25–29 cm).

32–38 cm: Large glass fragments (3 mm to 4 cm long) in calcite matrix = breccia. Less cement (10 volume %), lots of glass.

59–103 cm: Pillow unit, glass at top, grading into black aphanitic aphyric basalt, then dark gray (2.5Y 4/0) aphyric basalt; bottom inverse sequence of top. Irregular vesicles throughout unit; mainly empty above variolitic zone, calcite filled below this zone through aphyric basalt.

104–113 cm: Pieces of dark gray aphyric basalt. One piece within Piece 12 has a glass rind (devitrified).

115–135 cm: Pillow unit, only top half; down through sequence to aphyric basalt.

SECTION 2

APHYRIC PILLOW BASALT

Sequence consisting of:

1) Fine grained aphyric basalt (pillow interiors) generally weathered dark grayish brown (10YR 4/2) with occasional large (5 mm), irregular calcite-filled vesicles. Small (1 mm) vesicles up to 5% may be concentrated adjacent to variolitic zones. These are filled by calcite or part filled by dark bluish gray clay (shown by vertical dashes).

2) Variolitic pale brown (10YR 6/3) basalt (crosses in circles).

3) Black aphanitic basalt adjacent to pillow rims (white).

4) Fresh basalt glass (black) generally veined by, or forming angular fragments within white calcite. Moderately palagonitized around edges (calcite diagonally hatched).

SECTION 3

APHYRIC PILLOW BASALT SEQUENCE CONTINUED

0–76 cm: Lithology and symbols as for Section 2.

76–147 cm: Single aphyric pillow. Calcite veins as shown (diagonal hatch). Calcite present also along all fractures. Lithologies as for Section 2 except fresh fine grained aphyric dark gray (7.5YR N4) basalt from 118–147 cm.

SECTION 4

APHYRIC PILLOW BASALT

Dark gray (2.5Y 4/0). Calcite rims edges of most pieces; several are veined. Vesicles scattered, <1 mm in diameter.

16–20 cm: Piece of large (diameter ~8 mm) vesicle, calcite filled.

30–34 cm: Multiple pieces of dark gray aphyric basalt.

SITE 558, CORE 34 Depth 468.5–477.5 m

SECTION 1

APHYRIC PILLOW BASALT SEQUENCE

0–13 cm, Pieces 1A, B; 91–94 cm, Piece 4D; 103–106 cm, Piece 6A: Aphyric basalt, black, aphanitic with glass rims as shown. Grading to: Variolitic basalt, light brownish gray (10YR 6/2), moving inwards from pillow margins.

15–89 and 106–150 cm: Aphyric basalt, fine grained, dark gray (7.5YR N4) grading to brown (7.5YR 4/4) with alteration, especially adjacent to fractures. This rock type represents pillow interiors. Vesicles: scattered, irregular ~ 5 mm calcite filled. Small (<1 mm) bluish gray or green clay filled concentrated (up to 5%) just inside variolitic zones.

0–10, 52–70, and 107–115 cm: Calcite veinlets (diagonal hatched).

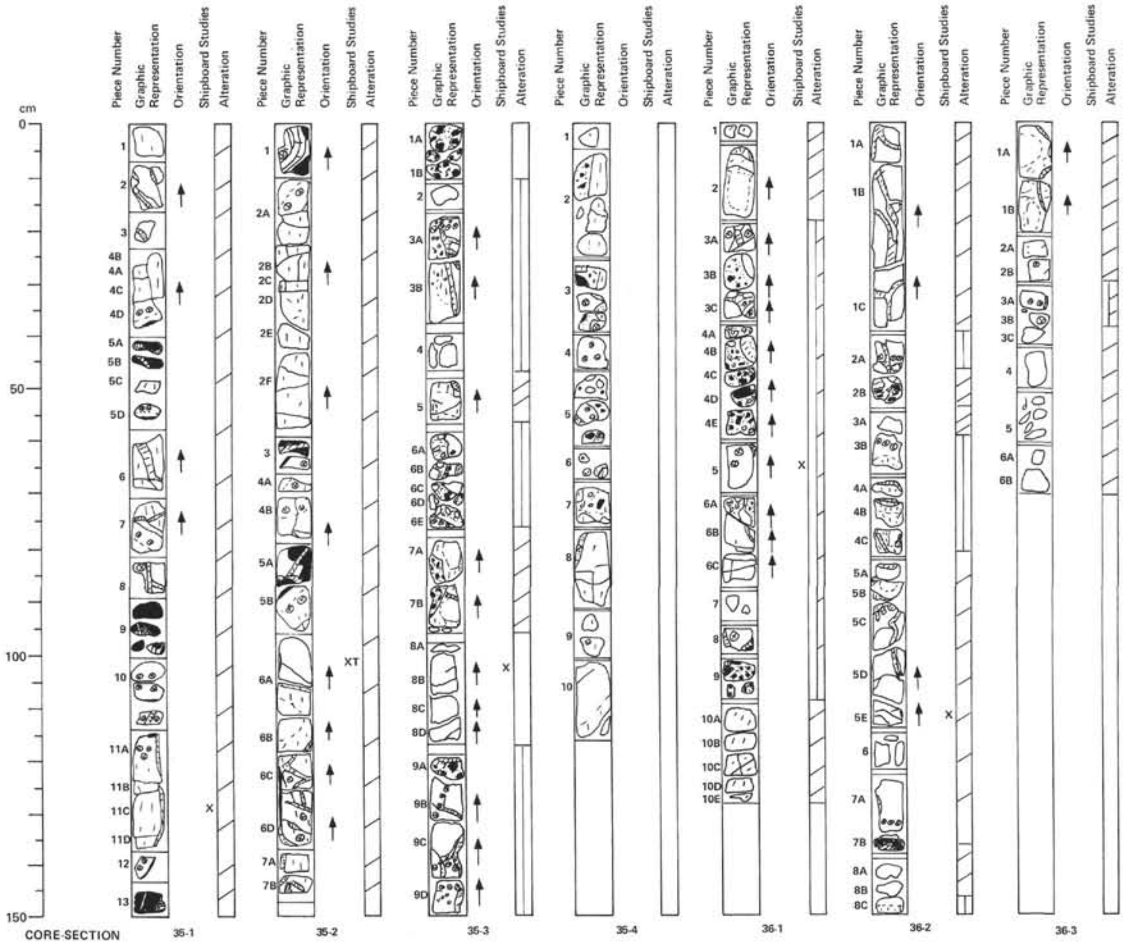

SITE 558, CORE 35 Depth 477.5–486.5 m

SECTION 1

APHYRIC PILLOW BASALT SEQUENCE

Lithologies and symbols as in Core 34, Section 1.

0–33, 58–76, and 119–135 cm: Aphyric basalt: fine-grained, altered grayish brown (10YR 5/2).

33–38, 54–57, 77–87, 100–111, and 137–147 cm: Aphyric basalt, black, aphanitic grading to variolitic basalt.

41–46, 82–98, and 144–148 cm: Aphyric black basalt glass, *moderately palagonitized and veined by calcite.*

Calcite veins throughout as shown and abundance is greater than in previous cores.

SECTION 2

APHYRIC PILLOW BASALT SEQUENCE

Lithology and symbols as for Core 34, Section 1.

8–58 and 94–122 cm: Fine grained basalt as in Section 1. Fresh(?) only at 33–37 and 107–115 cm.

0–20, 62–66, and 120–145 cm: Aphanitic and variolitic basalt as in Section 1.

0–10, 60–64, 80–88, and 120–130 cm: Basalt glass, moderately altered to palagonite and veined by calcite.

SECTION 3

APHYRIC PILLOW BASALT SEQUENCE

0–10 cm (Pieces 1A and B): Interpillow breccia of fresh glass.

80–90 cm (Pieces 7A and B): Clasts in calcite matrix.

58–77 cm (Pieces 6A–E): Interpillow breccia of altered light brownish gray (10YR 6/2) basalt clasts and black aphanitic basalt clasts in calcite matrix; some with fine bits of glass and basalt ground up in it (Pieces 6A–C).

17–58 cm (Pieces 2–5) and 77–117 cm (Pieces 7–8): Pieces of fine grained pillows with no variolitic edges (except at 18–20 cm) and 2% (<3 mm) rounded vesicles, some filled with clay, some with calcite. Fresher parts are gray (7.5YR N5) and more altered parts are light brownish gray (10YR 6/2).

117–120 cm (Piece 9A): Clasts of fresh and altered glass with calcite between.

120–140 cm: Single pillow of fine grained highly altered grayish brown (10YR 5/2) basalt with variolitic edge top (122–129 cm) and bottom (139–140 cm) grading into black aphanitic basalt.

140–150 cm: Top of second pillow with black aphanitic basalt grading through variolitic edge to same altered basalt interior. Both pillows have calcite in fractures and Piece 9D has 1% (<2 mm) rounded and irregular vesicles filled with calcite.

SECTION 4

PILLOW(?) BRECCIA, HYALOCLASTITE MATRIX

Basalt lithologies as in Core 34, Section 1 and Core 35, Section 1

0–24, 40–45, and 77–113 cm: Aphyric basalt, fine grained dark gray (7.5YR N4) grading to brown (7.5YR 4/4) with alteration (fresh only from 102–108 cm).

5–12 and 26–82 cm: Hyaloclastite breccia. Angular to subrounded clasts of variably altered aphanitic to variolitic basalt (< 5 cm) and generally completely palagonitized glass (< 1 cm). Matrix dominated by finely ground basaltic material with subordinate calcite.

SITE 558, CORE 36 Depth 486.5–495.5 m

SECTION 1

PILLOW BRECCIA, HYALOCLASTITE MATRIX

Basalt lithologies as in Core 34, Section 1 and Core 35, Section 1.

0–18 cm: Aphyric, fine grained basalt; color gray (2.5Y N5/0) to light brownish gray (2.5Y N6/2) in altered parts.

20–108 cm: Hyaloclastite breccia, consisting of angular to subrounded clasts of mostly palagonitized glass (< 30 mm) and aphanitic to variolitic basalt (< 15 cm). Breccia is mostly cemented by calcite, but fine grained matrix of basalt alteration products is also present.

109–127 cm: Aphyric fine grained basalt as in Pieces 1 and 2 (0–18 cm).

SECTION 2

APHYRIC PILLOW BASALT SEQUENCE

Series of isolated pillow pieces as in Section 1.

89–92 cm: 10% large (< 7 mm) irregular vesicles filled with calcite and some (< 1%) light yellowish brown (10YR 6/4) clay. Heavy calcite veining throughout.

SECTION 3

BASALT

1–70 cm: Aphyric, fine grained basalt; color gray (2.5Y N5/0) to light brownish gray (2.5Y N6/2) in altered zones along fractures and veins. Shows no vesicles.

25–38 cm: Aphanitic to variolitic textured basalt; varioles up to 5 mm. Veinlets are filled with calcite cement.

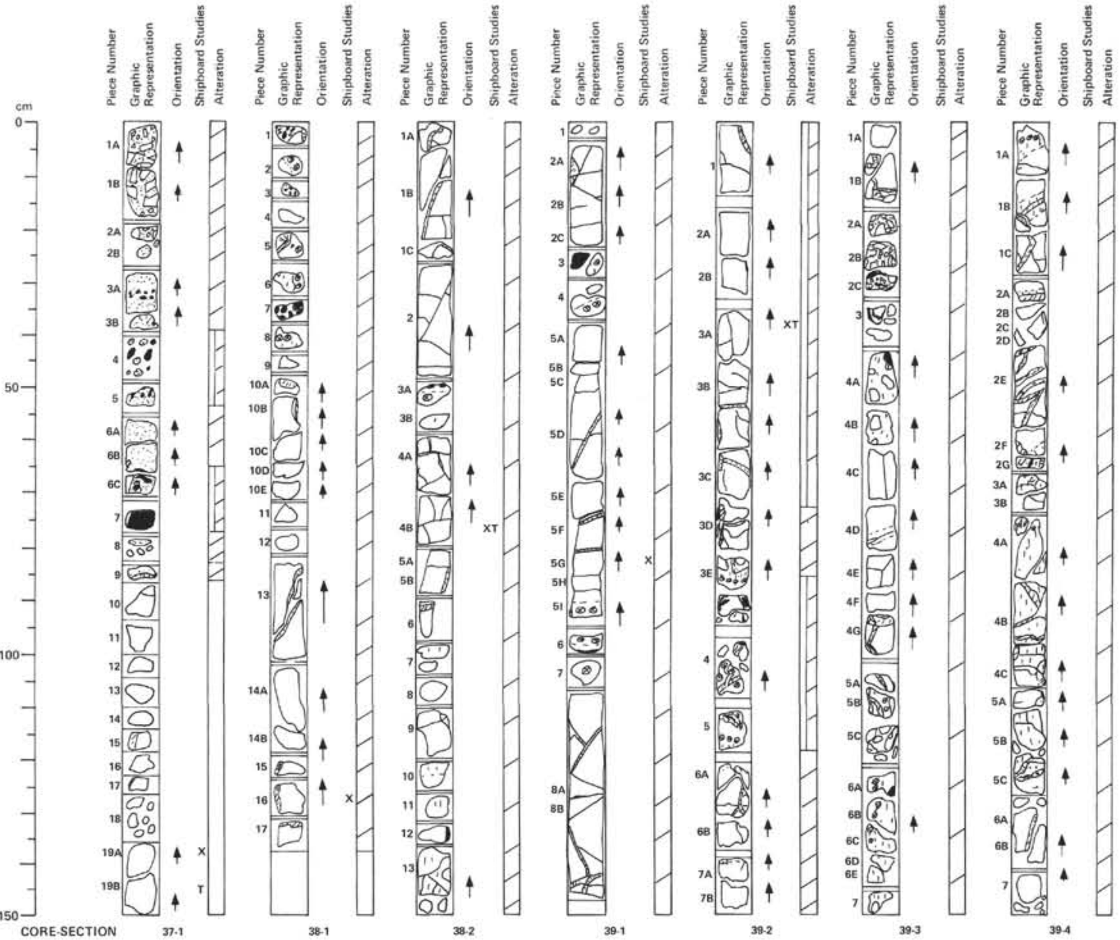

SITE 558, CORE 37 Depth 495.5–504.5 m

SECTION 1

0–82 cm: Basalt breccia, hyaloclastite and limestone.
82–150 cm: Basalt.
0–18 cm: Basalt breccia. Clasts of moderately to badly altered aphyric basalt (size <4 cm); the angular clasts "swim" within a limestone matrix – some cavities are cemented with calcite; color of clasts grayish brown (10YR 5/2).
19–82 cm: Limestone, color brownish white (10YR 8/2). Black MnO – dendrites are scattered throughout the sediment, which is partly interlayered by brecciated volcanic glass (hyaloclastite) (See Pieces 3A, 4, 5, 6B, and 6C). The glass is mostly altered to brown clay. Piece 7 (73–76 cm): Clast of drilled basalt glass with clayey alteration along fractures.
83–150 cm: Aphyric, fine grained fresh basalt color gray (7.5YR N5/0); vesicles are rare and filled with clay (size <1 mm).

SITE 558, CORE 38 Depth 504.5–509.0 m

SECTION 1

0–48 cm: Basalt breccia and pieces of aphanitic basalt/aphyric basalt.
48–134 cm: Aphyric basalt.
0–4, 11–13, and 34–37 cm: Basalt breccia. Clasts of aphanitic black (10YR 2.5/1) basalt and glass fragments set in calcite matrix. Aphanitic clasts ~1–2 cm in diameter. Vesicles irregularly scattered, some containing clay. Glass 2 mm–1 cm in diameter; majority of fragments slightly altered to palagonite. Clays observed along glass fractures.
4–11, 13–34, and 37–48 cm: Pieces of aphanitic basalt, dark gray (2.5Y N4/0) grading through variolitic texture to light brownish gray (10YR 6/2) altered aphyric basalt to aphyric basalt, gray (10YR 6/1).

48–134 cm: Aphyric basalt, gray (2.5Y N5/0). Some pieces are fractured, with calcite in/along the fractures. Calcite rims are observed on some pieces. Vesicles are variable in frequency; some are empty, most are calcite-filled (< 1 mm). Slight weathering to a different gray (10YR 5/1) is patchy and seen along the borders of most pieces.
Boundary of larger pillow unit at 55 cm?

SECTION 2

APHYRIC PILLOW BASALT
New Unit? – large pillows, narrower margins, no breccia, slightly coarser grained.
0–150 cm: Aphyric basalt, gray (5Y 5/1), fine grained (slightly coarser than overlying unit). Plagioclase laths (~ 0.5 mm) randomly altered or in radiating clusters altered deep green (~chlorite?). Weathered grayish brown (2.5Y 5/2 to 10YR 5/2) adjacent to fractures. Vesicles: 1–2% scattered throughout (<0.5 mm filled mainly with grayish green chlorite(?).
50–53 and 132–136 cm: Pillow rims – glass to black aphanitic basalt to grayish brown variolitic basalt.
0–70 cm: Minor veinlets and fracture fillings of calcite.

SITE 558, CORE 39 Depth 509.0–518.0 m

SECTION 1

PILLOW BASALT
Large pillow unit.
0–147 cm: Aphyric basalt as in Core 38, Section 2.
23–37 and 90–105 cm: Pillow margins as in Core 38, Section 2.
26 cm: Glass altered to dark green clay/chlorite(?) (grayish olive green – 5GY 3/2).
Calcite veinlets as shown, some with pale green (5G 7/2) clay.

SECTION 2

PILLOW BASALT
Large pillow units.
Aphyric basalt as in Core 38, Section 2 with small plagioclase laths randomly oriented.
84–86, 103–106, and 115–117 cm: Variolitic pillow margins as in Core 38, Section 2 and Core 39, Section 1. Minor veinlets and fracture fillings of calcite and pale green (5G 7/2) clay.
86–88 cm: Minor glass clasts.
111–114 cm: Glass rim of pillow.

SECTION 3

APHYRIC PILLOW BASALT
18–43, 107–120, and 143–150 cm: Aphanitic black basalt and altered aphyric basalt, interspersed with calcite veins (very small) and greenish alteration product, especially noticeable on surface. Colors same as in Core 38, Section 2 – aphyric basalt gray (5Y 5/1). Weathered and altered grayish brown (2.5Y 5/2 to 10YR 5/2) adjacent to aphanitic regions. Altered product possibly chlorite or smectite. Could imply hydrothermal processes in the region.
0–18, 43–107, and 120–143 cm: Aphyric basalt (5Y 5/1) relatively fine grained. Calcite fractures interspersed throughout section; weathered grayish brown (2.5Y 5/2 to 10YR 5/2) along fractures. Patches of pillow rims: black (10YR 2.5/1) aphanitic basalt to grayish brown variolitic basalt. Aphyric basalt pieces set within grayish brown "massive" region (as opposed to variolitic region). Minor veins of calcite, also present in fractures and some rim edges.
107–120 cm: olive green (5Y 5/3) alteration product referred to in above description especially evident. Same conclusion reached.

SECTION 4

APHYRIC PILLOW BASALT
Larger unit. Plagioclase laths are finer (~ 0.1–0.2 mm), aphyric gray (2.5Y N5) basalt with grayish brown (2.5Y N5/2) alteration (indicated ⁝.).
0–3 and 77–79 cm: Narrow variolitic edges, zoning to black aphanitic basalt, pillows are larger with narrower edges.

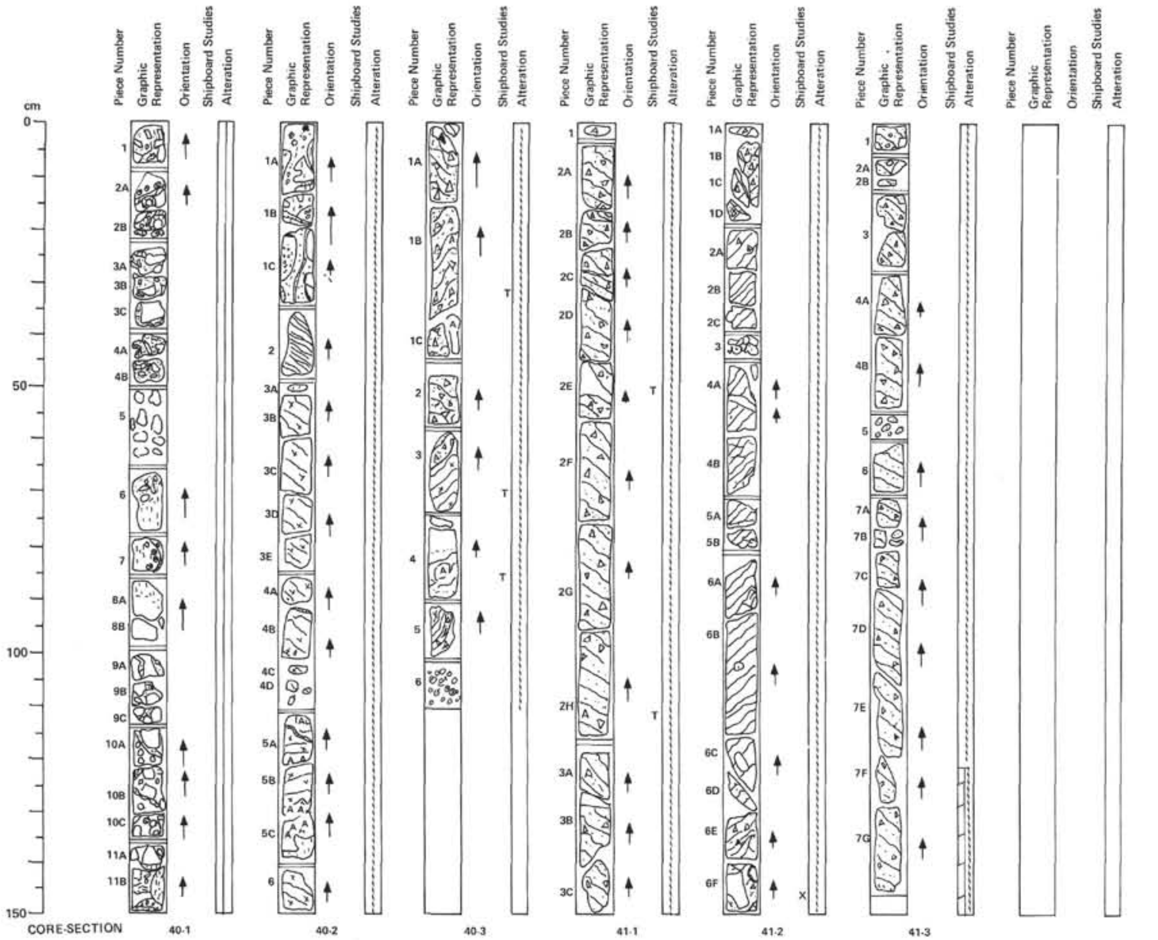

SITE 558, CORE 40 Depth 518.0–527.0 m

SECTION 1

BASALT BRECCIA

0–150 cm: Aphyric, grayish brown (10YR 5/2) altered; angular to subrounded basalt clasts.

0–88 cm: Matrix is combination of calcite (white) and limestone. Clasts (<10%) are rounded with black aphanitic cores and altered rims.

88–150 cm: Matrix is very fine basalt fragments with calcite in fractures. Smaller (<1 cm) clasts generally more altered including 20% reddish yellow (7.5YR 7/8) basalt clasts.

11–14 and 79–85 cm: Rounded clasts with variolitic texture (= pillow fragment?).

SECTION 2

0–34 cm: Basalt breccia. Aphyric, angular to subrounded basalt clasts of similar lithology to basalts higher in hole. Some have ~5% vesicles, often iron oxide filled. Matrix mainly comminuted basaltic material, lesser calcite.

36–47 cm: Mylonite. Soft, clay-rich mylonite. Strongly sheared with alternating, 1–2 cm, irregular bands of yellowish brown (10YR 5/8) and mottled greenish gray (5BG 5/1) with pale green (5G 6/2).

49–150 cm: Sheared gabbro. Weakly sheared, altered gabbro, overall dark grayish brown (10YR 4/2). Bronze reddish brown (5YR 5/4) relict pyroxene (5–10%).

126–136 cm: *Sheared anorthosite vein.* Relict coarse grains (1–2 cm) of plagioclase and pale green pyroxene separated by interlaced zones of white finely sheared material. Designated (A). Vein margins are highly irregular. Generally abuts fine grained dark reddish brown (5YR 3/3) material.

SECTION 3

0–66 cm: Sheared fault breccia. Polymict breccia composed of recognizable gabbro chunks and basalt clasts. Entire breccia is sheared, rendering individual boundaries undefinable. "Matrix" is brown (10YR 4/3) to yellowish brown (10YR 5/6). Basalt clast are gray (2.5Y N5/0) and range in size from 1 mm to <1 cm in diameter. Gabbro chunks range from olive (5Y 5/3) to olive gray (5Y 5/2). Clays abound.

37–43 and 82–89 cm: Sheared anorthosite. Anorthosite pieces roughly cemented together in a clay (calcite?) matrix then completely sheared. *Anorthosite piece at 37–43 cm is more massive and less "fragmented" then at* 82–89 cm. They are light gray/gray (2.5Y N6/0).

66–82 and 89–113 cm: Sheared gabbro. Gabbro, strongly altered and sheared pyroxenes and relict pyroxenes are observed, 1 mm – <5 mm diameter. Gabbro ranges from dark grayish brown (10YR 4/2) to reddish brown (5YR 5/4) relict pyroxene patches (5–10% in places) to light reddish brown (5YR 6/5) pyroxenes (5–10%). Clays worked into fabric throughout.

107–113 cm: Sheared gabbro rubble. Very small pieces (5 mm–1.5 cm) of sheared gabbro debris, with a large volume % of clays.

SITE 558, CORE 41 Depth 527.0–536.0 m

SECTION 1

0–150 cm: Sheared gabbro (breccia). The gabbro clasts are strongly altered to clay minerals and serpentine, which makes up the matrix, too. Altered opx occurs throughout the section (color light to dark brown, size<5 mm). The clasts (size from ~1 mm up to several centimeters) are colored from light brownish gray (2.5Y 6.2) to brown (10YR 5/3).

43–52 and 125–128 cm: Calcite veins; the lower one looks like sheared and shows some greenish clay beside it.

SECTION 2

SHEARED GABBRO (BRECCIA)

Similar to Section 1 but more altered and brecciated as it nears shear zone at 115–150 cm.

0–83 cm: Sheared gabbro, more altered and sheared than Core 40, Section 1.

83–150 cm: Gabbro breccia grading into shear zone of soft clay-rich mylonite with multiple irregular colored bands very dark grayish brown (10YR 3/2); brown (10YR 4/3); gray (10YR 5/1) grading into pale green (5G 6/2) with angular clasts (<5 mm) of same green. Mylonite zone also contains angular, moderately altered clasts of basalt with gray (7.5YR N/0) cores and narrow brownish yellow (10YR 6/8) altered rims.

143–148 cm: Note single larger (7 cm) basalt clast in Piece 6F.

SECTION 3

0–12 cm: Polymict breccia. Clasts: Serpentinized, olive (5Y 5/3) colored gabbro (size <5 mm) and aphyric basalt, fine-grained, color gray (10YR 5/1). Center is fresh, rim is altered to brown clay. One clast shows fresh black glass. Matrix: serpentine and other clays, greenish.

14–60 cm: Sheared fault breccia. Parallel textured multicolor layers of different clays (color ranges from dark brown over pale brown to dark green). Calcite within thin fissures is common. Subrounded clasts of serpentinized gabbro are scattered (size <8 mm).

61–70 cm: Larger clast of serpentinized gabbro. Dunite? (no visible opx). Color greenish gray (5GY 5/1).

71–145 cm: Sheared gabbro (breccia). Clasts of serpentinized gabbro (size <1 cm) are separated by fissures and veins, which are usually filled with calcite. In the lower part veinlets are filled with clay and chrysolite (asbestos). Color of rock dark green to dark brown. Orthopyroxene (~5 volume %) is moderately altered (size <6 mm).

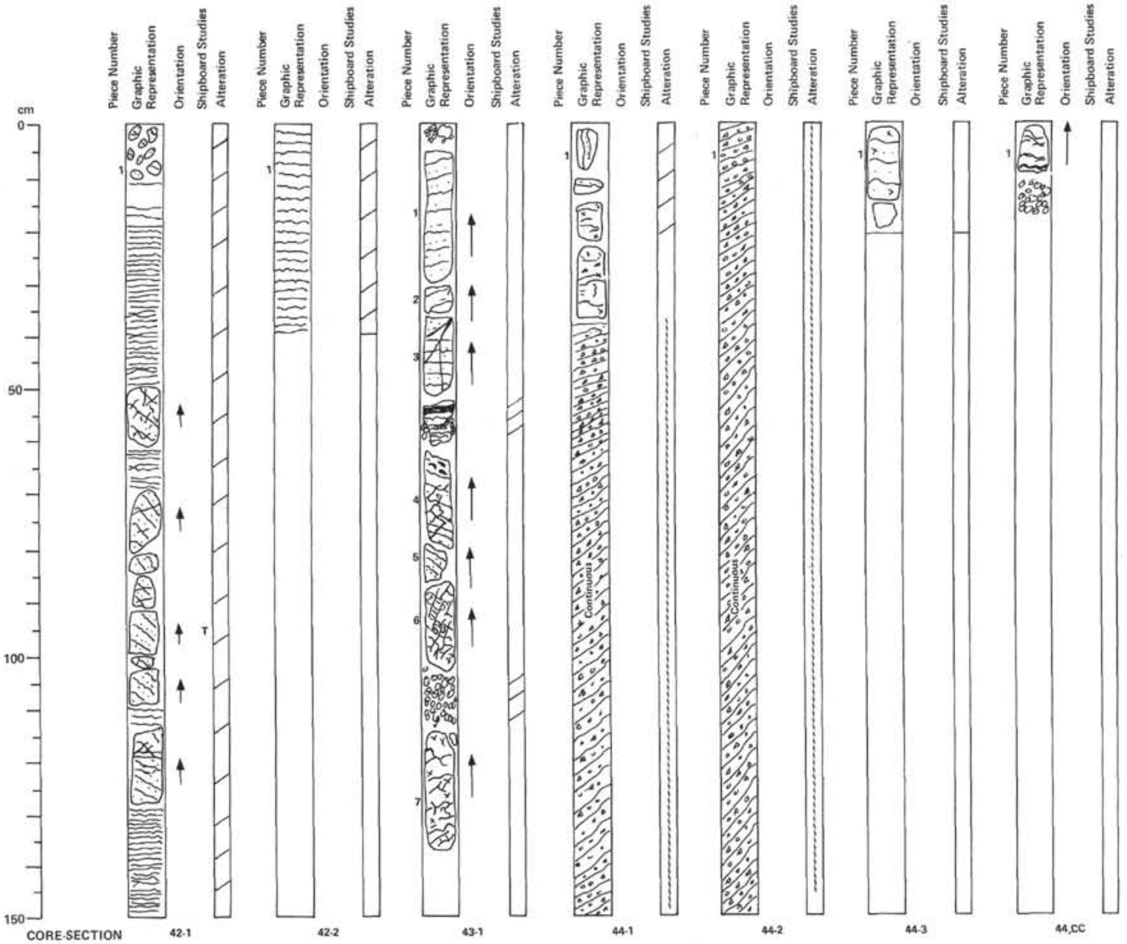

SITE 558, CORE 42 — Depth 536.0–545.0 m

SECTION 1

0–150 cm: Serpentinized gabbro (dunite?). Rock: black serpentinized gabbro (dunite?); serpentine is fresh to moderately altered. Small veinlets in the serpentinite are filled with white chrysotile (shown diagramatically as heavy black wavy lines). Clay (marked): these parts of the section probably consist of highly sheared serpentinite (ground by drilling?). Abundant chrysotile fibers may be an indicator of the occurrence of thicker chrysotile veins; color varies from white to dark gray.

SECTION 2

0–39 cm: Sheared serpentinite. Ground clayey serpentinite as described in Section 1.

SITE 558, CORE 43 — Depth 545.0–554.0 m

SECTION 1

SERPENTINITE

0–139 cm: Black (5Y 2.5/1) serpentinite, weakly–moderately sheared with varying abundance of sinuous veinlets of white chrysotile (represented by heavy black wavy lines).

0–5 cm: Several small aphyric basalt pebbles (fallen downhole?).

56–67 and 106–118 cm: Highly fractured (by drilling) serpentinite.

56–68 cm: 2 cm chrysotile vein.

70–149 cm: 10–30% large (< 1 cm), pale green (close to 5GY 7/2, grayish yellow green) crystals of antigorite(?).

SITE 558, CORE 44 — Depth 554.0–563.0 m

SECTION 1

SERPENTINITE AND SERPENTINITE FAULT BRECCIA

0–38 cm: Serpentinite as in Core 43, Section 1.

38–150 cm: Serpentinite fragments (< 1 cm) in shear-layered, soft, clay matrix.

SECTION 2

SERPENTINITE FAULT BRECCIA

As in Section 1.

SECTION 3

SERPENTINITE

0–20 cm: Serpentinite with large (<1 cm) antigorite(?) crystals as in Core 43, Section 1.

CORE-CATCHER

SERPENTINITE

0–9 cm: Serpentinite as in Core 43, Section 1; large augens (≤1 cm) of antigorite crystals. Chrysotile veins represented by heavy wavy lines.

10–16 cm: Serpentinite rubble.

SITE 558 HOLE A CORE 1 CORED INTERVAL 0.0–0.5 m

TIME – ROCK UNIT	BIOSTRATIGRAPHIC ZONE	FORAMINIFERS	NANNOFOSSILS	RADIOLARIANS	DIATOMS	SECTION	METERS	GRAPHIC LITHOLOGY	DRILLING DISTURBANCE	SEDIMENTARY STRUCTURES	SAMPLES
Pleistocene	N23/N22 (early to late Pleistocene) CN14–15 (NN20–21) *Emiliania huxleyi* zone; *Gephyrocapsa oceanica* zone (late Pleistocene)	AG	AG			1	0.5	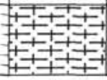			• * #

10YR 7/3
10YR 6/3
10YR 7/3

LITHOLOGIC DESCRIPTION

DOMINANT LITHOLOGY SILICEOUS FORAM-NANNOFOSSIL OOZE

Pale brown (10YR 6/3) to very pale brown (10YR 7/3)

Soft and soupy, but with some "gelatinous" cohesiveness. No bedding or bioturbation observable, but faint lighter-pale brown mottling may be bioturbation.

Principal constituents: nannos, forams, volcanic glass, siliceous organisms.

SMEAR SLIDE SUMMARY (%):

	1, 50 D	1, 55 D
Composition:		
Feldspar	Tr	Tr
Heavy minerals	–	1
Clay	?	6
Volcanic glass (incl. clay size)	10	5
Carbonate unspec.	–	1
Foraminifers	20	25
Calc. nannofossils	60	50
Diatoms, Radiolarians, Sponge spicules, Silicoflagellates	10	12

Carbonate Bomb (%):
1, 55–56 = 75

SITE 558 HOLE A CORE 2 CORED INTERVAL 0.5–10.0 m

TIME – ROCK UNIT	BIOSTRATIGRAPHIC ZONE	FORAMINIFERS	NANNOFOSSILS	RADIOLARIANS	DIATOMS	SECTION	METERS	GRAPHIC LITHOLOGY	DRILLING DISTURBANCE	SEDIMENTARY STRUCTURES	SAMPLES
Pleistocene	N23/N22 (early to late Pleistocene) (CN13–14) (NN19) *Gephyrocapsa oceanica* zone, *Crenalithus doronicoides* zone (early to late Pleistocene)	AG	AG			1, 2, 3, 4, 5, 6, 7, CC	0.5, 1.0	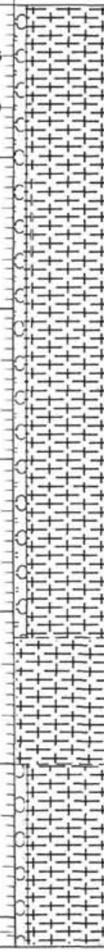			

10YR 7/2
5YR 7/1
5YR 7/2
5YR 8/1
10YR 8/2
10YR 7/2
10YR 6/2
10YR 5/1
5YR 8/1
5YR 7/2
5YR 8/1
7.5YR N8

LITHOLOGIC DESCRIPTION

DOMINANT LITHOLOGY SILICEOUS FORAM-NANNOFOSSIL OOZE

Light gray to pinkish gray to white to light brownish gray with occasional gray streaks; dark streaks in Section 4

Soft to firm; disturbed

Faintly mottled and indistinctly bioturbated; no evidence of bedding or other structures

Dominant components are calcareous nannofossils and forams. Siliceous biogenic content variable.

SMEAR SLIDE SUMMARY (%):

	1, 80 D	3, 80 D	5, 80 D	6, 25 D	6, 120 D
Composition:					
Feldspar	2	1	Tr	Tr	Tr
Heavy minerals	–	–	Tr	Tr	Tr
Clay	5	9	5	2	2
Volcanic glass	2	Tr	1	Tr	Tr
Opaques	–	1	1	1	–
Carbonate unspec.	3	–	–	1	2
Foraminifers	20	25	10	10	10
Calc. nannofossils	50	45	75	65	75
Diatoms	3	1	1	2	1
Radiolarians	3	8	5	5	2
Sponge spicules	7	8	Tr	10	6
Silicoflagellates	5	1	2	3	1

Carbonate Bomb (%):
3, 80–81 = 70

SITE 558 HOLE A CORE 3 CORED INTERVAL 10.0–19.5 m

TIME-ROCK UNIT	BIOSTRATIGRAPHIC ZONE	FORAMINIFERS	NANNOFOSSILS	RADIOLARIANS	DIATOMS
Pliocene? and Pleistocene?	N22–N21 (early Pleistocene to late Pliocene) CN13 (NN19) *Crenolithus doronicoides* zone (early Pleistocene)	AG	AG		

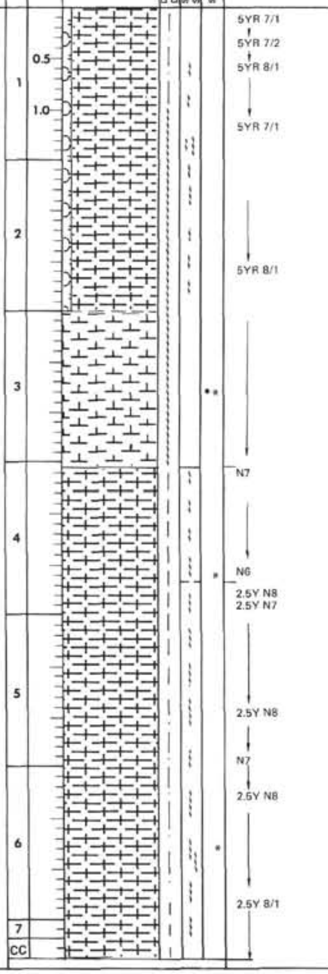

LITHOLOGIC DESCRIPTION

DOMINANT LITHOLOGIES:
(1) FORAM-NANNOFOSSIL OOZE TO NANNOFOSSIL OOZE

White to light gray with faint gradual color changes

Soft to firm; disturbed

Moderately to mildly bioturbated; massive bedding; distinct contact at Section 4, 5 cm, between nanno ooze (white) and foram-nanno ooze (light gray).

The nanno oooze may contain more clay; the foram-nanno ooze is more siliceous and has >25% forams.

(2) SILICEOUS FORAM-NANNOFOSSIL OOZE

Continues from Core 2, with gradual decrease in siliceous material and increase in carbonate.

SMEAR SLIDE SUMMARY (%):

	3, 80	4, 110	6, 80
	D	D	D
Composition:			
Feldspar	1	Tr	Tr
Heavy minerals	–	Tr	–
Clay	15	8	9
Volcanic glass	–	Tr	Tr
Opaques	Tr	–	–
Micronodules	–	–	1
Carbonate unspec.	2	–	–
Foraminifers	9	25	25
Calc. nannofossils	70	64	60
Diatoms	1	3	5
Radiolarians	1		
Sponge spicules	1		
Silicoflagellates	Tr		

Carbonate Bomb (%):
3, 80 = 81

SITE 558 HOLE A CORE 4 CORED INTERVAL 19.5–29.0 m

TIME-ROCK UNIT	BIOSTRATIGRAPHIC ZONE	FORAMINIFERS	NANNOFOSSILS	RADIOLARIANS	DIATOMS
Pliocene	N21 (late Pliocene) CN12d (NN18) *Discoaster brouweri* zone–*Calcidiscus macintyrei* subzone (latest Pliocene)	AG	AM		

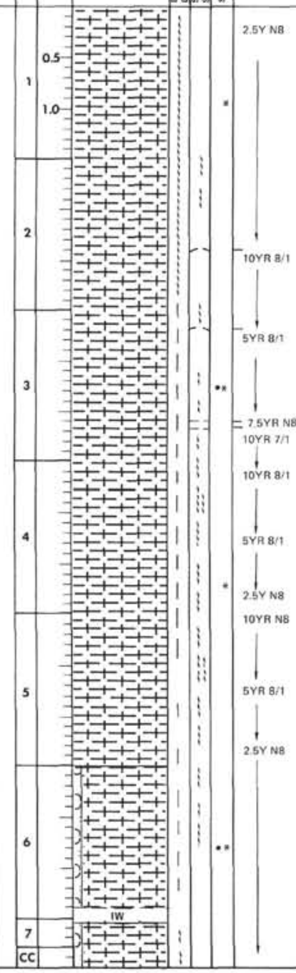

LITHOLOGIC DESCRIPTION

DOMINANT LITHOLOGIES:
(1) FORAM-NANNOFOSSIL OOZE

White, with subtle color variations to other shades of white; light gray to gray bed in Section 3, indistinct contact with white. Black (MnO_2?) streaks and spots in Sections 1 and 6.

Soft to firm; disturbed

Mottled and mildly bioturbated; massive bedding, and indistinct bed contacts marked by subtle color changes.

Principal constituents are nannofossils and forams, with variable quantities of siliceous components and clay.

(2) SILICEOUS FORAM-NANNOFOSSIL OOZE

As in Core 2.

SMEAR SLIDE SUMMARY (%):

	1, 45	3, 80	4, 120	6, 80
	D	D	D	D
Composition:				
Feldspar	1	1	1	1
Heavy minerals	Tr	–	–	–
Clay	9	14	9	13
Volcanic glass	2	2	1	1
Opaques	3	1	–	–
Micronodules	Tr?	–	–	–
Carbonate unspec.	–	–	3	–
Foraminifers	15	14	10	13
Calc. nannofossils	65	60	70	62
Diatoms	4	8	6	12
Radiolarians				
Sponge spicules				
Silicoflagellates				

Carbonate Bomb (%):
3, 80 = 74
6, 80 = 75

SITE 558 HOLE A CORE 5 CORED INTERVAL 29.0–38.5 m

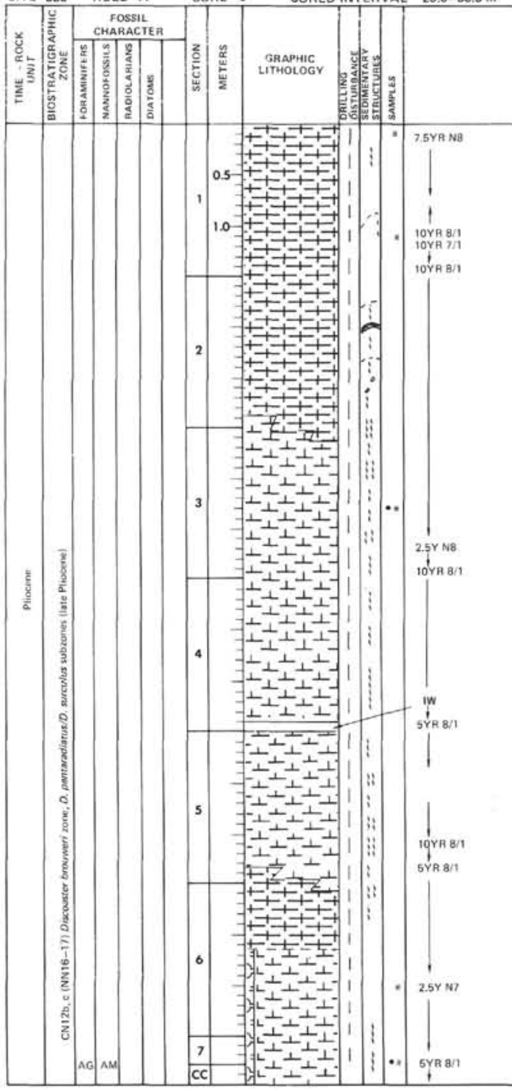

LITHOLOGIC DESCRIPTION

DOMINANT LITHOLOGIES:

(1) FORAM-NANNOFOSSIL OOZE TO NANNOFOSSIL OOZE

White, grading subtly into other shades of white and light gray, with black streaks and spots common, and light gray to white mottling

Soft to firm, moderately disturbed

Mildly bioturbated throughout with faint mottling; massive parallel bedding indicated by indistinct to distinct color contacts

Principal components are calcareous nannofossils, foraminifers, and varying amounts of siliceous organisms

(2) SILICEOUS NANNOFOSSIL OOZE

Light gray to gray with mottles of darker gray to white

Soft to firm

Mildly bioturbated

Decrease in CO_3 content and increase in siliceous organisms and clay(?) (slight), as well as slightly darker color, distinguish this litho.

SMEAR SLIDE SUMMARY (%):

	1, 92	1, 110	3, 80	6, 120	7, 30
	D	D	D	M	D
Composition:					
Feldspar	1	1	1	1	1
Heavy minerals	–	–	–	–	Tr
Clay	9	9	9	3	12
Volcanic glass	Tr	Tr	1	2	2
Opaques	Tr	Tr	Tr	7	Tr
Foraminifers	10	10	8	13	5
Calc. nannofossils	70	70	76	70	65
Diatoms, Radiolarians, Sponge spicules, Silicoflagellates	8	9	5	4	15

Carbonate Bomb (%):
3, 80 = 84
7, 30 = 70

SITE 558 HOLE A CORE 6 CORED INTERVAL 38.5–48.0 m

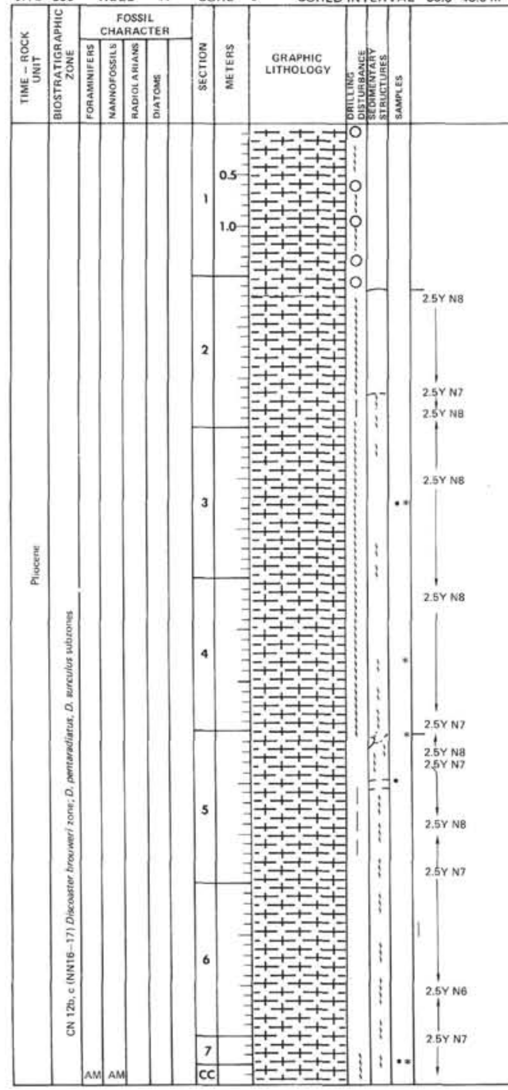

LITHOLOGIC DESCRIPTION

Caved material Section 1–Section 2, 20 cm.

DOMINANT LITHOLOGY FORAM NANNOFOSSIL OOZE

White to light gray with darker streaks and gray to light gray to white mottling

Soft to firm, disturbed

Mottled and mildly bioturbeted; evidence for bioturbation increases in lower part where clay content probably increases (decrease in CO_3 %).

Massive bedding; a few bed contacts are suggested by subtle color changes; disturbed bedding and flow-in deformation through Section 4.

Principal constituents are nannofossils, forams, and varying amounts of clay. Estimates of foram abundance are higher where CO_2 content decreases and clay is believed to increase.

Note: Section 7 has 50 cm.

SMEAR SLIDE SUMMARY (%):

	3, 80	4, 80	5, 52	7, 50
	D	D	D	D
Composition:				
Feldspar	Tr	2	1	Tr
Heavy minerals	–	–	–	Tr
Clay	7	9	18	19
Micronodules	1	–	1	–
Foraminifers	15	15	18	29
Calc. nannofossils	73	73	58	50
Diatoms, Radiolarians, Sponge spicules, Silicoflagellates	4	1	5?	2

Carbonate Bomb (%):
3, 80 = 88
5, 50 = 76
7, 50 = 79

SITE 558 HOLE A CORE 7 CORED INTERVAL 48.0–57.5 m

TIME – ROCK UNIT: Pliocene

BIOSTRATIGRAPHIC ZONE: CN12a (NN16) *Discoaster brouweri* zone–*D. tamalis* subzone (early late Pliocene)

FOSSIL CHARACTER: FORAMINIFERS AG; NANNOFOSSILS AM; RADIOLARIANS; DIATOMS

SECTION: 1, 2, 3, 4, 5, 6, CC

METERS: 0.5, 1.0

GRAPHIC LITHOLOGY | DRILLING DISTURBANCE | SEDIMENTARY STRUCTURES | SAMPLES

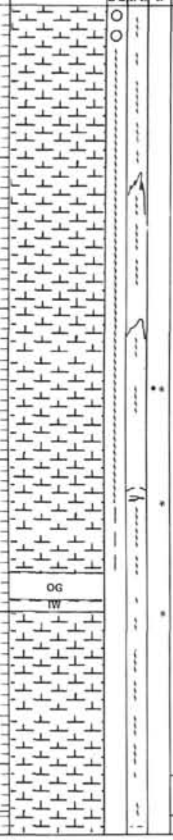

2.5Y N8 to N7
2.5Y N7
2.5Y N8
2.5Y N7 to N8
2.5Y N7
2.5Y N8
2.5Y N7
2.5Y N8
2.5Y N7
2.5Y N8
2.5Y N7
2.5Y N8
2.5Y N7
2.5Y N8

LITHOLOGIC DESCRIPTION

DOMINANT LITHOLOGY NANNOFOSSIL OOZE

White to light gray to gray with faint mottling, black streaks, and indistinct color banding

Soft to firm; disturbed to Section 4

Mildly bioturbated and mottled throughout; intense flow-in deformation through Section 4, 37 cm.

Massive bedding with faint color banding

Principal constituents are calcareous nannofossils; quantity of clay appears to be variable.

SMEAR SLIDE SUMMARY (%):

	3, 80	4, 43	5, 3
	D	M	D
Composition:			
Feldspar	Tr	Tr	Tr
Heavy minerals	Tr	–	–
Clay	20	10	10
Micronodules	Tr	–	2
Carbonate unspec.	1	5	Tr
Foraminifers	8	5	7
Calc. nannofossils	65	75	80
Diatoms, Radiolarians, Sponge spicules, Silicoflagellates	5	5?	Tr?

Carbonate Bomb (%):
3, 80 – 74

SITE 558 HOLE A CORE 8 CORED INTERVAL 57.5–67.0 m

TIME – ROCK UNIT: Pliocene

BIOSTRATIGRAPHIC ZONE: CN11–CN12a (NN15–16) *D. brouweri* zone–*Reticulofenestra pseudoumbilica* zone (early to late Pliocene)

FOSSIL CHARACTER: FORAMINIFERS AG; NANNOFOSSILS AG; RADIOLARIANS; DIATOMS

SECTION: 1, 2, 3, 4, 5, 6, CC

METERS: 0.5, 1.0

GRAPHIC LITHOLOGY | DRILLING DISTURBANCE | SEDIMENTARY STRUCTURES | SAMPLES

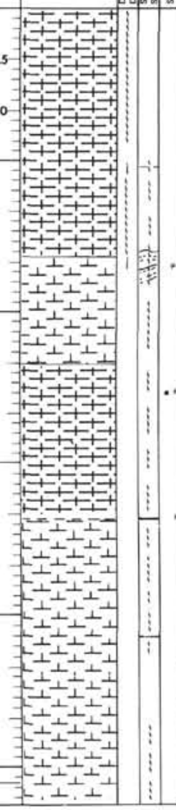

2.5Y N8
2.5Y N7
2.5Y N8
2.5Y N6
2.5Y N8
2.5Y N7
2.5Y N6
2.5Y N7
2.5Y N8
2.5Y N7
2.5Y N8
2.5Y N2
2.5Y N8
2.5Y N8

LITHOLOGIC DESCRIPTION

DOMINANT LITHOLOGY FORAM-NANNOFOSSIL OOZE TO NANNOFOSSIL OOZE

White to light gray, subtly grading, except where color bands define color changes; black streaks common throughout

Soft to firm, disturbed through Section 2, 95 cm

Bioturbation and mottling probably throughout, though very indistinct in some portions; bands 1–2 cm wide in Section 2 indicate more rapid alternation of lithologic character and suggest parallel bedding.

Principal constituents are nannofossils and varying amounts of forams and clay.

Minor lithology:
Manganiferous(?) nanno ooze

Black streaks, as in Sections 4, 5, and 6 are concentrations of opaque minerals possibly marking bedding planes or depositional discontinuities.

SMEAR SLIDE SUMMARY (%):

	2, 103	3, 80	4, 52
	D	D	M
Composition:			
Feldspar	Tr	1	1
Heavy minerals	Tr	–	–
Clay	10	13	8
Palagonite	Tr	–	–
Opaques	–	–	15
Micronodules	1	1	–
Carbonate unspec.	–	1	–
Foraminifers	5	15	1
Calc. nannofossils	80	68	75
Diatoms, Radiolarians, Sponge spicules, Silicoflagellates	3?	1?	–

Carbonate Bomb (%):
3, 80 – 84

SITE 558 HOLE A CORE 9 CORED INTERVAL 67.0–74.0 m

TIME-ROCK UNIT: Pliocene

BIOSTRATIGRAPHIC ZONE: N19 (early Pliocene); CN10 a, b (NN12) *Amaurolithus tricorniculatus* zone–*Ceratolithus acutus* or *Triquetrorhabdulus rugosus* subzone (early Pliocene)

FOSSIL CHARACTER: Foraminifers AG; Nannofossils AM

SECTION: 1, 2, 3, 4, CC

METERS: 0.5, 1.0

GRAPHIC LITHOLOGY:

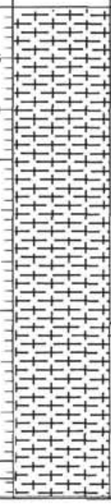

SAMPLES: •• (Section 3)

Colors: 2.5Y N8; 7.5YR N8; 2.5Y N8; 7.5YR N8; 7.5YR N8; 2.5Y N8

LITHOLOGIC DESCRIPTION

DOMINANT LITHOLOGY FORAM-NANNOFOSSIL OOZE

White, with dark spots and streaks

Soft; soupy, and disturbed to Section 3; then only slightly disturbed

No evidence of bioturbation or bedding, except dark streaks

Principal constituent is calcareous nannofossils

SMEAR SLIDE SUMMARY (%):

Composition:	3, 80
Feldspar	Tr
Clay	10
Palagonite	Tr
Foraminifers	10
Calc. nannofossils	78
Diatoms, Radiolarians, Sponge spicules, Silicoflagellates	2?

Carbonate Bomb (%):
3, 80 = 88

SITE 558 HOLE A CORE 10 CORED INTERVAL 74.0–77.0 m

TIME-ROCK UNIT: Pliocene? upper Miocene?; Miocene?–Pliocene?

BIOSTRATIGRAPHIC ZONE: N19 (early Pliocene); CN10a (NN12) *Triquetrorhabdulus rugosus* subzone of *Amaurolithus tricorniculatus* zone (late Miocene)

FOSSIL CHARACTER: Foraminifers CM; Nannofossils AM

SECTION: 1, 2, CC

METERS: 0.5, 1.0

GRAPHIC LITHOLOGY:

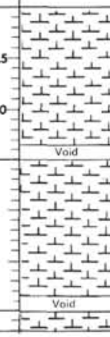

SAMPLES: •• (Section 2)

Colors: 2.5Y N8; 2.5Y N8; 2.5Y N8; 7.5YR N8

LITHOLOGIC DESCRIPTION

DOMINANT LITHOLOGY NANNOFOSSIL OOZE

White, with subtle gradation to other white in CC

Soft and soupy in Section 1; Section 2 is moderately to very disturbed

Mottling and bioturbation faint and indistinct; no bedding structure evident

Nannofossils are principal component

SMEAR SLIDE SUMMARY (%):

Composition:	2, 80
Feldspar	1
Clay	10
Palagonite	Tr
Foraminifers	3
Calc. nannofossils	84
Diatoms, Radiolarians, Sponge spicules, Silicoflagellates	2?

Carbonate Bomb (%):
2, 80 = 87

SITE 558 HOLE A CORE 11 CORED INTERVAL 77.0–86.5 m

TIME – ROCK UNIT	BIOSTRATIGRAPHIC ZONE	FORAMINIFERS	NANNOFOSSILS	RADIOLARIANS	DIATOMS	SECTION	METERS
Miocene?–Pliocene?; lower Pliocene? upper Miocene?	N19–N18? (early Pliocene–late Miocene) CN10a (NN12) *Triquetrorhabdulus rugosus* subzone of *Amaurolithus tricorniculatus* zone (*A. primus* subzone of *D. quinqueramus* zone (late Miocene)	AG	AM			1, 2, 3, 4, 5, 6, 7, CC	0.5, 1.0

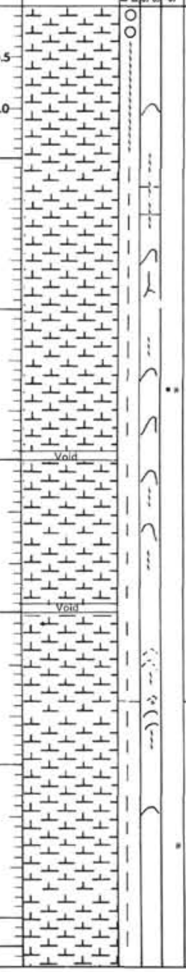

LITHOLOGIC DESCRIPTION

2.5Y N8
2.5Y N8
7.5YR N8
2.5Y N8
7.5YR N8
2.5Y N8

DOMINANT LITHOLOGY NANNOFOSSIL OOZE

White, grading subtly to other shades of white; dark streaks present in every section

Soft to firm; moderately to severely disturbed

Very mildly bioturbated and faint mottling; dark patches may represent bioturbation. Dark streaks may be parallel with bedding surfaces but are deformed vertically by drilling disturbance.

Principal constituent is calcareous nannofossils

Note: Section 7 has 50 cm.

SMEAR SLIDE SUMMARY (%):

Composition:	3, 80	6, 80
Feldspar	Tr	–
Clay	9	10
Carbonate unspec.	3	5
Foraminifers	2	–
Calc. nannofossils	85	85
Diatoms, Radiolarians, Sponge spicules, Silicoflagellates	1?	–

Carbonate Bomb (%):
3, 80 = 90

SITE 558 HOLE A CORE 12 CORED INTERVAL 86.5–96.0 m

TIME – ROCK UNIT	BIOSTRATIGRAPHIC ZONE	FORAMINIFERS	NANNOFOSSILS	RADIOLARIANS	DIATOMS	SECTION	METERS
Miocene; upper Miocene	N17 (late Miocene) CN10a (NN12) *Triquetrorhabdulus rugosus* subzone of *Amaurolithus tricorniculatus* zone (late Miocene)	AM	AG			1, 2, 3, 4, 5, 6, CC	0.5, 1.0

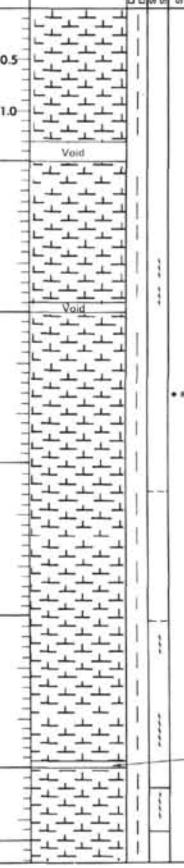

LITHOLOGIC DESCRIPTION

2.5Y N8
2.5Y N8
7.5YR N8
2.5Y N8
7.5YR N8
2.5Y N8
7.5YR N8
2.5Y N8
void
7.5YR N8
2.5Y N8

DOMINANT LITHOLOGY NANNOFOSSIL OOZE

White, grading subtly within various shades of white; dark streaks and patches soft to firm

Moderately deformed to slightly deformed

Bioturbation not prominent but may be indicated by streaks and dark patches in Sections 2, 5, and 6. Dark spots and streaks throughout. Massive bedding with indistinct color contacts.

Principal constituents are nannofossils

SMEAR SLIDE SUMMARY (%):

Composition:	3, 80
Feldspar	1
Clay	5
Carbonate unspec.	2
Foraminifers	3
Calc. nannofossils	88
Diatoms, Radiolarians, Sponge spicules, Silicoflagellates	1

Carbonate Bomb (%):
3, 80 = 93

SITE 558 HOLE A CORE 13 CORED INTERVAL 96.0–103.0 m

TIME–ROCK UNIT	BIOSTRATIGRAPHIC ZONE	FORAMINIFERS	NANNOFOSSILS	RADIOLARIANS	DIATOMS	SECTION
upper Miocene	CN9b (NN11) *D. quinqueramus* zone—*A. primus* subzone (late Miocene)	CM	AM			1, 2, 3, 4, 5

METERS: 0.5, 1.0

GRAPHIC LITHOLOGY

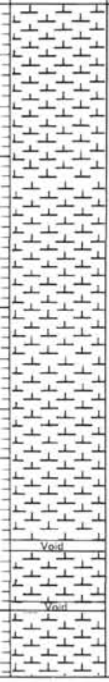

DRILLING DISTURBANCE · SEDIMENTARY STRUCTURES · SAMPLES

LITHOLOGIC DESCRIPTION

2.5Y N8
2.5Y N8
2.5Y N7
2.5Y N8
2.5Y N7
2.5Y N8
2.5Y N7
2.5Y N8
2.5Y N7
2.5Y N8
2.5Y N7
2.5Y N8

DOMINANT LITHOLOGY NANNOFOSSIL OOZE

White to light gray with gradual gradation from lighter to darker zones; darker mottling and dark streaks

Soft and soupy to firm; disturbed

Slightly bioturbated; mottling associated with darker areas; indistinct contacts of colors suggest massive parallel bedding

Principal constituents are nannofossils

SMEAR SLIDE SUMMARY (%):

	3, 80
Composition:	
Feldspar	1
Clay	9
Micronodules	Tr
Carbonate unspec.	5
Foraminifers	1
Calc. nannofossils	83
Diatoms, Radiolarians, Sponge spicules, Silicoflagellates	1?

Carbonate Bomb (%):
3, 80 = 89

SITE 558 HOLE A CORE 14 CORED INTERVAL 103.0–112.5 m

TIME–ROCK UNIT	BIOSTRATIGRAPHIC ZONE	FORAMINIFERS	NANNOFOSSILS	RADIOLARIANS	DIATOMS	SECTION
upper Miocene	CN9b (NN11) *D. quinqueramus* zone—*A. primus* subzone	AM	AG			1, 2, 3, 4, 5, 6, 7, CC

METERS: 0.5, 1.0

GRAPHIC LITHOLOGY

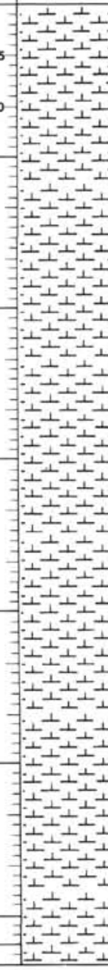

DRILLING DISTURBANCE · SEDIMENTARY STRUCTURES · SAMPLES

LITHOLOGIC DESCRIPTION

2.5Y N8
2.5Y N8
2.5Y N8
2.5Y N8
2.5Y N7
2.5Y N8
2.5Y N8
volcanic ash
2.5Y N8
2.5Y N8

DOMINANT LITHOLOGY NANNOFOSSIL OOZE

White with black streaks in lower part and a band of gray at Section 4, 69 cm.

Soupy; highly disturbed through Section 3; then firm and only moderately disturbed.

Mildly bioturbated and mottled, massive bedded with no bedding structure except the thin band at Section 4, 69 cm.

Principal contituents are nannofossils

Minor lithology:
Altered volcanic ash in a small "pellet". At Section 5, 20 cm: Volcanic ash with abundant nannofossils and clay.

SMEAR SLIDE SUMMARY (%):

	4, 80	5, 70 M
Composition:		
Feldspar	Tr	–
Clay	7	15
Volcanic glass	–	3
Palagonite	Tr	1
Micronodules	–	3
Carbonate unspec.	2	5
Foraminifers	1	Tr
Calc. nannofossils	89	73
Diatoms, Radiolarians, Sponge spicules, Silicoflagellates	Tr?	–

Carbonate Bomb (%):
4, 80 = 92

SITE 558 HOLE A CORE 15 CORED INTERVAL 112.5–122.0 m

TIME-ROCK UNIT	BIOSTRATIGRAPHIC ZONE	FOSSIL CHARACTER (FORAMINIFERS, NANNOFOSSILS, RADIOLARIANS, DIATOMS)	SECTION	METERS	GRAPHIC LITHOLOGY	DRILLING DISTURBANCE	SEDIMENTARY STRUCTURES	SAMPLES	LITHOLOGIC DESCRIPTION

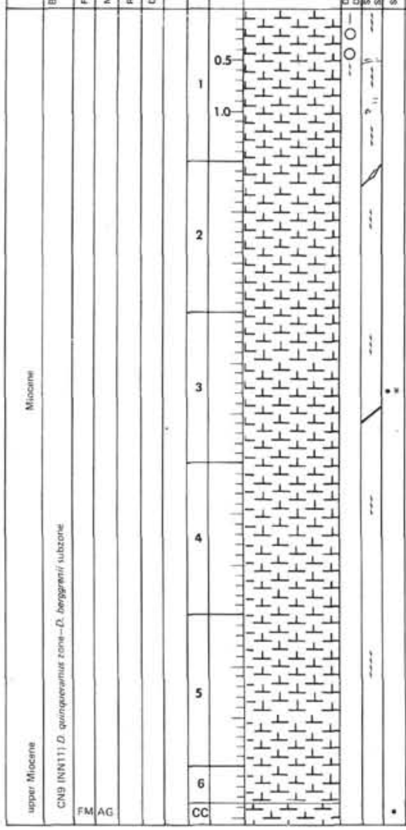

2.5Y N8
2.5Y N7
2.5Y N8
2.5Y N8
2.5Y N8
2.5Y N2
2.5Y N8
2.5Y N8
2.5Y N8

DOMINANT LITHOLOGY NANNOFOSSIL OOZE

White with slight mottling and occasional dark thin (2 mm) streaks in Sections 2 and 3.

Soft to firm; apparently no deformation except at top of Section 1.

Mildly bioturbated at sporadic intervals. Massive bedding; inclined dark streaks suggest (inclined) parallel bedding (probably deformation by coring?).

Principal constituents are nannofossils.

SMEAR SLIDE SUMMARY (%):
3, 80

Composition:	
Feldspar	1
Clay	8
Carbonate unspec.	3
Foraminifers	3
Calc. nannofossils	85

Carbonate Bomb (%):
3, 80 = 91
CC = 89

SITE 558 HOLE A CORE 16 CORED INTERVAL 122.0–131.5 m

TIME-ROCK UNIT	BIOSTRATIGRAPHIC ZONE	FOSSIL CHARACTER (FORAMINIFERS, NANNOFOSSILS, RADIOLARIANS, DIATOMS)	SECTION	METERS	GRAPHIC LITHOLOGY	DRILLING DISTURBANCE	SEDIMENTARY STRUCTURES	SAMPLES	LITHOLOGIC DESCRIPTION

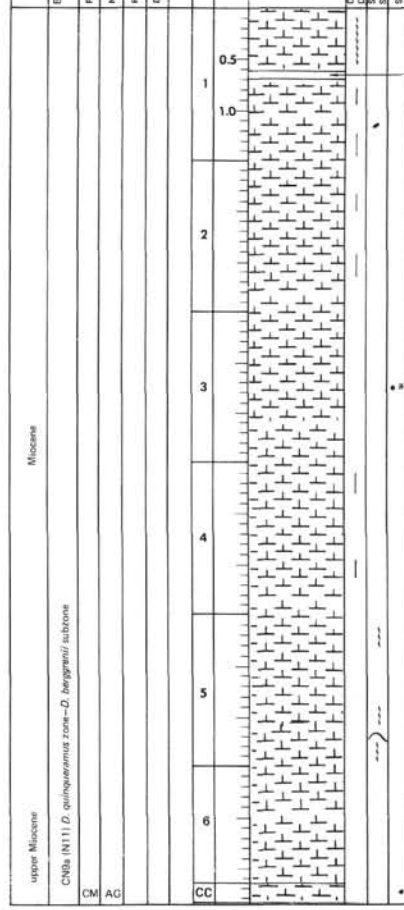

2.5Y N8
void
2.5Y N8
2.5Y N8
2.5Y N8
2.5Y N8
2.5Y N8

DOMINANT LITHOLOGY NANNOFOSSIL OOZE

White with black streaks in Section 3 and an irregular 3 mm dark layer in Section 5; a black nodule in Section 1.

Soft to firm, relatively undisturbed

Very slightly bioturbated and faintly mottled in lower part of core. No bedding structure apparent except for the irregular dark lamina in Section 5.

Principal constituents are nannofossils. The carbonate content is 84% (as compared with 91% in Core 15), but there is no apparent increase in siliceous components.

SMEAR SLIDE SUMMARY (%):
3, 80

Composition:	
Feldspar	1
Clay	13
Palagonite	Tr
Micronodules	Tr
Carbonate unspec.	5
Foraminifers	Tr
Calc. nannofossils	80
Diatoms	Tr?
Radiolarians	Tr?
Sponge spicules	Tr?
Silicoflagellates	Tr?

Carbonate Bomb (%):
3, 80 = 84
CC = 91

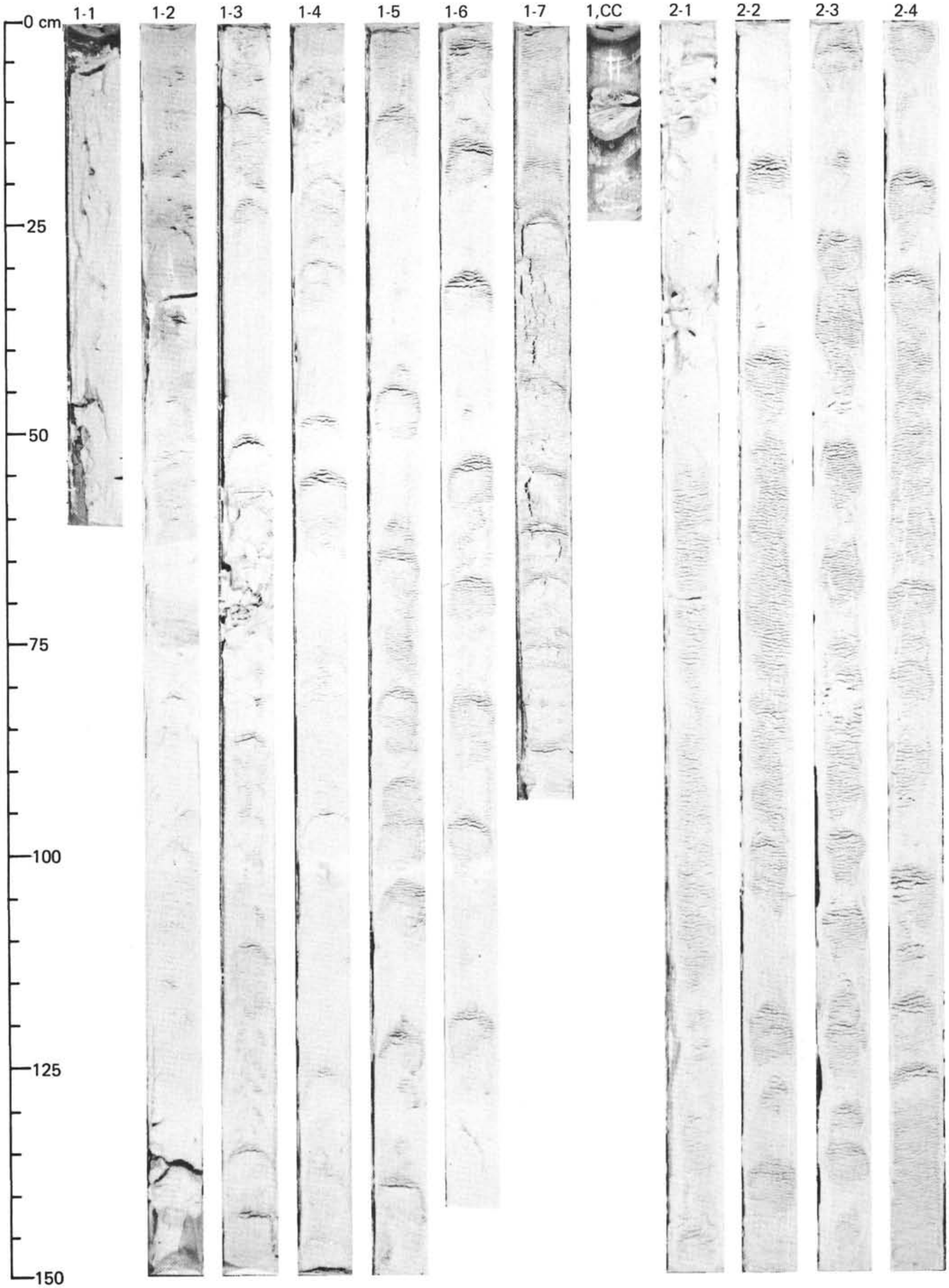
0 cm
25
50
75
100
125
150
1-1
1-2
1-3
1-4
1-5
1-6
1-7
1,CC
2-1
2-2
2-3
2-4

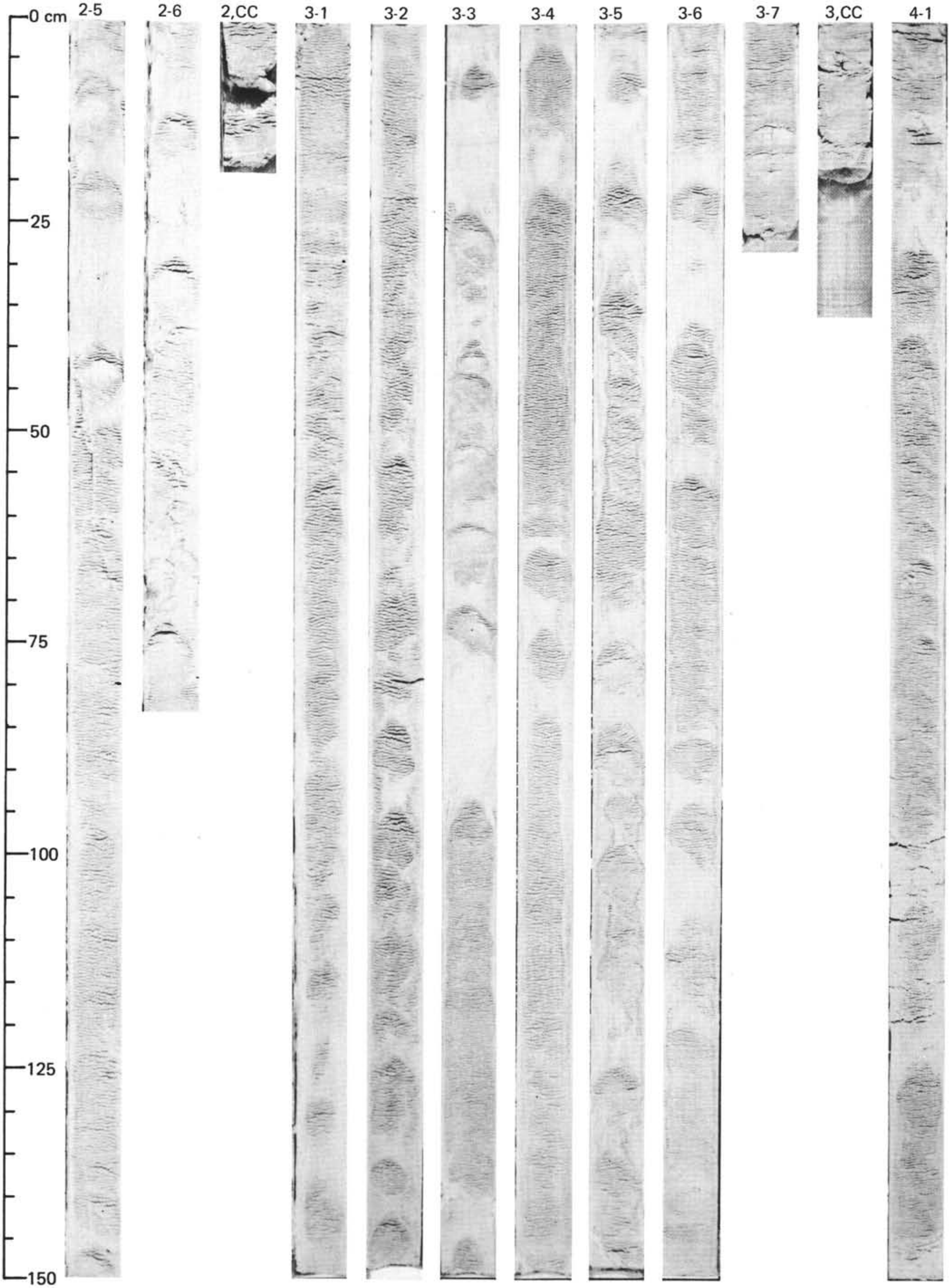
0 cm
25
50
75
100
125
150
2-5
2-6
2,CC
3-1
3-2
3-3
3-4
3-5
3-6
3-7
3,CC
4-1

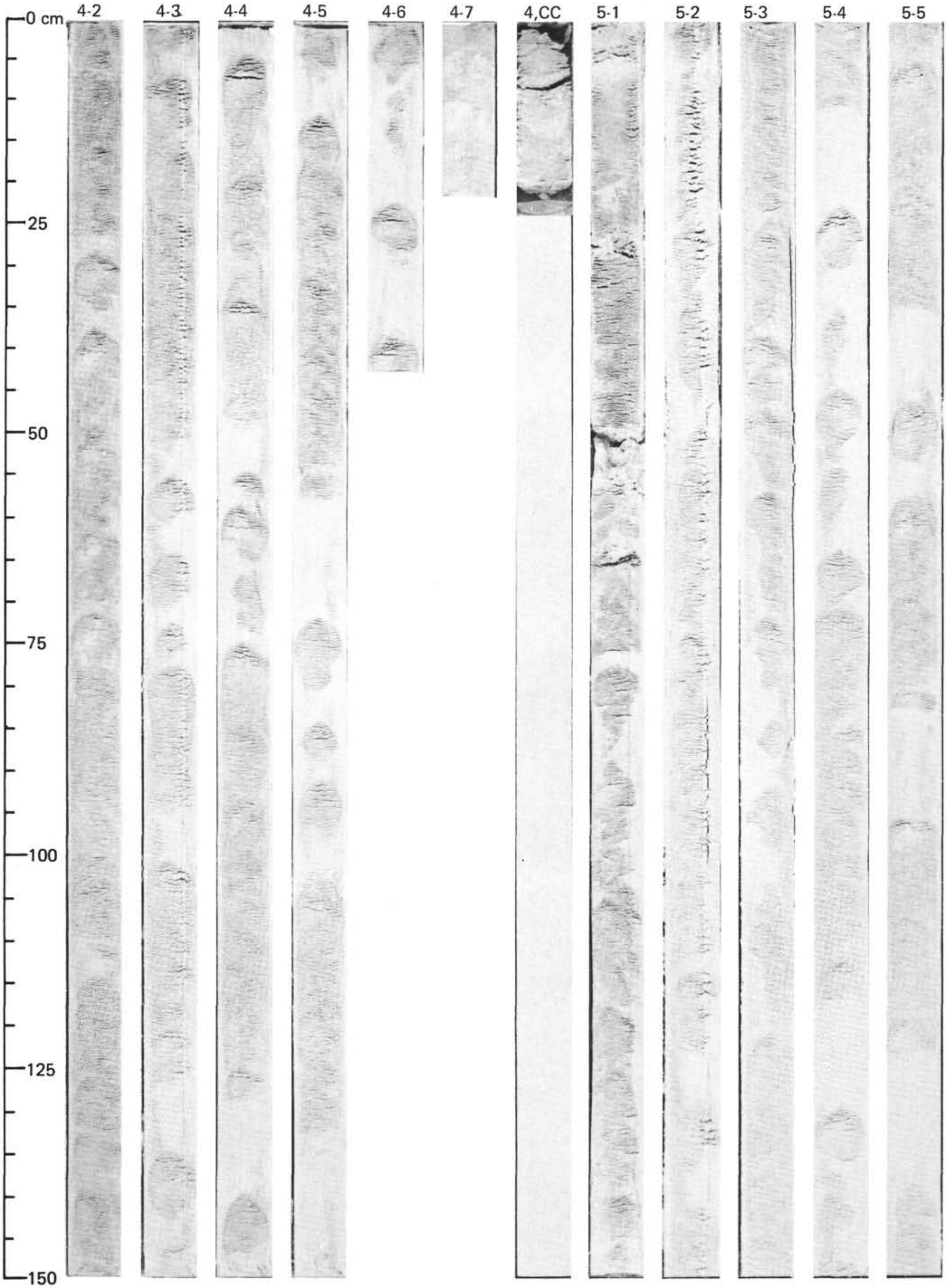
0 cm
25
50
75
100
125
150
4-2
4-3
4-4
4-5
4-6
4-7
4,CC
5-1
5-2
5-3
5-4
5-5

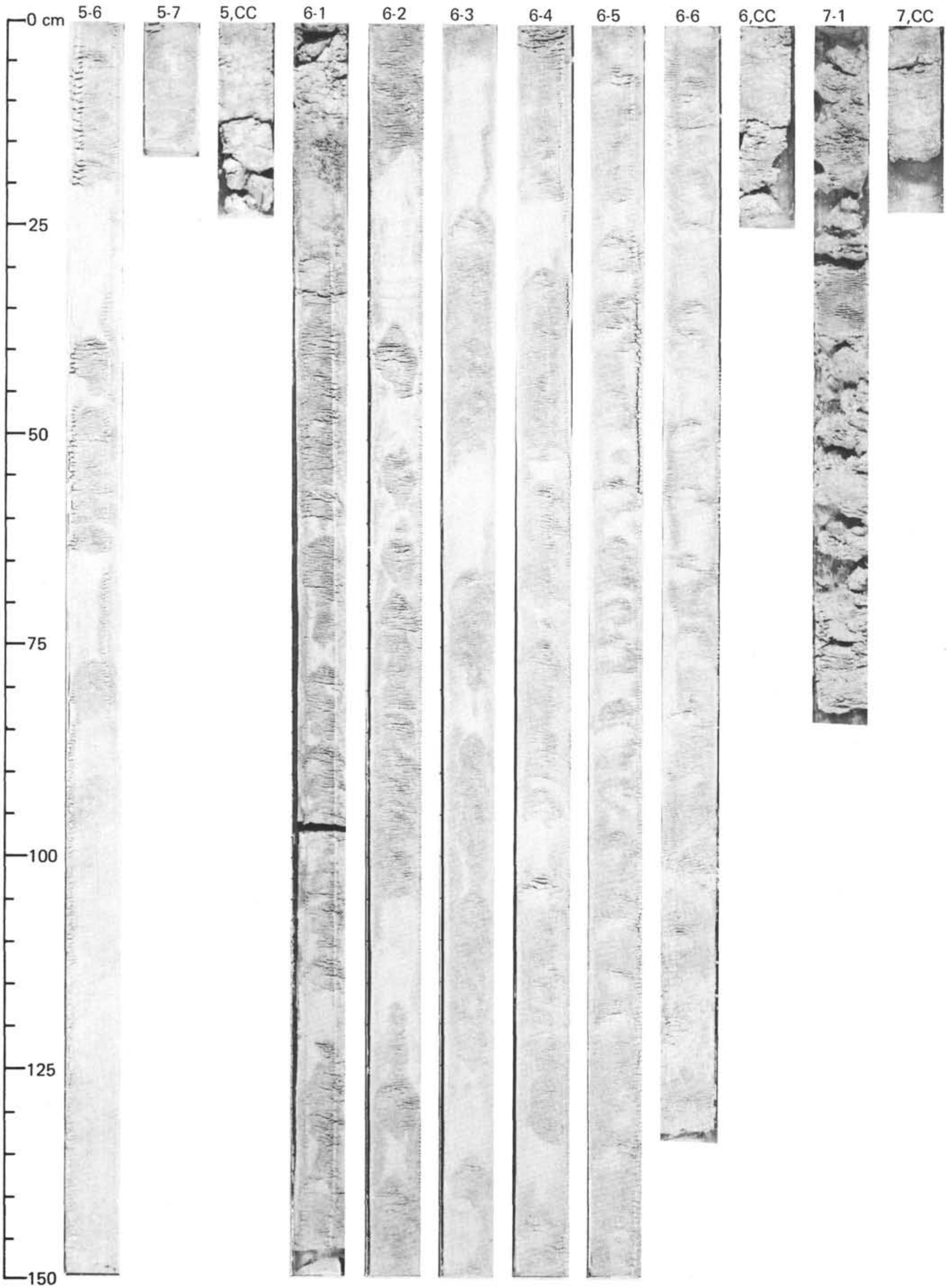
0 cm
25
50
75
100
125
150
5-6
5-7
5,CC
6-1
6-2
6-3
6-4
6-5
6-6
6,CC
7-1
7,CC

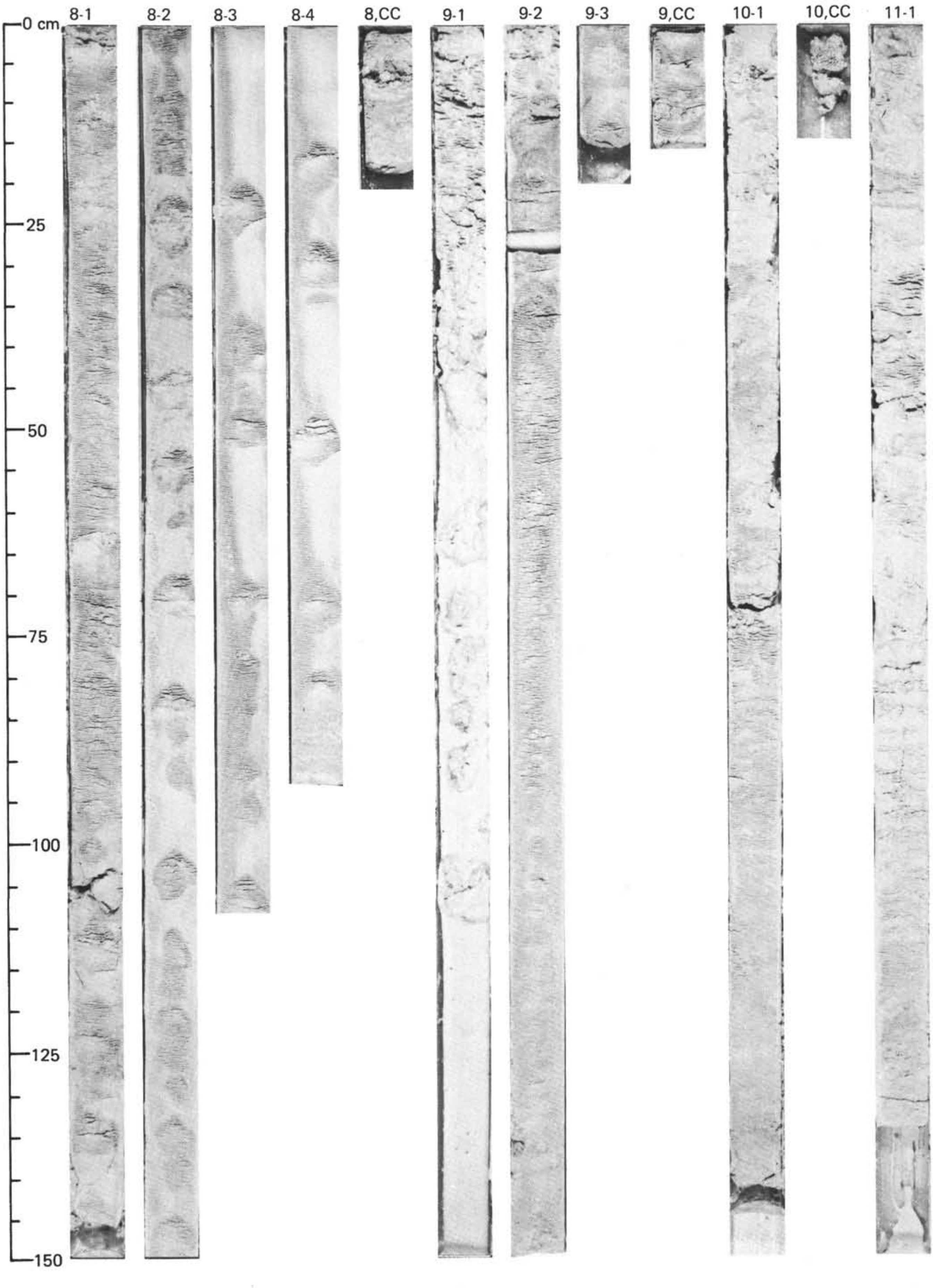
8-1
8-2
8-3
8-4
8,CC
9-1
9-2
9-3
9,CC
10-1
10,CC
11-1
0 cm
25
50
75
100
125
150

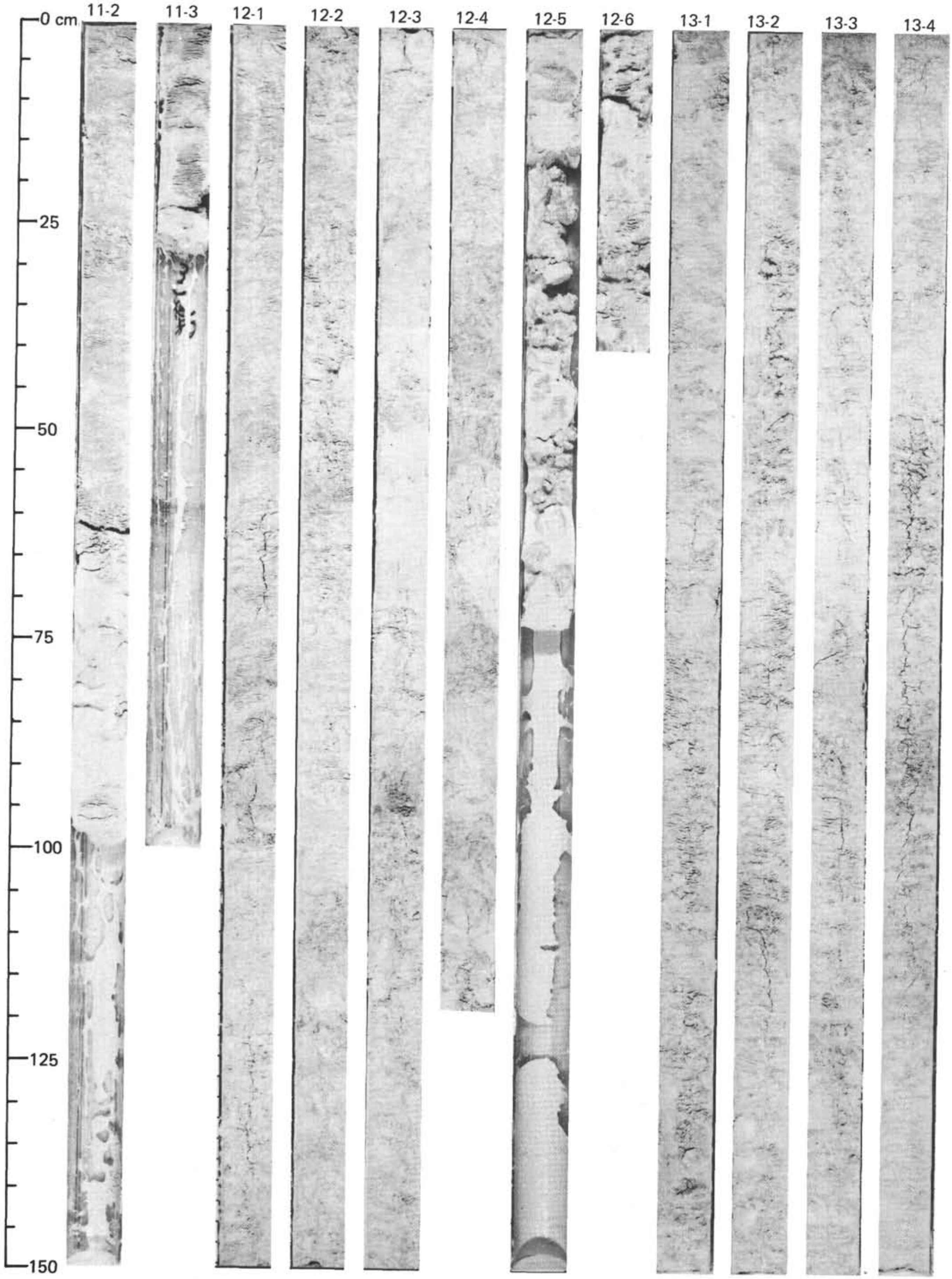
0 cm
25
50
75
100
125
150
11-2
11-3
12-1
12-2
12-3
12-4
12-5
12-6
13-1
13-2
13-3
13-4

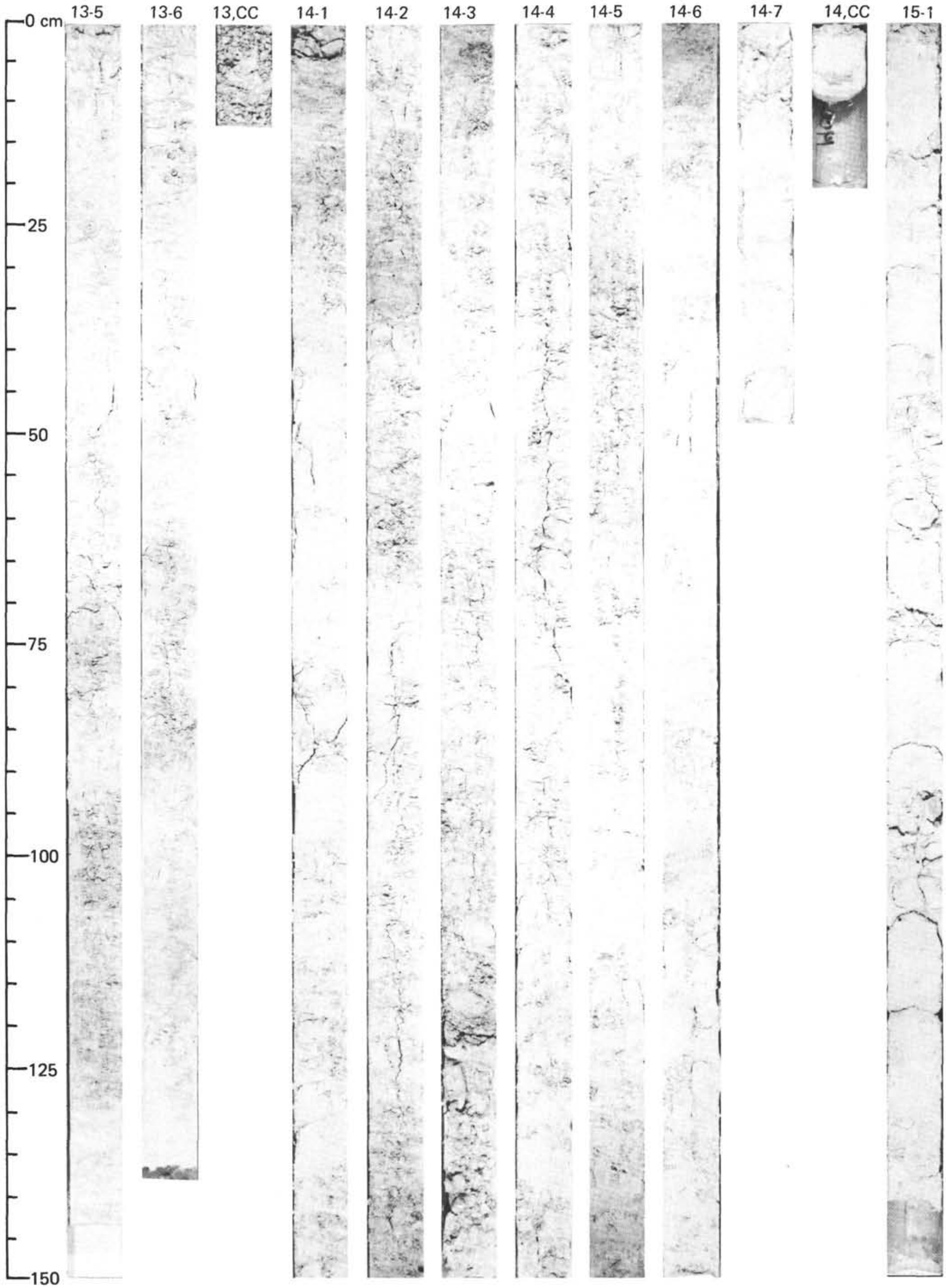
0 cm
25
50
75
100
125
150
13-5
13-6
13,CC
14-1
14-2
14-3
14-4
14-5
14-6
14-7
14,CC
15-1

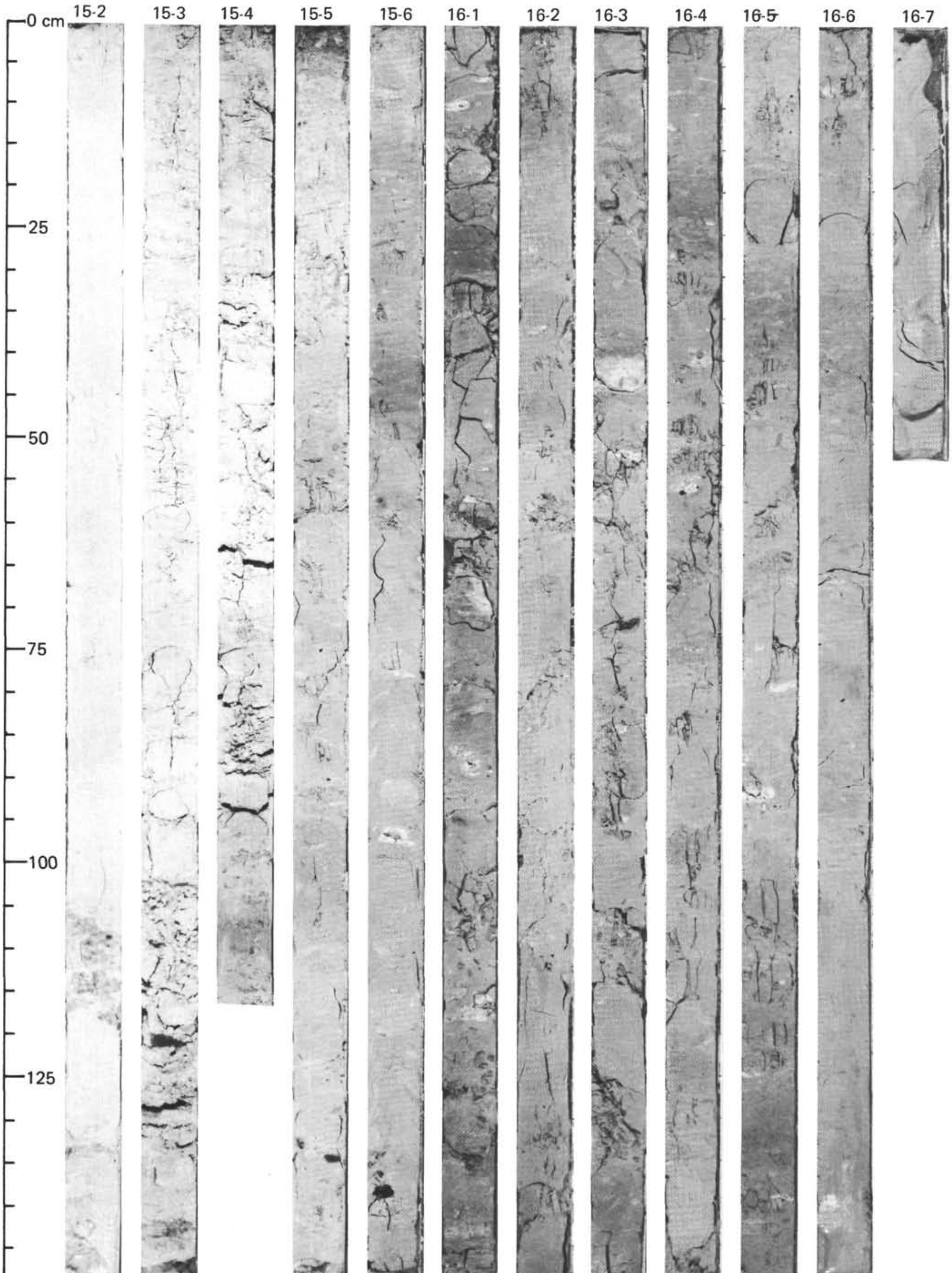
0 cm
25
50
75
100
125
150
15-2
15-3
15-4
15-5
15-6
16-1
16-2
16-3
16-4
16-5
16-6
16-7

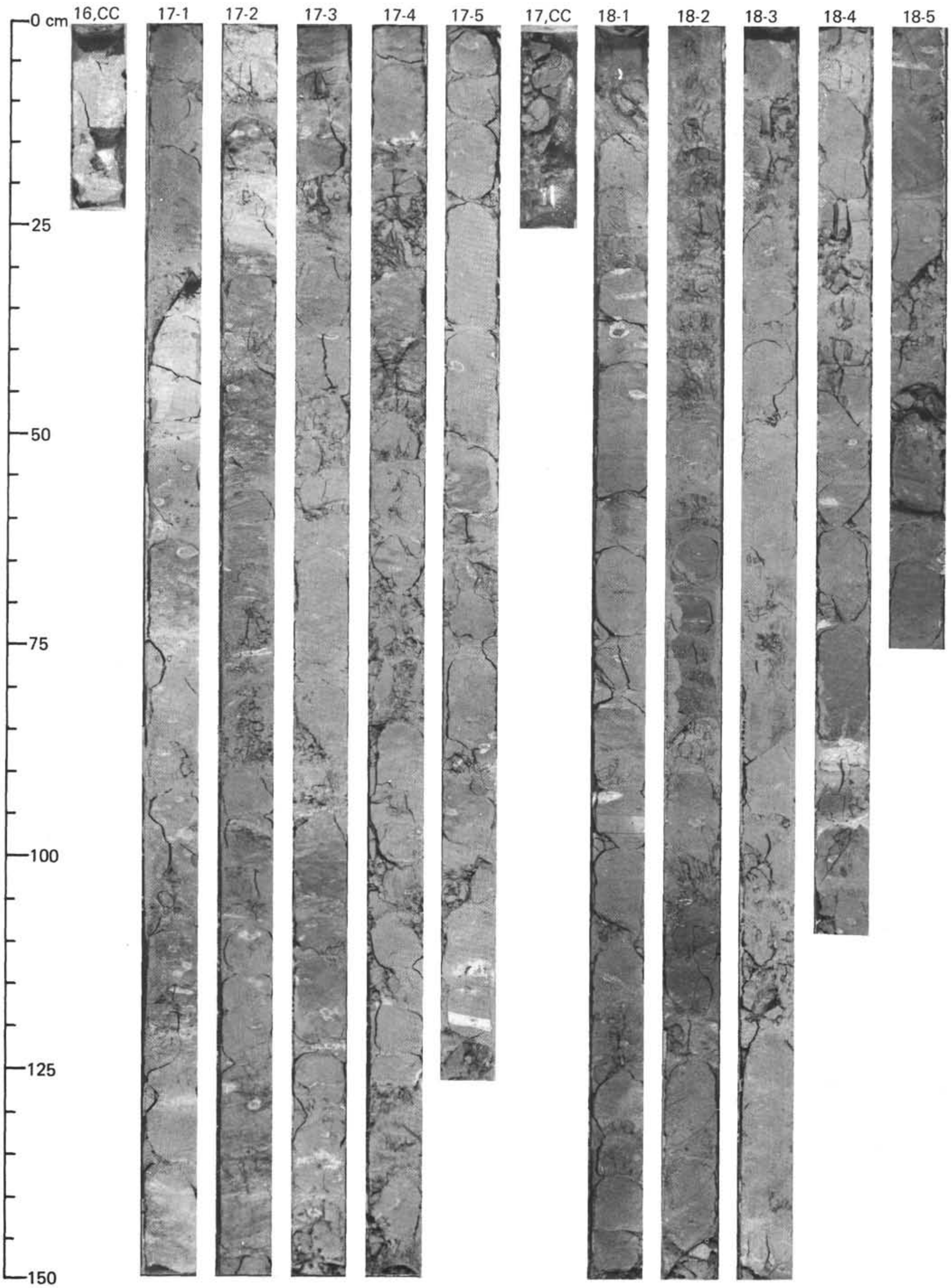
0 cm
25
50
75
100
125
150
16,CC
17-1
17-2
17-3
17-4
17-5
17,CC
18-1
18-2
18-3
18-4
18-5

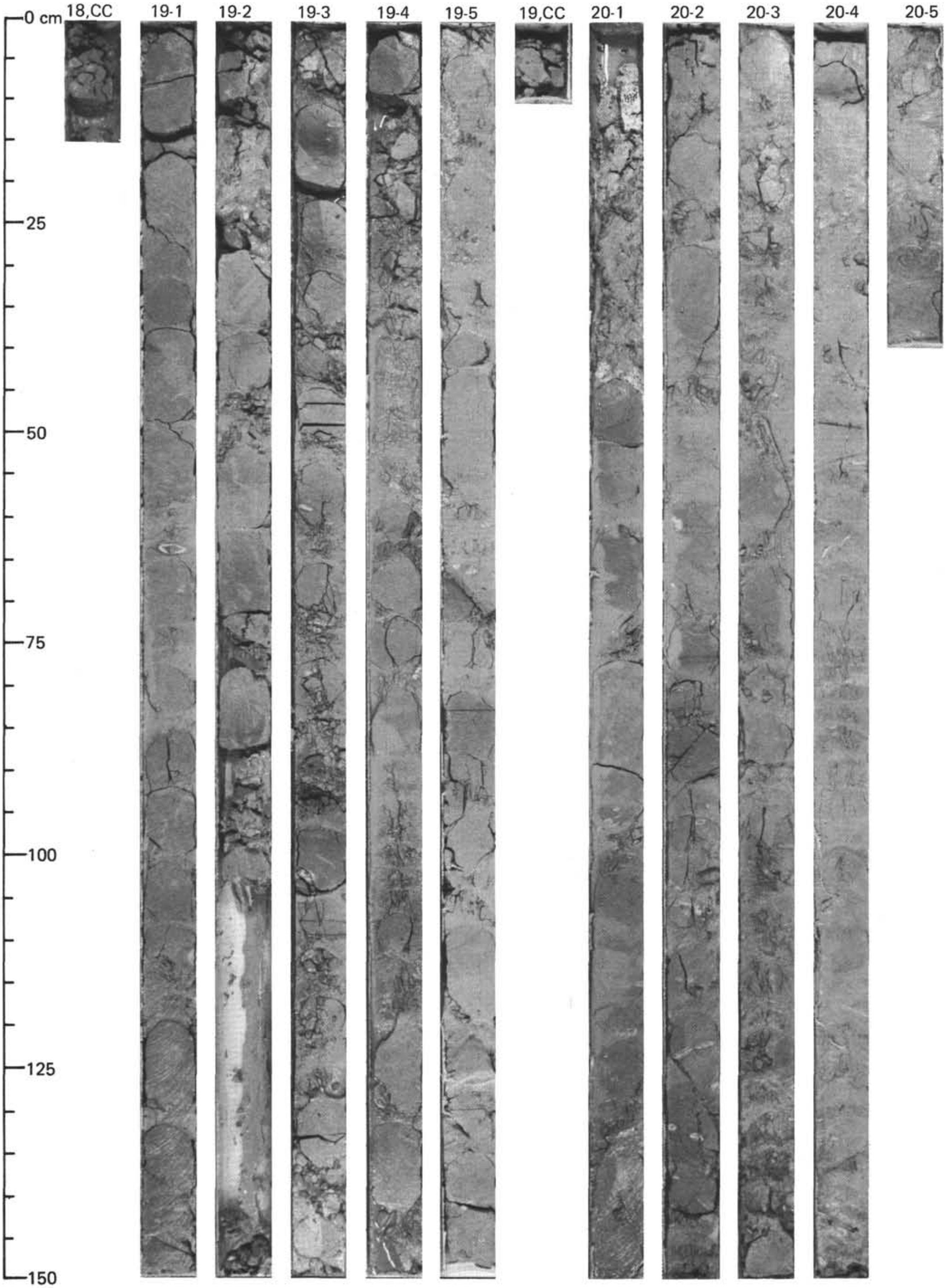
0 cm
25
50
75
100
125
150
18,CC
19-1
19-2
19-3
19-4
19-5
19,CC
20-1
20-2
20-3
20-4
20-5

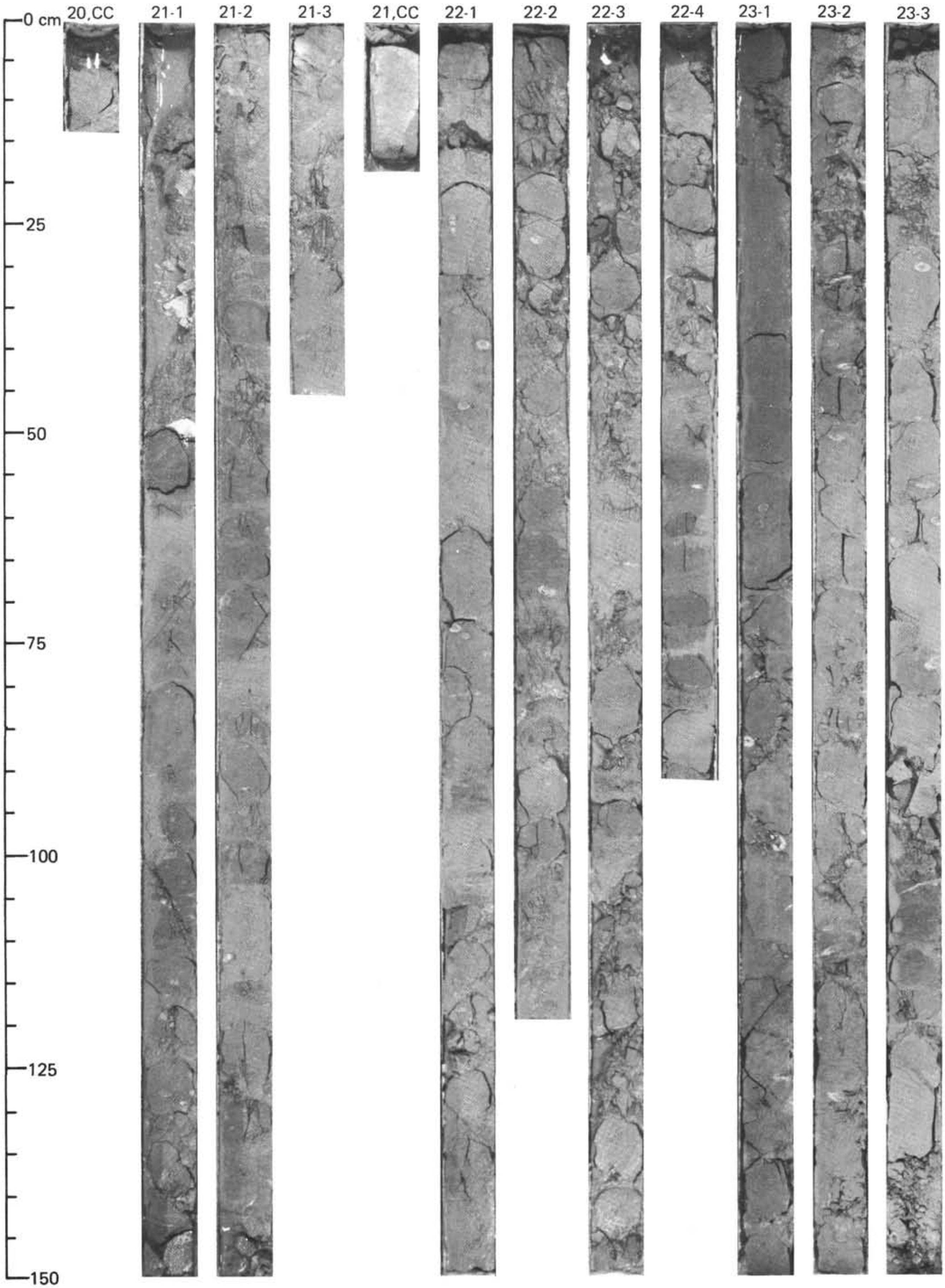
0 cm
25
50
75
100
125
150
20,CC
21-1
21-2
21-3
21,CC
22-1
22-2
22-3
22-4
23-1
23-2
23-3

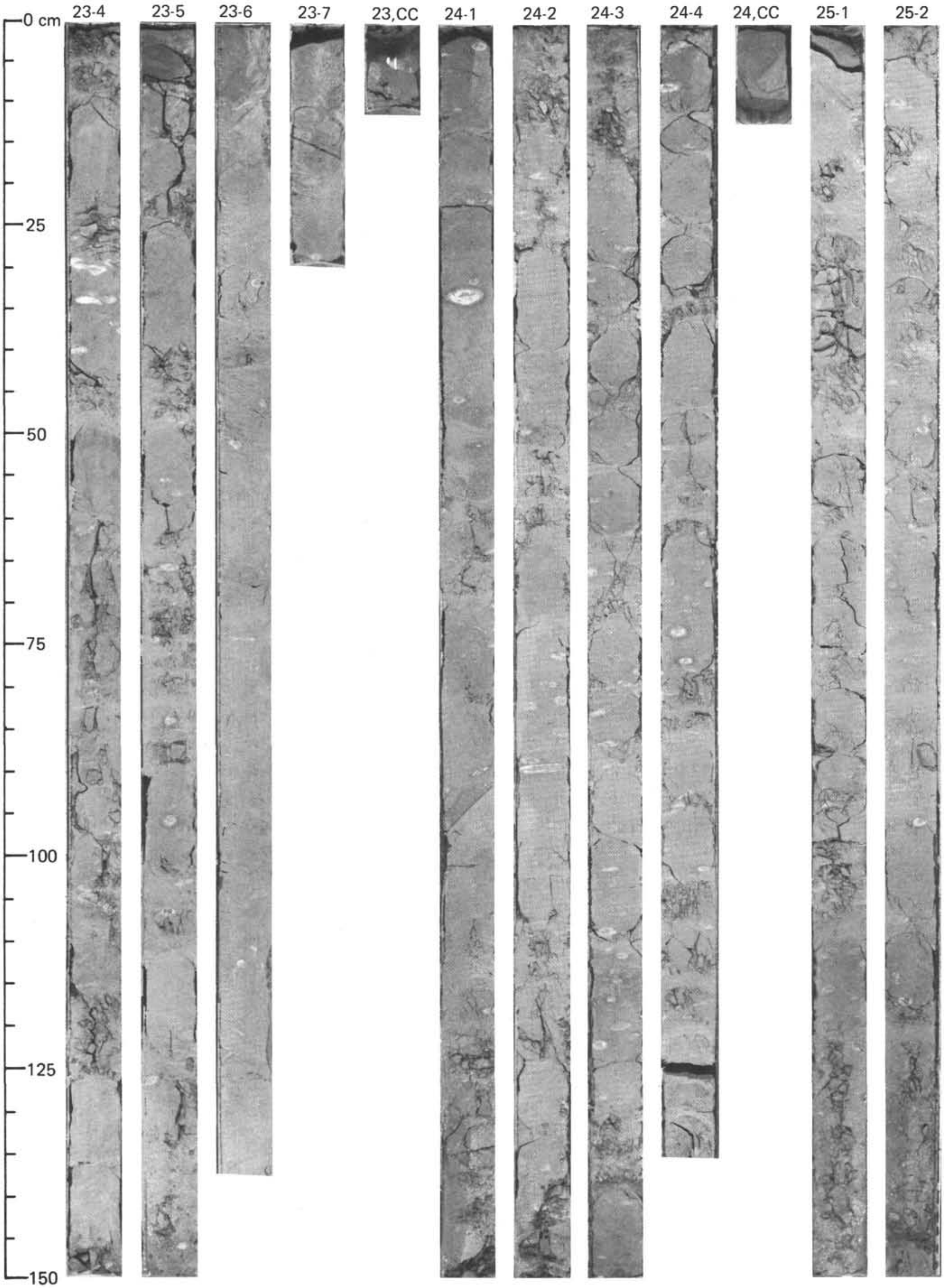
0 cm
25
50
75
100
125
150
23-4
23-5
23-6
23-7
23,CC
24-1
24-2
24-3
24-4
24,CC
25-1
25-2

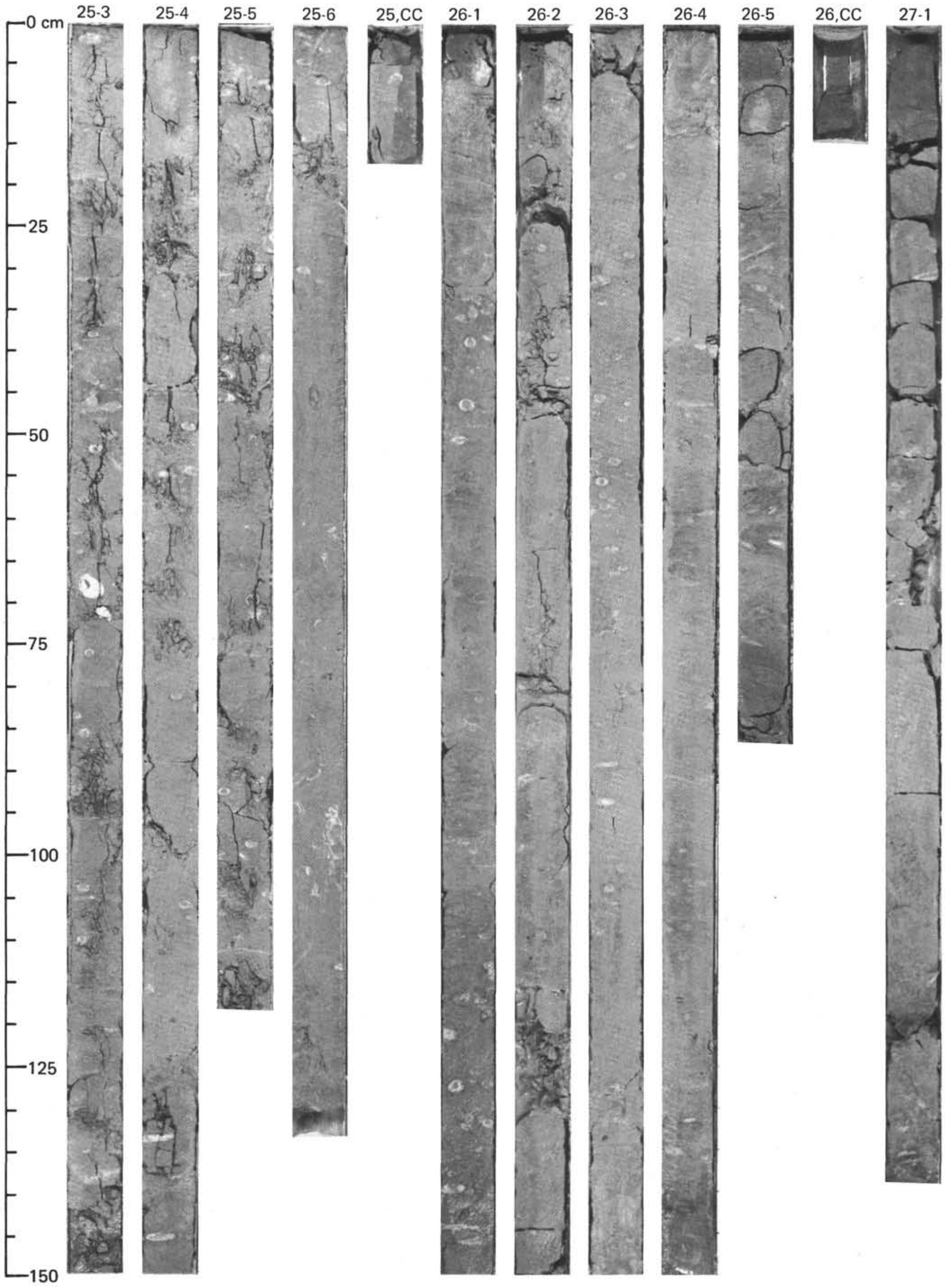
0 cm
25
50
75
100
125
150
25-3
25-4
25-5
25-6
25,CC
26-1
26-2
26-3
26-4
26-5
26,CC
27-1

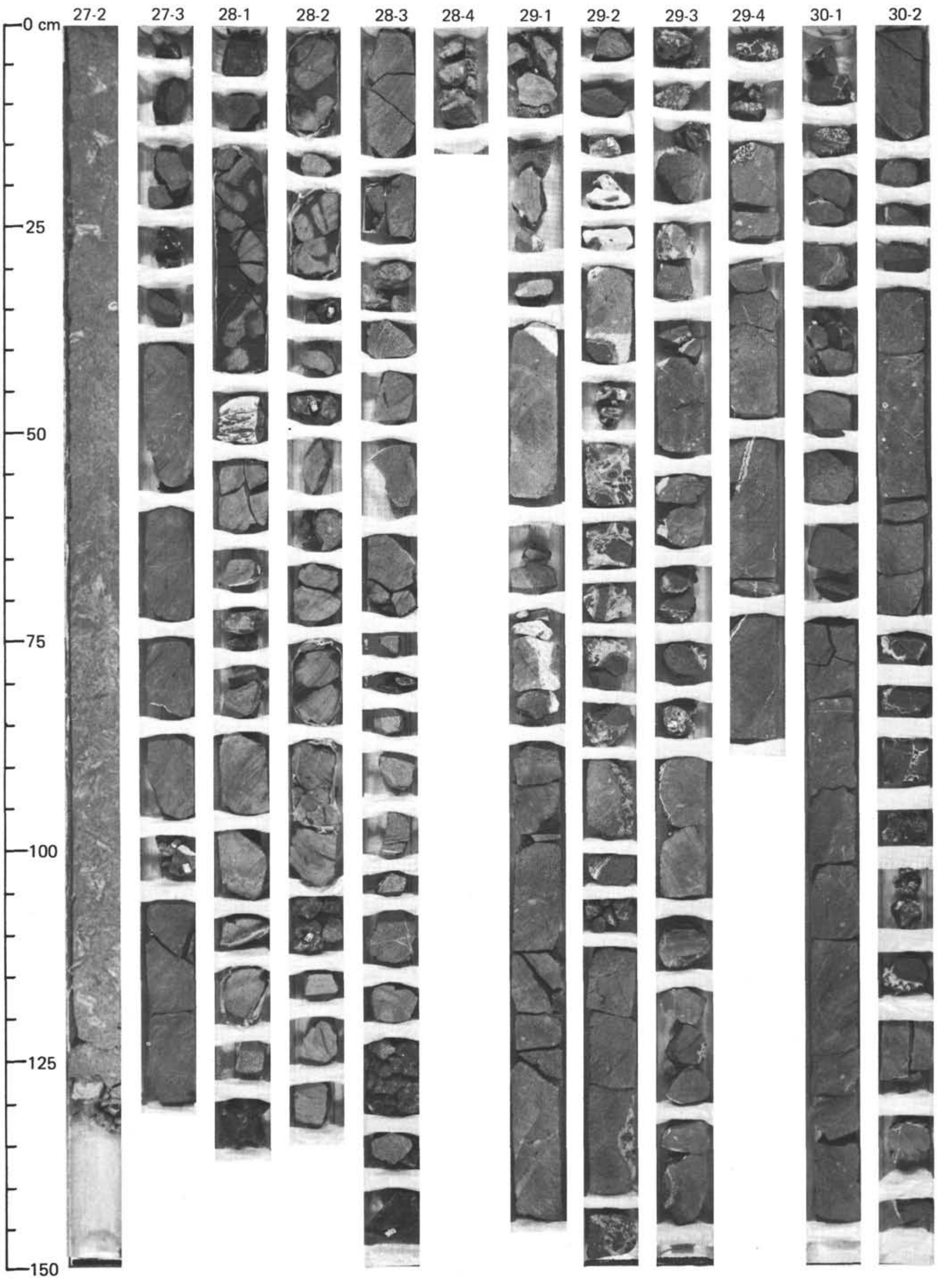
0 cm
25
50
75
100
125
150
27-2
27-3
28-1
28-2
28-3
28-4
29-1
29-2
29-3
29-4
30-1
30-2

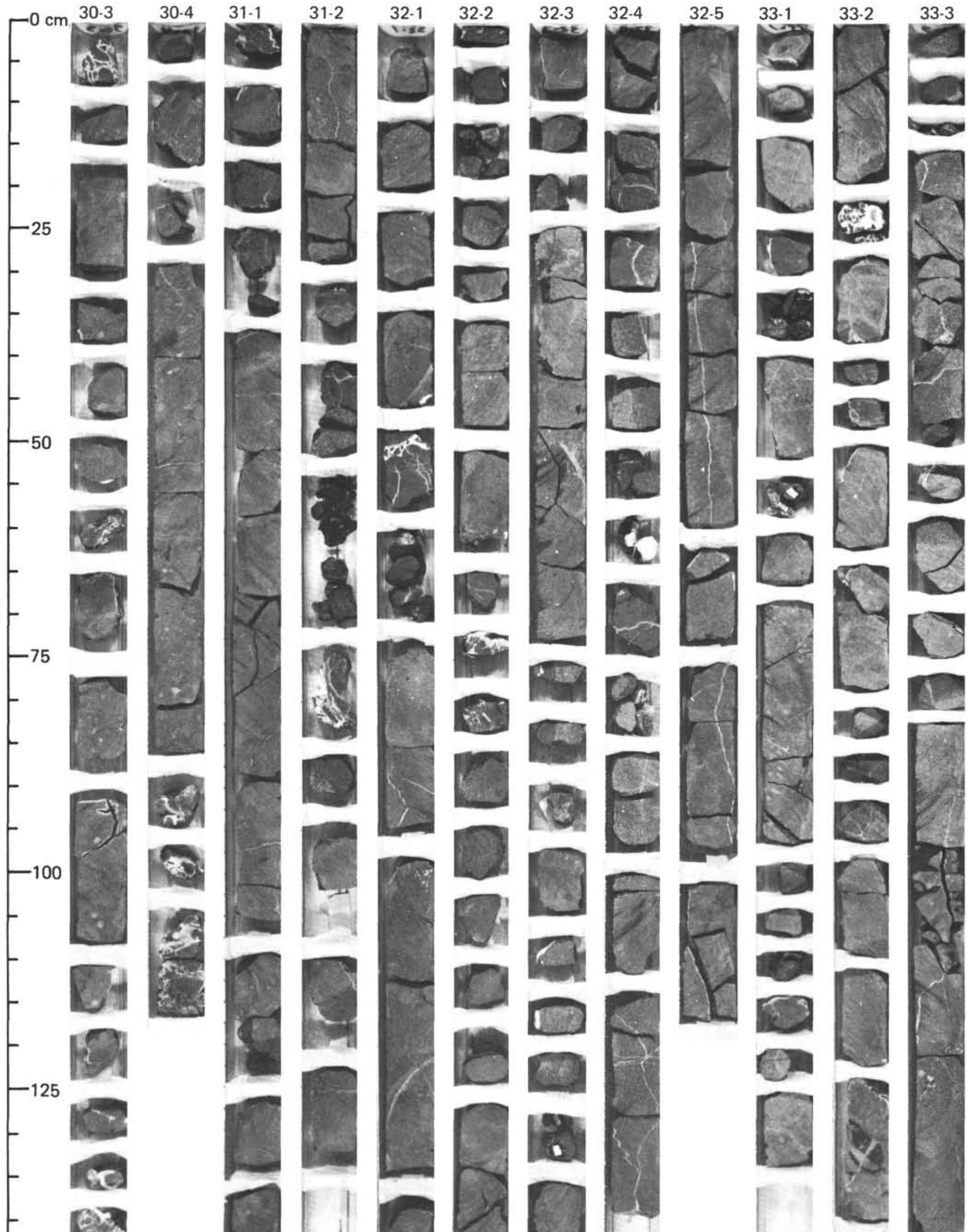
0 cm
25
50
75
100
125
150
30-3
30-4
31-1
31-2
32-1
32-2
32-3
32-4
32-5
33-1
33-2
33-3

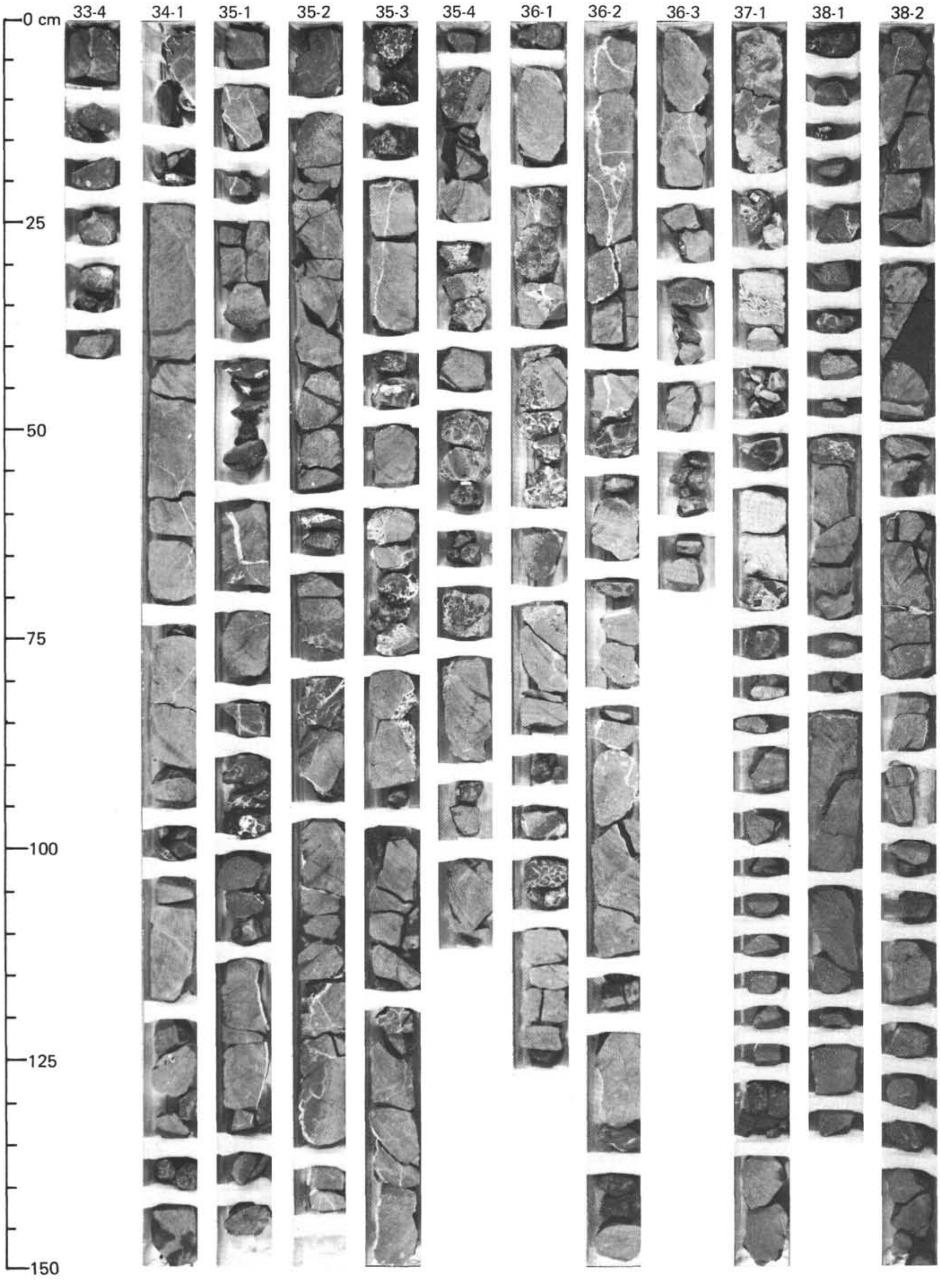
33-4
34-1
35-1
35-2
35-3
35-4
36-1
36-2
36-3
37-1
38-1
38-2
0 cm
25
50
75
100
125
150

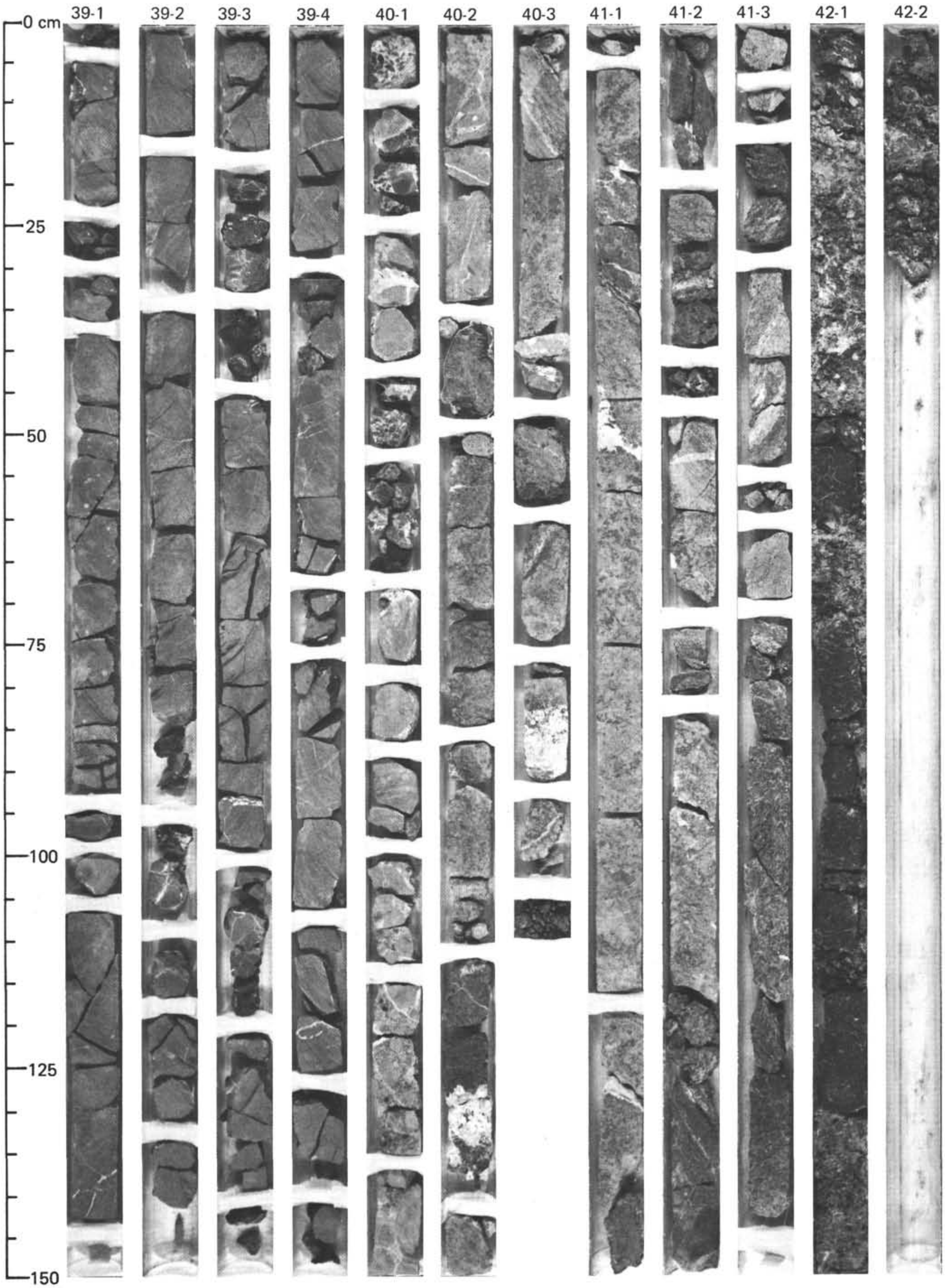
39-1
39-2
39-3
39-4
40-1
40-2
40-3
41-1
41-2
41-3
42-1
42-2
0 cm
25
50
75
100
125
150

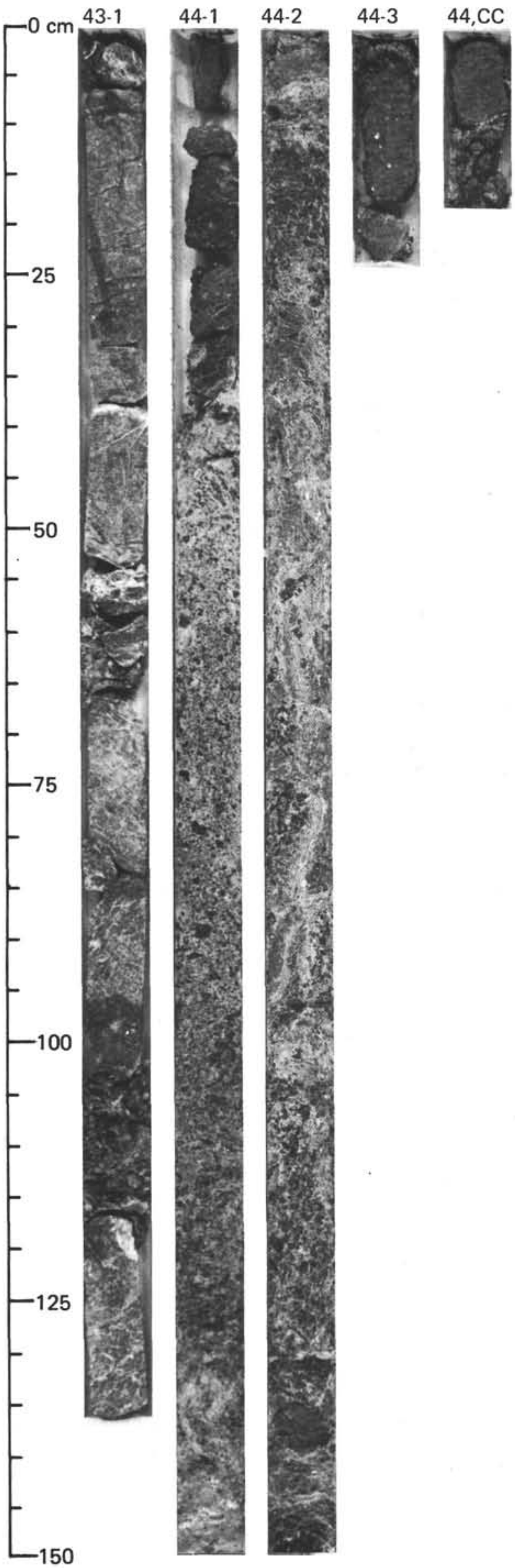
0 cm
25
50
75
100
125
150
43-1
44-1
44-2
44-3
44,CC

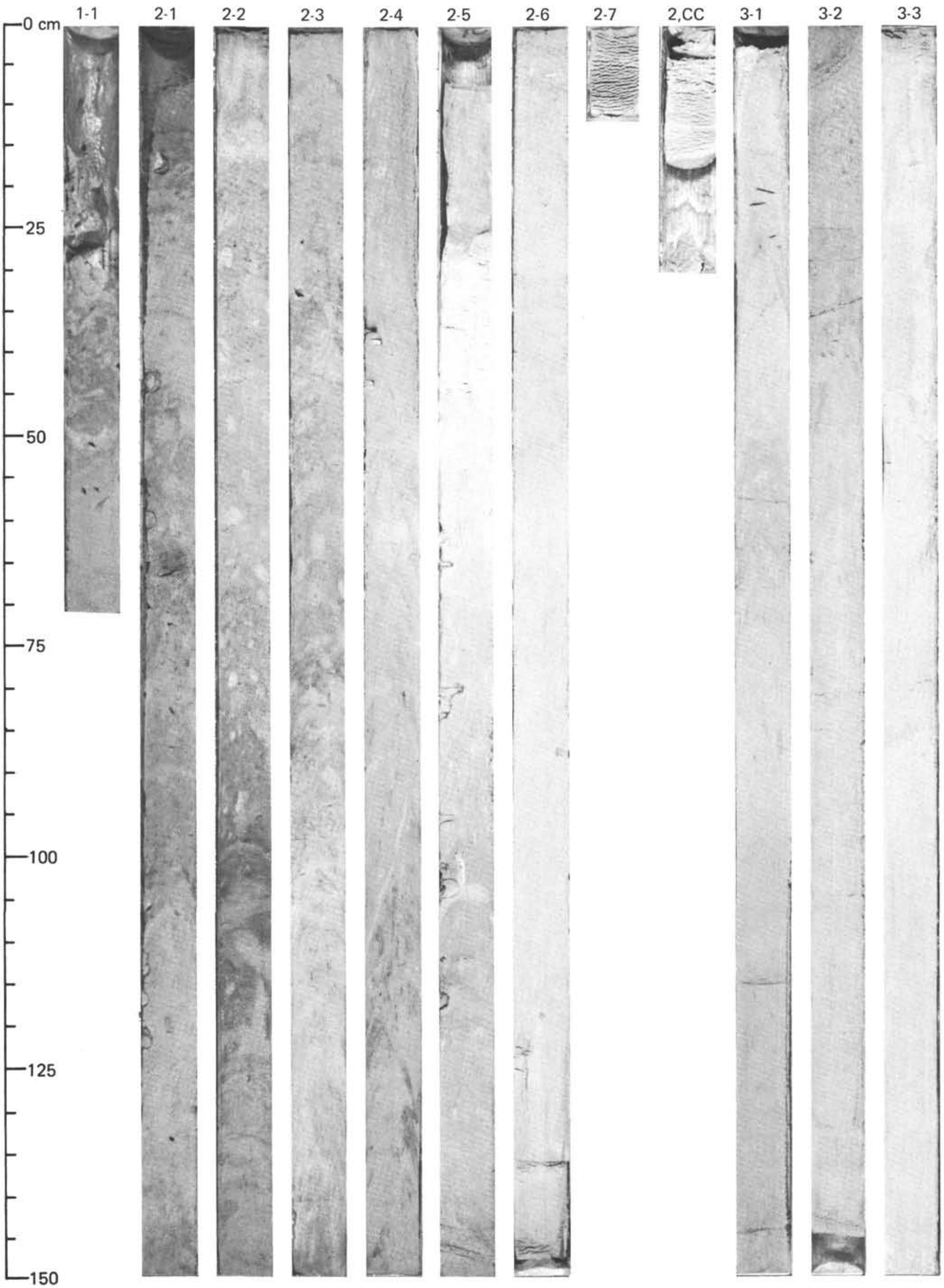
1-1
2-1
2-2
2-3
2-4
2-5
2-6
2-7
2,CC
3-1
3-2
3-3
0 cm
25
50
75
100
125
150

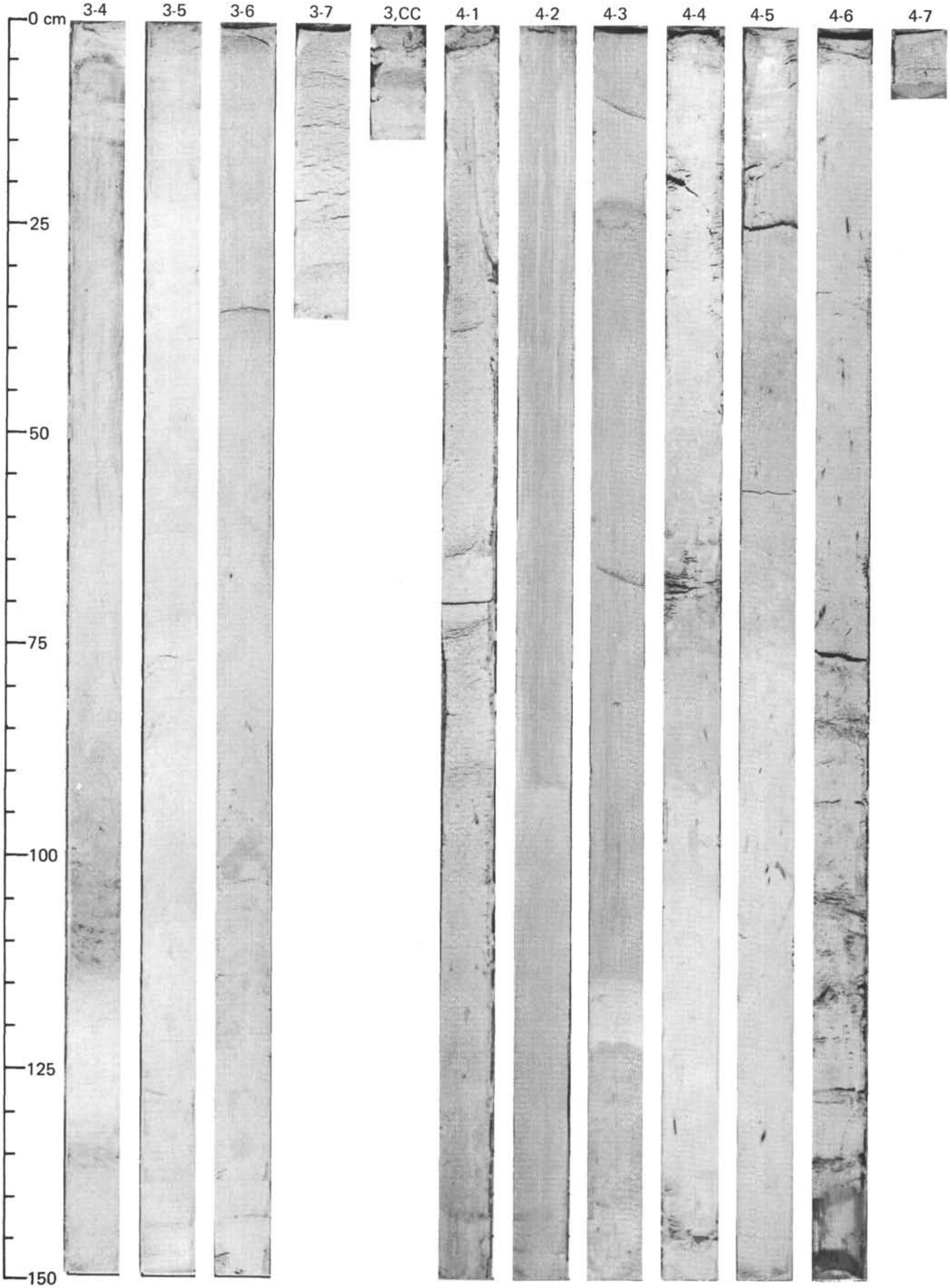
0 cm
25
50
75
100
125
150
3-4
3-5
3-6
3-7
3,CC
4-1
4-2
4-3
4-4
4-5
4-6
4-7

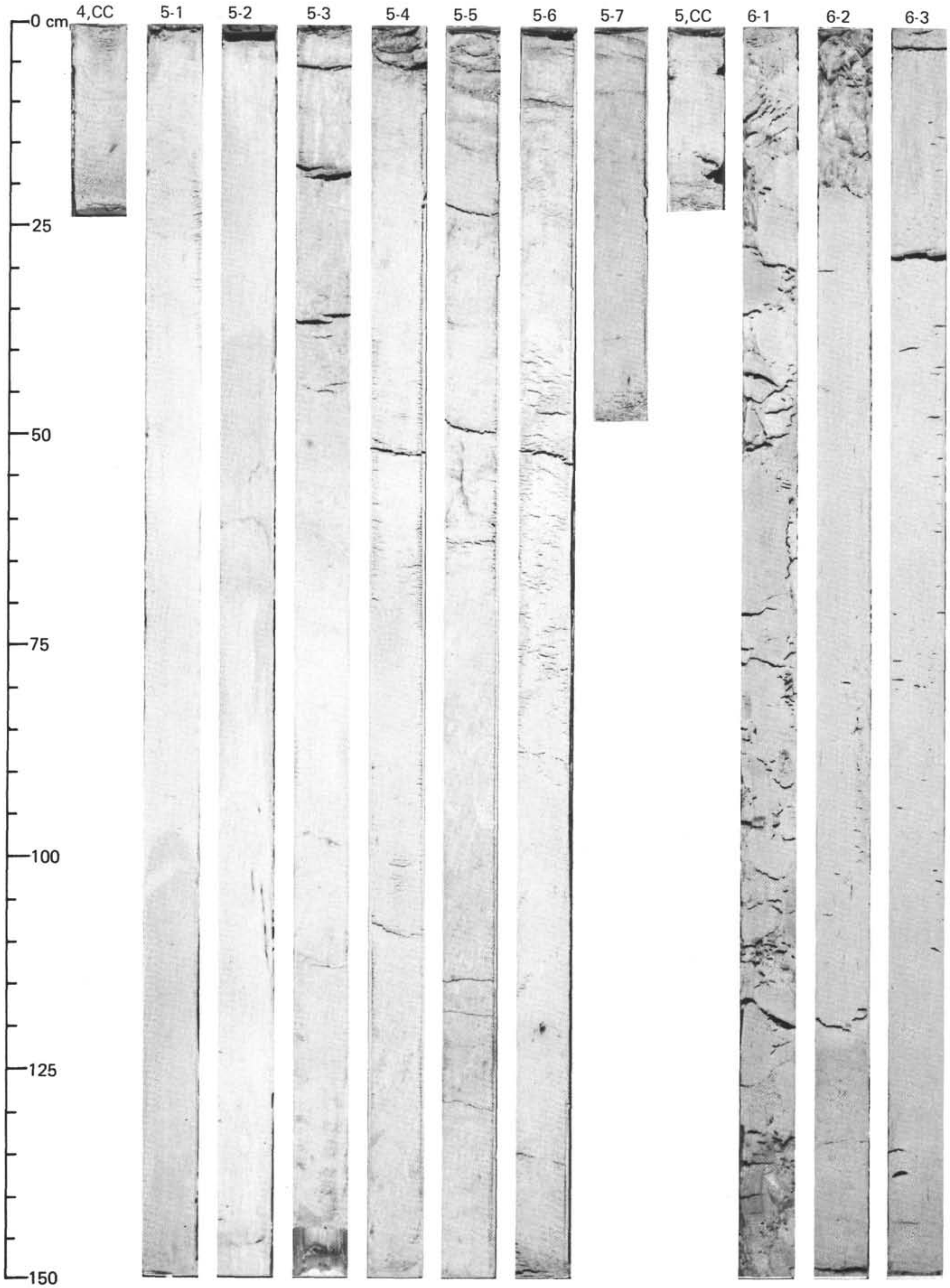
0 cm
25
50
75
100
125
150
4,CC
5-1
5-2
5-3
5-4
5-5
5-6
5-7
5,CC
6-1
6-2
6-3

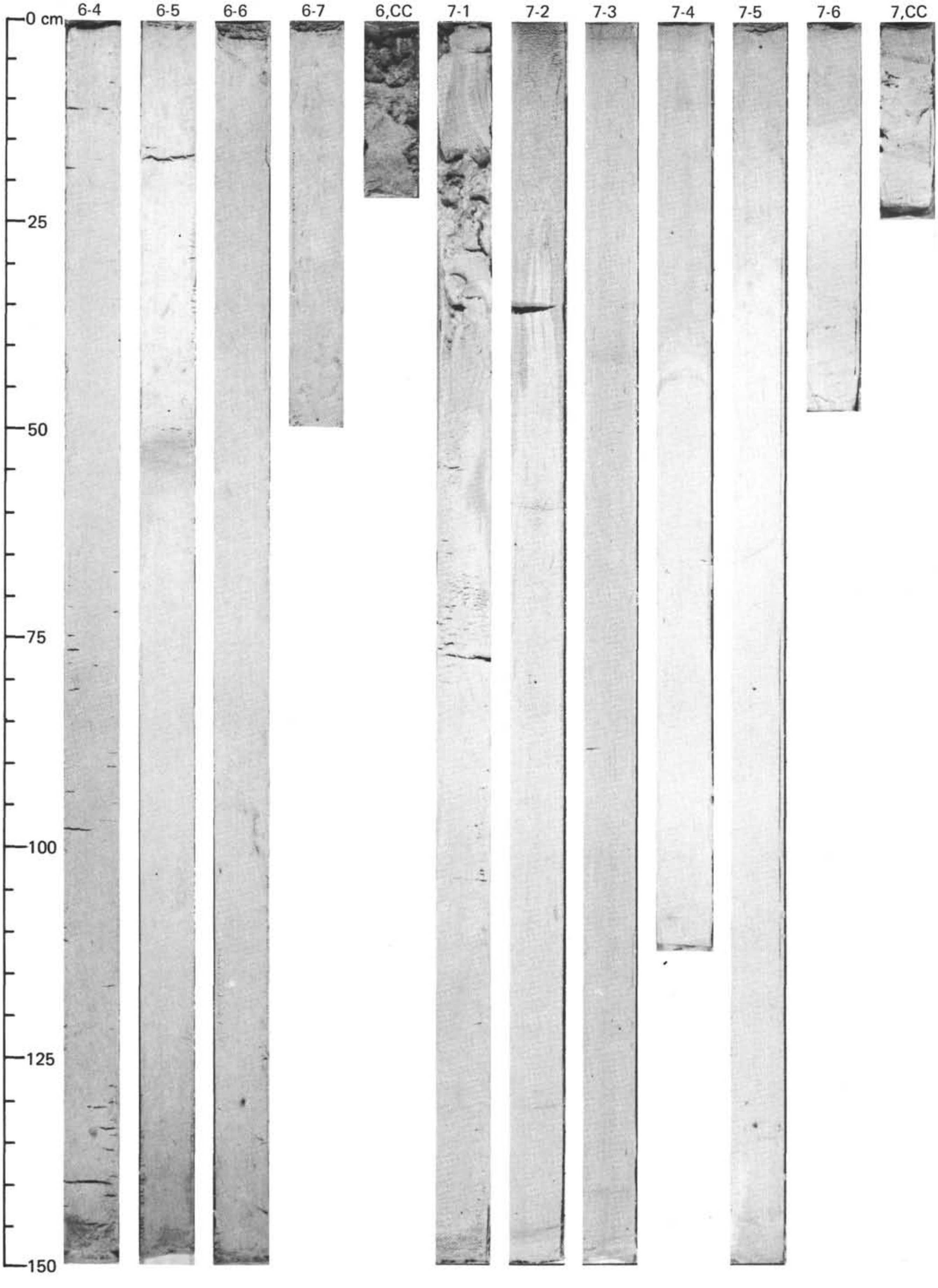
0 cm
25
50
75
100
125
150
6-4
6-5
6-6
6-7
6,CC
7-1
7-2
7-3
7-4
7-5
7-6
7,CC


8-1
8-2
8-3
8-4
8-5
8-6
8,CC
9-1
9-2
9-3
9-4
9,CC
0 cm
25
50
75
100
125
150

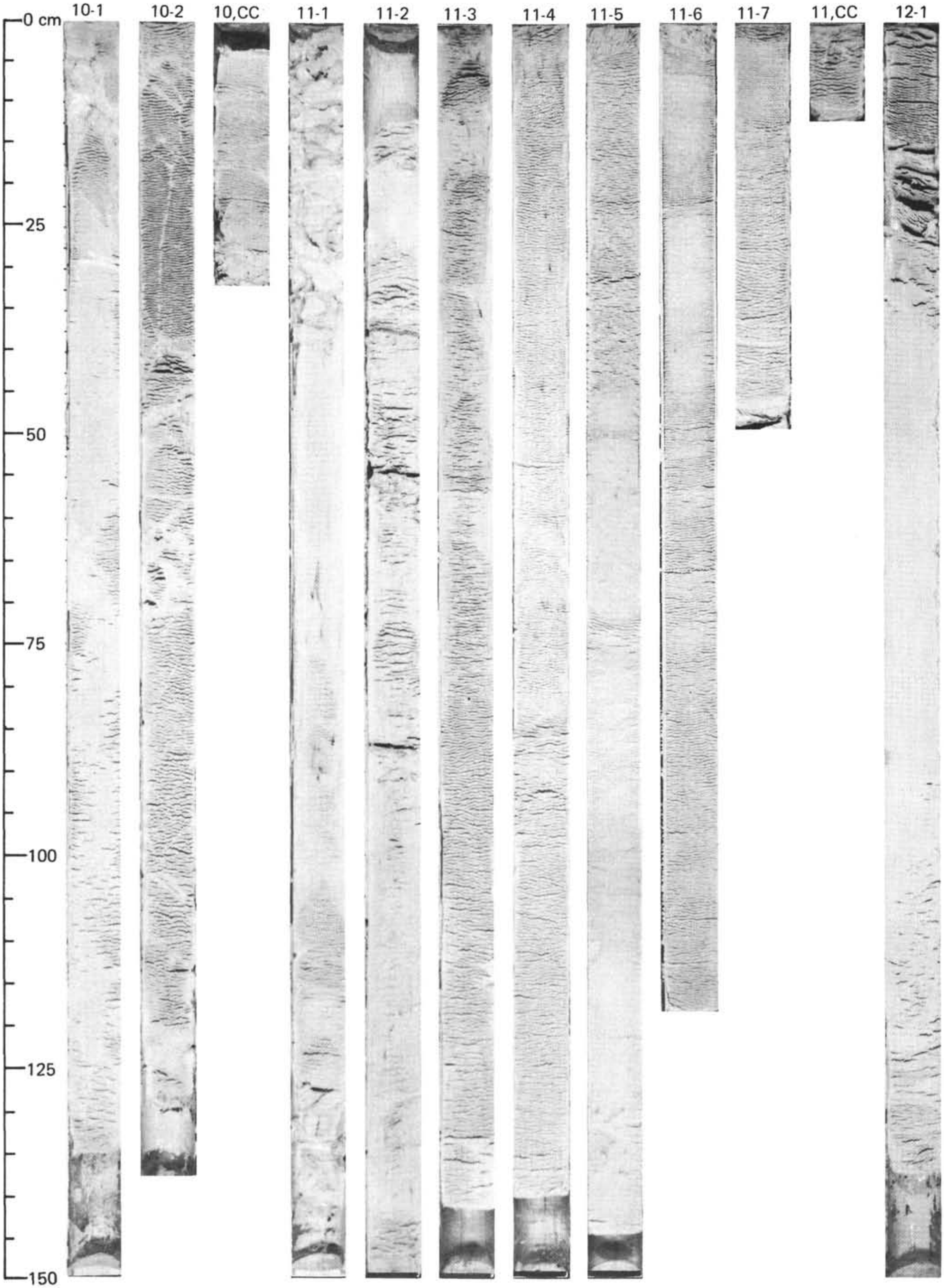
0 cm
25
50
75
100
125
150
10-1
10-2
10,CC
11-1
11-2
11-3
11-4
11-5
11-6
11-7
11,CC
12-1

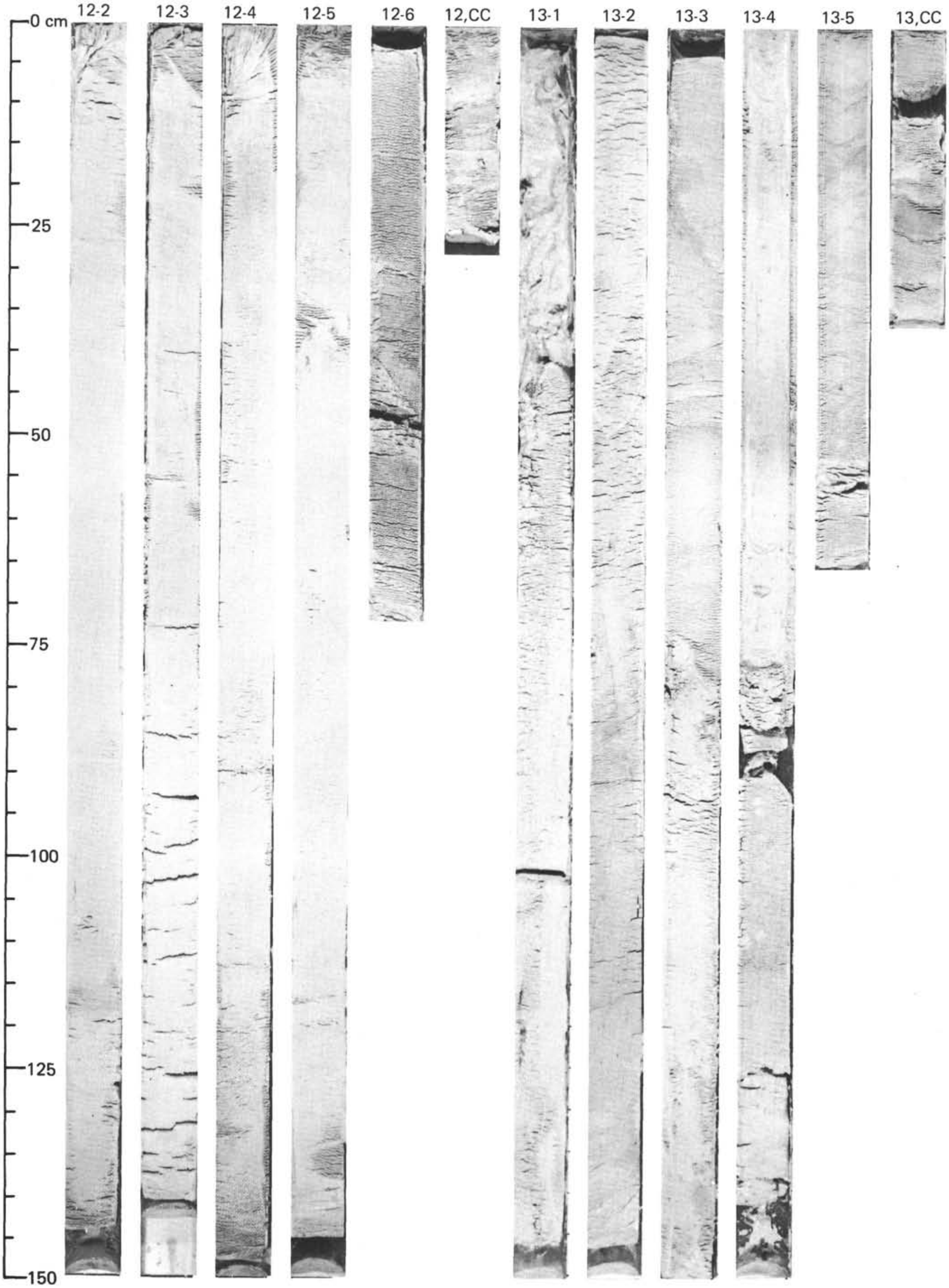

12-2
12-3
12-4
12-5
12-6
12,CC
13-1
13-2
13-3
13-4
13-5
13,CC
0 cm
25
50
75
100
125
150


0 cm
25
50
75
100
125
150
14-1
14-2
14-3
14-4
14-5
14-6
14-7
14,CC
15-1
15-2
15-3
15-4

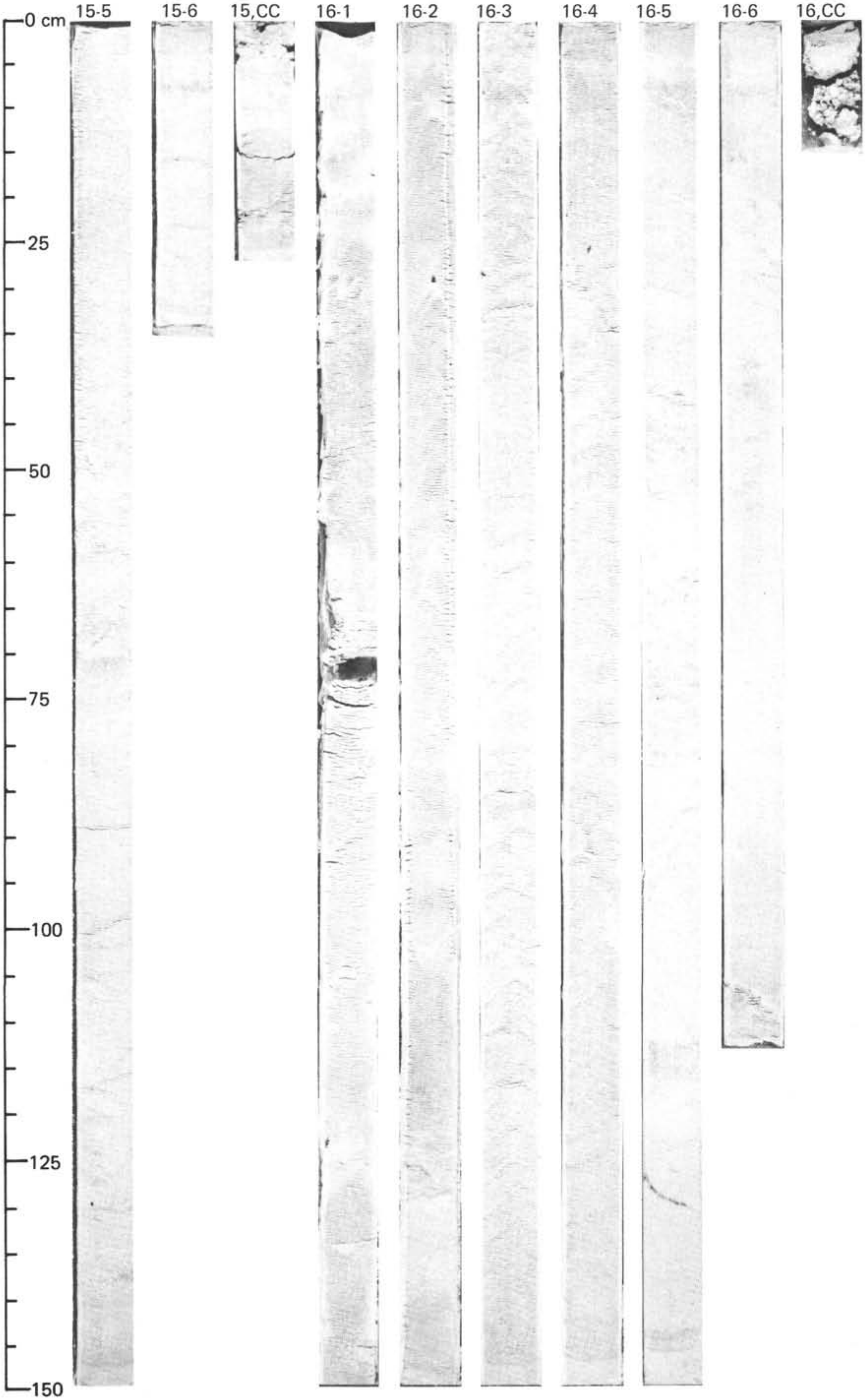
0 cm
25
50
75
100
125
150
15-5
15-6
15,CC
16-1
16-2
16-3
16-4
16-5
16-6
16,CC